Ultrafiltration and Nanofiltration of E-stage bleaching plant effluent of a sulphite pulp mill

Teófilo Rodrigo Leitão São Pedro

Thesis to obtain the Master of Science Degree in

Chemical Engineering

Supervisors: Professor Ann-Sofi Jönsson (LTH)
Professor Maria Norberta Neves Correia de Pinho (IST)

Examination Committee

Chairperson: Professor Francisco Manuel da Silva Lemos (IST)
Supervisor: Professor Maria Norberta Neves Correia de Pinho (IST)
Members of the Committee: Professor Luís Miguel Minhalma (ISEL)

December 2016

Acknowledgments

I would like to address special thanks to Professor Maria Norberta de Pinho, as a supervisor, for the opportunity to carry out this work abroad, for the knowledge transmitted and for its essential suggestions.

This master thesis has been performed at the Department of Chemical Engineering at the Faculty of Engineering, LTH, Lund University, which I would like to thank everyone at the department for the friendly and supportive environment during my presence in Lund, especially my supervisor Ann-Sofi Jönsson for receiving me, treating and providing me everything so kindly through this challenging journey of my life. The experimental work could not have been conducted without the help, expertise and support from Johan Thuvander and Sandra Farran-Lee to which I am very grateful. To Frank Lipnizki from Alfa Laval, my sincerely thanks for having provided the Alfa Laval membranes and the necessary advices about that.

I also would like to thank *Caima - Indústria de Celulose, S.A.* for providing the bleach plant effluent used during the experiments and especially Eng. António Prates for being available to discuss, to have trust in my work and for guiding me into a field trip in the mill.

I will be forever grateful to all professors and colleagues who I had shared so many ideas and experiences during my academic performance at *Instituto Superior Técnico, Universidade de Lisboa*.

Finally and not least, my sincere gratitude to my closest friends and family who have been with me at all time. I dedicate this thesis to my wonderful parents and, of course, to my sister Carolina for being an extra motivation in all actions of my life.

Abstract

With the continuous increase of the environmental constraints in the pulp and paper industry, efforts have been made to find possible ways that minimize water consumption by reusing treated process streams and improving the quality of the final effluent. In addition, the use of by-products from this industry increase its economic sustainability. The treatment of sectorial streams in the pulp mills can be an attractive alternative due to its lower volumes and more specific characterizations in comparison to the final effluents.

Thus, the aim of this work was to evaluate the use of a membrane separation process in the treatment of a bleaching plant effluent, specifically, the alkaline extraction filtrate of a sulphite pulp mill that use the bleaching sequence, E-O-P. The process that concentrates the effluent was optimized, taken into account the use of the lignin and hemicelluloses of the final retentate, as well as the possibility of reusing the treated permeate obtained.

Nanofiltration membrane ALFA-LAVAL - NF99HF was found to be the most suitable when operating at 70°C, with a CFV of 0,8 m/s and a transmembrane pressure of 13 bar. An average permeate flux of 24,2 $Lh^{-1}m^{-2}$, lignin and hemicelluloses rejections between 94 and 97%, and an increase in total solids content from 3% to 7%(w/w) for a volumetric concentration factor of 3,1 were obtained. A total cost of 2,14€ per m^3 of permeate for a new plant that processes 70 m^3/h of the studied effluent was determined.

Keywords: Bleach plant effluent, Ultrafiltration/Nanofiltration, Concentration, Lignin, Hemicelluloses, Sulphite pulp

Resumo

Com o aumento das restrições ambientais na indústria da pasta de celulose, têm sido feitos esforços para encontrar opções que minimizem o consumo de água, como reutilizar correntes de processo tratadas e melhorar a qualidade do efluente final. Para além disso, a sustentabilidade económica desta indústria passa também pelo aproveitamento de subprodutos que possam constituir um valor acrescentado ao processo de fabricação da polpa. O tratamento de correntes setoriais das fábricas pode assim constituir uma alternativa atrativa face aos seus menores volumes e caracterizações mais específicas que os efluentes finais.

O objetivo deste trabalho passou por avaliar o uso de um processo de separação por membranas no tratamento de um efluente de branqueamento, especificamente o filtrado da extração alcalina de uma fábrica de pasta de celulose que usa uma sequência de branqueamento, E-O-P. Foi otimizado o processo de concentração do efluente, tendo em vista o aproveitamento das lenhinas e hemiceluloses dos concentrados obtidos bem como o possível reaproveitamento do permeado obtido.

A membrana NF99HF da Alfa-laval foi a que se apresentou mais adequada quando a operar a 70°C, uma velocidade de 0,8 m/s e à pressão transmembranar de 13 bar. Obtendo-se um fluxo médio de permeado de 24,2 $Lh^{-1}m^{-2}$, rejeição a lenhinas e hemiceluloses entre 94 e 97% e aumento da concentração de sólidos totais de 3% para 7% (w/w) para um fator de concentração volumétrico de 3,1. O custo total obtido para uma nova planta que opere 70 m^3/h do efluente seria 2,14€ por m^3 de permeado tratado.

Palavras-chave: Efluente de branqueamento, Ultrafiltração/Nanofiltração, Concentração, Lenhina, Hemiceluloses, Processo ao sulfito

Table of Contents

1. Introduction 1

1.1. Background 1

1.2. Aim of the thesis 3

1.3. Outline of the thesis 3

2. Membrane processes 5

2.1. Pressure-driven membrane processes 5

2.1.1. Membrane classification 6

2.1.2. Membrane characterization 9

2.1.3. Polarization phenomena and fouling 11

3. Literature review 17

3.1. Environmental protection and water recovery 17

3.1.1. Bleach plant effluents treatment 17

3.2. Energy-efficiency and sub-products valorization 22

3.3. Fouling and cleaning 25

3.4. Molar mass of solutes in pulp mill streams 26

4. Materials and methods 27

4.1. Bleaching plant effluent 27

4.2. Membranes 28

4.2.1. Membrane selection by SEC analysis 28

4.2.2. Tested membranes 28

4.3. Equipment 28

4.3.1. Parametric studies 29

4.3.2. Concentration studies 29

4.4. Operating procedure 30

4.4.1. Initial cleaning and PWF of new membranes 30

4.4.2. Parametric studies 30

4.4.3. Concentration studies 31

4.4.4. Membrane regeneration 31

4.5. Analysis 32

4.5.1. Total solids, ash and total suspended solids 32

4.5.2. Total lignin 32

4.5.3. Acid hydrolysis, acid-insoluble (Klason), acid-soluble lignin and hemicelluloses 32

4.5.4. Total carbon, organic carbon and inorganic carbon 33

4.5.5. Molecular mass distribution of hemicelluloses and lignin 33

5. Results and discussion 35

5.1. Size exclusion chromatography of the BPE 35

5.2. Hydraulic permeability of the membranes 36

5.3. Parametric studies 38

5.3.1. Permeate fluxes vs TMP 38

5.3.2. Lignin retention 40

5.3.3. Other retentions 41

5.3.4. SEC of permeates 43

5.3.5. Membrane resistances 45

5.3.6. Membranes regeneration 48

5.4. Concentration studies 49

5.4.1. Permeate fluxes vs VR 49

5.4.2. Characterization of fractionated streams 51

5.4.3. SEC of fractionated streams 54

5.4.4. Membrane regeneration 56

5.5. Cost estimates 58

5.5.1. Investment cost 59

5.5.2. Operating costs 60

6. Conclusion and future work 63

6.1. Contributions 63

6.2. Future work 64

7. References 67

8. Annexes A1

List of Acronyms and Nomenclature

Acronyms

AOX	Absorbable organic halides
ASP	Activated sludge plant
BOD	Biochemical oxygen demand
BPE	Bleach plant effluent
CFV	Cross-flow velocity
COD	Chemical oxygen demand
E-stage	Alkaline extraction stage
ECF	Elemental chlorine free
E_{OP}	Alkali extraction re-enforced by oxygen and peroxide
EOX	Extracted organic halides
MF	Microfiltration
MWCO	Molecular weight cut-off
NF	Nanofiltration
P&P	Pulp and paper
PWF	Pure water flux
RI	Refractive index
RO	Reverse osmosis
SWM	Spiral-wound membranes
SEC	Size exclusion chromatography
TC	Total carbon
TCF	Total chlorine free
TDS	Total dissolved solids
TMP	Transmembrane pressure
TOC	Total organic carbon
TOX	Total organic halides
TS	Total solids
TSS	Total suspended solids

UF	Ultrafiltration
UV	Ultraviolet
VR	Volume reduction
VRF	Volume reduction factor

Nomenclature

$\boldsymbol{\delta}$	Thickness of the laminar sub-layer
$\boldsymbol{\rho}$	Density
$\boldsymbol{D}$	Diffusivity
$\boldsymbol{R}$	Gas constant
$\boldsymbol{T}$	Temperature
$\boldsymbol{k}$	Mass transfer coefficient
$\boldsymbol{t}$	Time
$\boldsymbol{\varepsilon}$	Porosity
$\boldsymbol{\tau}$	Tortuosity
$\boldsymbol{\bar{M}_w}$	Mass average molecular mass
$\boldsymbol{C_b}$	Bulk solution concentration
$\boldsymbol{C_c}$	Retentate concentration
$\boldsymbol{C_f}$	Feed concentration
$\boldsymbol{C_g}$	Gel concentration
$\boldsymbol{C_i}$	Concentration of component i
$\boldsymbol{C_m}$	Membrane surface concentration
$\boldsymbol{C_p}$	Permeate concentration
$\boldsymbol{C_0}$	Initial concentration in the feed
$\boldsymbol{J_{w^*}}$	Fouled membrane pure water flux
$\boldsymbol{J_\infty}$	Limiting flux
$\boldsymbol{J_{av}}$	Average permeate flux
$\boldsymbol{J_v}$	Permeate flux
$\boldsymbol{J_w}$	Regenerated membrane pure water flux (after chemical cleaning)

J_{wi}	New membranes pure water flux
L_{w^*}	Hydraulic permeability of fouled membranes
L_p	Hydraulic permeability
L_v	Permeability of the solution
L_w	Hydraulic permeability of regenerated membranes (after chemical cleaning)
P_{out}	Outlet pressure
P_{in}	Inlet pressure
P_p	Permeate side pressure
Q_{feed}	Feed flow
R_a	Adsorption resistance
R_b	Pore blocking resistance
R_{cp}	Concentration polarization resistance
R_g	Gel layer resistance
R_{irrev}	Irreversible fouling resistance
R_{obs}	Observed/apparent retention
R_{rev}	Reversible fouling resistance
R_t	Total resistance
R_{tr}	True retention
V_p	Permeate volume
V_0	Initial feed volume
W	Energy required per m^3 of permeate
d_{pore}	Pore diameter
l_{pore}	Pore width
μ_p	Dynamic viscosity of permeate
μ_w	Dynamic viscosity of water
π_m	Membrane surface osmotic pressure
π_p	Permeate osmotic pressure
ΔP	Frictional pressure drop
$\Delta \pi$	Osmotic pressure difference

List of Figures

Figure 1 - Schematic illustration of the bleaching process at Caima - Indústria de Celulose, S.A. pulp mill and the point where the process liquid used in this investigation was withdrawn (‘E’ bleaching effluent bolded). 2

Figure 2 - Schematic representation of the nominal pore size for the pressure-driven membrane separation processes. Adapted from (Baker, 2004) 6

Figure 3 - Sketch of a cross-flow membrane process 6

Figure 4 - Principal types of membranes. Adapted from (Baker, 2004) 7

Figure 5 - Schematic of (a) Hollow-fiber module, (b) Tubular module, (c) Plant-and-frame modules, (d) Spiral-wound module. Adapted from (Baker, 2004) 8

Figure 6 - Typical variation of permeation flux against time, with polarization phenomena and fouling. Adapted from (Mulder, 1996) 12

Figure 7 - Concentration profile in the boundary layer in a polarization situation 12

Figure 8 - Resistance types to mass transfer in membrane processes. Adapted from (Mulder, 1996) 15

Figure 9 - Flow sheet of the equipment used in the flat-sheet membrane for parametric studies experiments. F = flowmeter, PI = pressure indicator, TS = temperature sensor 29

Figure 10 - Flow sheet of the equipment used in the flat-sheet membrane for concentration studies experiments. F = flowmeter, PI = pressure indicator, TS = temperature sensor 30

Figure 11 - Molecular mass distribution of lignin (measured as UV absorbance at 280 nm) and hemicelluloses (measured as refractive index) of untreated BPE. 35

Figure 12 - Pure water fluxes (J_{wi}) in function of TMP for the new membranes tested (before 1st usage). T = 30°C, CFV = 0,3 ms^{-1} 36

Figure 13 - Influence of the TMP and CFV on the permeate fluxes (J_v) for the first membrane series. T = 70°C 39

Figure 14 - Influence of the TMP and CFV on the permeate fluxes (J_v) for the second membrane series. T = 50°C 39

Figure 15 - Influence of the TMP on total lignin retention for the 1st membrane series tested in the parametric studies. T = 70°C, CFV = 0,8 ms^{-1} 40

Figure 16 - Influence of the TMP on total lignin retention for the 2nd membrane series tested in the parametric studies. T = 50°C, CFV = 0,8 ms^{-1} 41

Figure 17 - Influence of the TMP on hemicelluloses, TS and ash retention for the MPF36 membrane. T = 70°C, CFV = 0,8 ms^{-1} 42

Figure 18 - Influence of the TMP on hemicelluloses, TS and ash retention for the NF99HF membrane. T = 50°C, CFV = 0,8 ms^{-1} 42

Figure 19 - Molecular mass distribution of lignin (measured as UV absorbance at 280 nm) and hemicelluloses (measured as refractive index) in the BPE, BPE after sieving and permeate of MPF36 membrane. T = 70°C, P = 15 bar, CFV = 0,8 ms^{-1} 43

Figure 20 - Molecular mass distribution of lignin (measured as UV absorbance at 280 nm) and hemicelluloses (measured as refractive index) in the BPE, BPE after sieving and permeate of NF99HF membrane. T = 50°C, P = 13 bar, CFV = 0,8 ms^{-1} 44

Figure 21 - Permeate fluxes (J_v) in the linear region. 45

Figure 22 - Pure water fluxes (J_{w^*}) in function of TMP after parametric studies (fouled membranes). T = 30°C, CFV = 0,3 ms^{-1} 46

Figure 23 - Pure water fluxes (J_w) in function of TMP after cleaning the membranes. T = 30°C, CFV = 0,3 ms^{-1} 48

Figure 24 - Flux during concentration of process solution with NF99HF membrane. T = 50°C, TMP = 13 bar, CFV = 0,8 ms^{-1} 50

Figure 25 - Moving average of frictional pressure drop during the concentration studies of the BPE. NF99HF, T = 50°C, TMP = 13 bar, CFV = 0,8 ms^{-1} 51

Figure 26 - Concentration values for retentate streams 53

Figure 27 - Concentration values for permeate streams 53

Figure 28 - Variation of apparent retentions with volume reduction (VR) for each component 53

Figure 29 - TOC concentrations for retentate and permeate streams 54

Figure 30 - Variation of TOC retention with volume reduction (VR) 54

Figure 31 - Molecular mass distribution of hemicelluloses (measured as refractive index) for the feed (retentate at VR of 0%), concentrate and permeate for a VR of 68% 55

Figure 32 - Molecular mass distribution of lignin (measured as UV absorbance at 280 nm) for the feed (retentate at VR of 0%), concentrate and permeate for a VR of 68% 55

Figure 33 - Pure water fluxes (PWF) in function of TMP for the new, fouled and cleaned membranes after the concentration experiment 56

Figure 34 - Single-stage feed and bleed system for the industrial scale-up process. Adapted from (Cui & Muralidhara, 2010) 59

Figure 35 - HPLC standards concentrations 1 and 2 ..... A3

Figure 36 - HPLC standards concentrations 3 and 4 ..... A4

Figure 37 - HPLC standard concentration 5 and Permeate VR=0% A5

Figure 38 - HPLC Permeate VR=68% and Retentate VR=0% A6

Figure 39 - HPLC Retentate VR=68% and summarized tables 1 .... A7

Figure 40 - HPLC summarized tables 2 .... A8

Figure 41 - HPLC summarized tables 3 .... A9

Figure 42 - SEC diagram for retentate and permeate streams at VR=0% A10

Figure 43 - SEC diagram for retentate and permeate streams at VR=30% A10

Figure 44 - SEC diagram for retentate and permeate streams at VR=40% A11

Figure 45 - SEC diagram for retentate and permeate streams at VR=68% A11

List of Tables

Table 1 - Different pressure-driven membrane processes 5

Table 2 - Parameters for membrane module design 9

Table 3 - Design data for the UF planta t Nymölla mill. Adapted from (Nordin & Jönsson, 2006) 21

Table 4 - Some characteristics of the BPE used in this investigation 27

Table 5 - Data for the polymeric membranes tested in the experiments 28

Table 6 - Mass average molecular mass of lignin and hemicelluloses of untreated BPE. 36

Table 7 - Hydraulic permeability (L_p) of the membranes tested (1st usage). 37

Table 8 - Permeate flux (J_v) and total lignin retention ($R_{total\ lignin}$) at the maximum TMP within the linear region, for membranes tested at CFV = 0,8 ms^{-1}. 41

Table 9 - Mass average molecular mass of lignin and hemicelluloses for feed BPE, MPF36 (T = 70°C, P = 15 bar, CFV = 0,8 ms^{-1}) and NF99HF (T = 50°C, P = 13 bar, CFV = 0,8 ms^{-1}) permeates. 44

Table 10 - BPE permeability values. CFV = 0,8 $ms-^{1}$ 45

Table 11 - Hydraulic permeability (L_{w*}) after parametric experiments (fouled membranes). 46

Table 12 - Different resistance types to permeation of BPE. 48

Table 13 - Hydraulic permeability (L_w) after cleaning the membranes. 49

Table 14 - Permeability recovery after washing and after cleaning. 49

Table 15 - Physicochemical characterization of the feed (retentate at VR of 0%), concentrate and permeate for a VR of 68% 52

Table 16 - Mass average molecular mass of lignin and hemicelluloses for the feed (retentate at VR of 0%), concentrate and permeate for a VR of 68% 56

Table 17 - Hydraulic permeability values and permeability recovery after washing and after cleaning 57

Table 18 - Experimental data used in the cost estimates 58

Table 19 - Technico-economical data 58

Table 20 - Cost estimates for NF installation with full-time use (8000h.$year^{-1}$) 61

Table 21 - Physicochemical characterization of retentates and permeates for a VR of 0%, 10% and 20% A1

Table 22 - Physicochemical characterization of retentates and permeates for a VR of 30%, 40% and 50% A2

Table 23 - Physicochemical characterization of retentates and permeates for a VR of 60%, 65% and 68% A2

1. Introduction

1.1. Background

Pulp and paper (P&P) industry is one of the major sources of industrial water pollution, thus waste water reuse is a globally imperative component of sustainable water management. The volume and characteristics of waste water differ according to the type of raw material, the process technologies, whether or not there is internal recirculation of the effluent, and the type of pulp and paper produced. (Ebrahimi, et al., 2015)

The production of sulphite pulp is much smaller than the production of kraft pulp, the main reason is that sulphite pulps generally do not have good strength properties as those of kraft pulp. However for some specialty pulp applications sulphite pulp provides other advantageous properties. Sulphite pulps produced by different processes have different properties, which make them suitable for particular products. Most pulp is produced for the purpose of subsequent manufacture of paper, but some is destined for other uses such as thick fibreboard or textile products manufactured from dissolving pulp. For now, producers of dissolving pulp are producing low kappa (an indication of the residual lignin content) products that are predominantly sold to the viscose textile industry. (Suhr, et al., 2015)

One example on this framework is *Caima - Indústria de Celulose, S.A.*, a Portuguese pulp mill with a capacity to produce 125 000 tons per year of bleached hardwood (eucalyptus globulus) sulphite dissolving pulp. The bleaching process is totally chlorine free (TCF) and the bleaching sequence E-O-P starts with an alkaline extraction (E) followed by an oxygen delignification (O) and a final bleaching with hydrogen peroxide (P) to enhance the removal of lignin, hemicelluloses and color to achieve the low kappa aforementioned. The schematic illustration of the bleaching sequence used in *Caima - Indústria de Celulose, S.A.* is presented in Figure 1.

The E-stage is an alkaline extraction with sodium hydroxide. Since sodium causes clogging of the recovery boilers the effluent from the E-stage cannot be recycled to the recovery boilers of the mill. (Nordin & Jönsson, 2008)

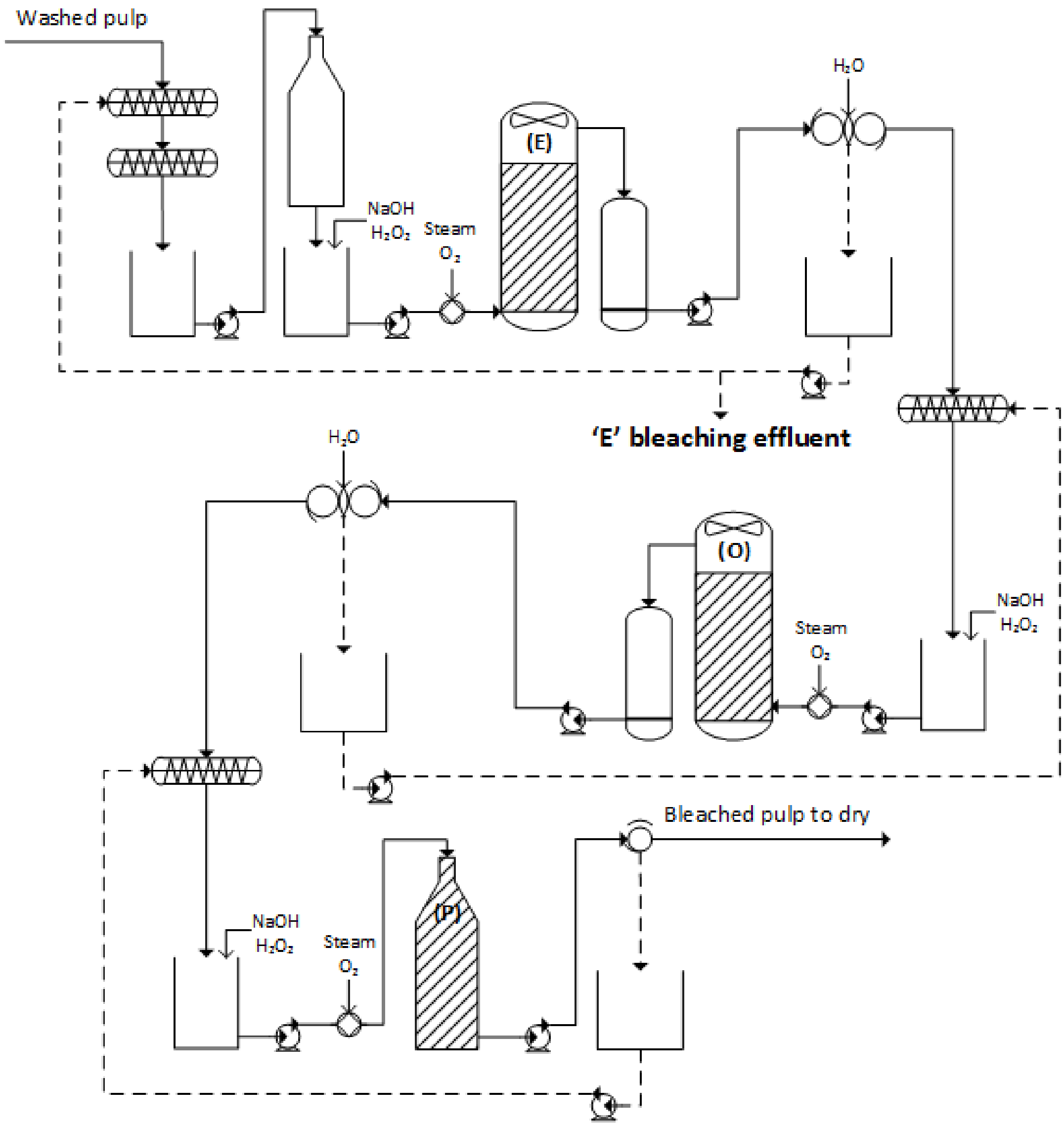

Figure 1 - Schematic illustration of the bleaching process at Caima - Indústria de Celulose, S.A. pulp mill and the point where the process liquid used in this investigation was withdrawn ('E' bleaching effluent bolded).

Usually each bleaching stage is composed of a reactor followed by a pulp washer. The bleaching plant effluent (BPE) filtrates from the washers constitute the major source of effluent sent to the effluent treatment plant, particularly the alkaline filtrate from E-stage contributes significantly to the final effluent's high organic load. Furthermore, process streams in pulp mills are commonly dilute and the treatment of specific in-plant streams seems to be an attractive technical and economical approach because it allows for the use of advanced technologies such as membrane filtration. (Quezada, et al., 2014) (Jönsson, 2016)

In the case of P&P industry, membrane filtration has been studied and applied in recent years for various purposes, including treatment of end-of-pipe effluents and particularly for processing of in-plant streams for water, energy and sub-products recovery. Lignin and hemicelluloses valorization constitutes a major subject of research and development in the biorefinery framework. (He, et al., 2012)

1.2. Aim of the thesis

The main purpose of this work is to contribute for the improvement of the current knowledge on pressure-driven membrane processes applied in the P&P industry streams, exploring its capacity to use both in an environmental protection and water reuse, and in energy efficiency and sub-product valorization.

The main aim of the present work is to propose an alternative way to treat an E-stage BPE from a sulphite pulp mill with a TCF bleaching process that works on an E-O-P sequence to produce dissolving pulp. This treatment by UF/NF focused not only on the concentration of the stream for possible water reuse and energy-efficiency, as also evaluates the fractionated streams for sub-products valorization in the perspective of future works in the biorefinery point of view.

The strategy to achieve the aim presupposes the following partial objectives:

1. Characterization of the BPE to be treated
2. Select a membrane and the optimal operating conditions of UF/NF by parametric studies
3. Concentrate the BPE in batch concentration mode and evaluate the fractionated streams
4. Analyze the efficiency of membrane washing and chemical cleaning
5. Brief cost estimates for the industrial scale-up of the process

1.3. Outline of the thesis

In the context presented before, this thesis follows a sequence divided in five main chapters.

2. Membrane processes
3. Literature review
4. Materials and methods
5. Results and discussion
6. Conclusion and future work

The first two chapters (2 and 3) provide background information and put this work into the perspective of the state of the art. A theoretical background of pressure-driven membrane processes and previous investigations of membrane processes in the P&P industry are presented.

In chapter 4, the feed solutions and experimental equipment and procedures are presented. All experiments were performed at the Department of Chemical Engineering, Lund University, Lund, Sweden.

In chapter 5, results obtained from the experimental parts are presented and discussed.

Finally, concluding remarks and suggestions for future work, are given in chapter 6.

2. Membrane processes

2.1. Pressure-driven membrane processes

Most common membrane separation processes are those in which the driving force is the difference in pressure between the feed and the permeate channel: microfiltration (MF), ultrafiltration (UF), nanofiltration (NF) and reverse osmosis (RO). The main differences between these membrane processes, presented in Table 1, are based on the different types of molecules that are involved in the separation or in the different pore sizes, as shown in Figure 2, that vary depending on the materials used and the manufacturing method.

Table 1 - Different pressure-driven membrane processes

Membrane Separation	Membrane Type	Transmembrane pressure	Osmotic pressure	Mechanism	Applications
Microfiltration (MF)	Symmetric and Asymmetric microporous	Low (< 2 bar)	Negligible	Size exclusion	Separation of colloids and particles
Ultrafiltration (UF)	Asymmetric microporous	Low (1 to 10 bar)	Negligible	Size exclusion and electrostatic interaction forces	Separation of macromolecules
Nanofiltration (NF) and Reverse Osmosis (RO)	Asymmetric, composite with homogeneous skin	High (10 to 60 bar)	High (1 to 25 bar)	Solution-diffusion	Separation of low-molecular-weight solutes (salts, and small organic compounds)

Adapted from (Mulder, 1996)

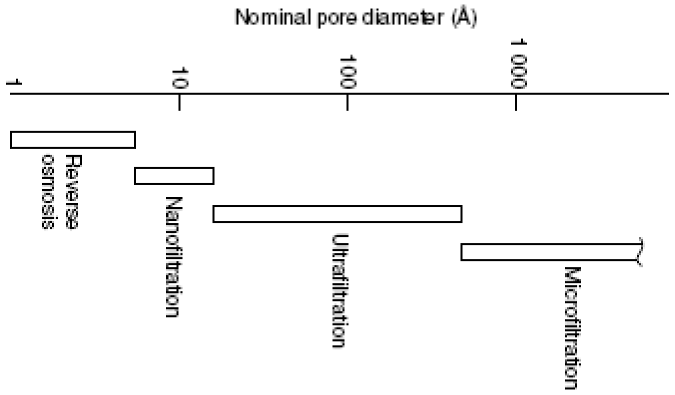

Figure 2 - Schematic representation of the nominal pore size for the pressure-driven membrane separation processes. Adapted from (Baker, 2004)

These processes are mostly carried out in cross-flow mode, i.e. the feed solution circulates tangentially to the membrane and, due to the pressure applied (transmembrane pressure (TMP), equation (1)), the feed stream is divided in two: a permeate stream, which passes through the membrane, and a concentrate/retentate stream that contains the portion of solution that was rejected by the membrane, as shown in Figure 3. Cross-flow operation has the advantage that it reduces the formation of a filter cake on the membrane surface, thereby allowing a continuous operation.

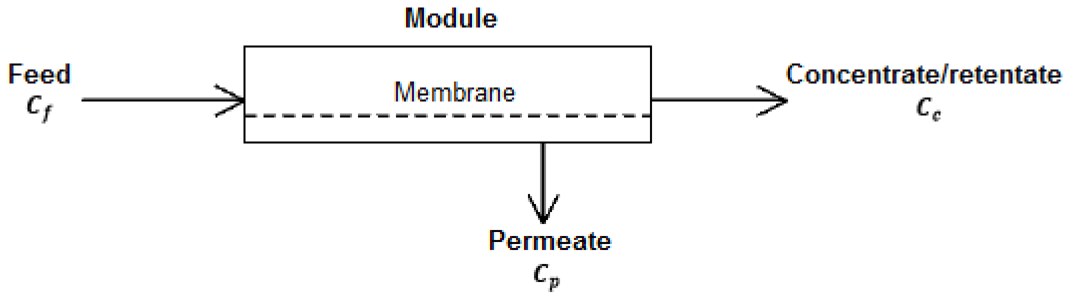

Figure 3 - Sketch of a cross-flow membrane process

$$TMP = \frac{P_{in} + P_{out}}{2} - P_p \tag{1}$$

Where P_{in} and P_{out} are the pressures at the inlet of the feed and the outlet of the retentate, P_p is the pressure on the permeate side and C_f, C_c and C_p are the concentrations on the feed, retentate and permeate streams, respectively.

2.1.1. Membrane classification

Membranes can be classified according to their nature, biological or synthetic, and these differ in their structure and functionality. (Mulder, 1996) These can be solid or liquid and can be neutral or may carry negative and/or positive charges. (Strathmann, 1986)

According to its structure, the membranes can be classified into two classes: symmetric and asymmetric membranes, as shown in Figure 4. Symmetric membranes include the microporous and the homogeneous, while asymmetric membranes can be integral or composed. (Strathmann, 1986) (Mulder, 1996)

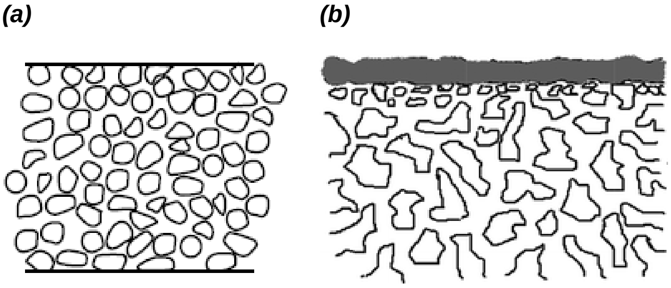

Figure 4 - Principal types of membranes. Adapted from (Baker, 2004)

The selective barrier is distributed throughout the thickness, in the case of symmetric membranes, ranging between 10-200 µm. (Mulder, 1996) On asymmetric composite membranes (b), the selective barrier consists in a very thin and homogeneous layer, also referred to as active layer or "skin", with its varying thickness between 0,1-1 µm in a porous layer, called support layer, with thickness of 100-200 µm. One of the advantages of this type of structure is that they retain the particles to the surface of the membrane, thus preventing from fouling, unlike symmetric membranes (a), which act as filters and retain particles in their pores, which can lead to a higher decrease of the permeate fluxes. (Strathmann, 1986)

The membranes are classified according to their morphological and physicochemical characteristics and can be arranged in different module configurations. The choice of membranes and membrane modules is a very important factor for the optimization of a given separation, since it is necessary to consider several operating factors and normally the cleaning processes.

Membrane materials

Synthetic membranes can be made of different types of materials within the two major classes of organic /polymeric or inorganic. Basically all polymers can be used as a barrier or membrane material, but the physicochemical characteristics differ greatly between the polymers, making possible the use of a limited amount. (Scott, 1998)

Due to its regular and crystalline structure, cellulose polymers are hydrophilic (not soluble in water). Derivatives of cellulose, such as cellulose nitrate or cellulose acetate are commonly used to UF and MF. The cellulose esters are very sensitive to chemical, biological and thermal degradation. To avoid degradation, the pH has to be maintained in the range of 4 to 7. (Mulder, 1996)

Another important group of polymers are polyamides, which contains functional amide groups (-CO-NH-). The preference is to use aromatic polyamides, due to its remarkable chemical, physical and thermal stability, and its selective capacity, particularly in NF and/or RO.

The morphological (pore size and pore density, represented by the number of pores per surface area of the membrane), chemical and electrical properties of the membrane affect membrane-solute-solvent interactions. In this way, the knowledge of the electrical surface charge of the membrane, the acid/basic character and hydrophilicity/hydrophobicity becomes crucial in the performance of membrane separation processes. (Cheryan, 1998)

Module configuration

In order to give membranes their operational function, they are arranged and packed in an operating system called module. This can be of various types and the most common geometries are hollow fiber, tubular, plate-and-frame and spiral-wound, presented in Figure 5. The choice of one type or another depends on certain factors, including manufacturing economy, providing good contact between the membrane and the feed stream, the ratio between the permeation area and the volume of the module, the possibility of exchanging the membranes, the fouling resistance, the characteristics of the mixture to be fractionated, the ease of permeate passage and the cleaning and maintenance easiness. (Mulder, 1996)

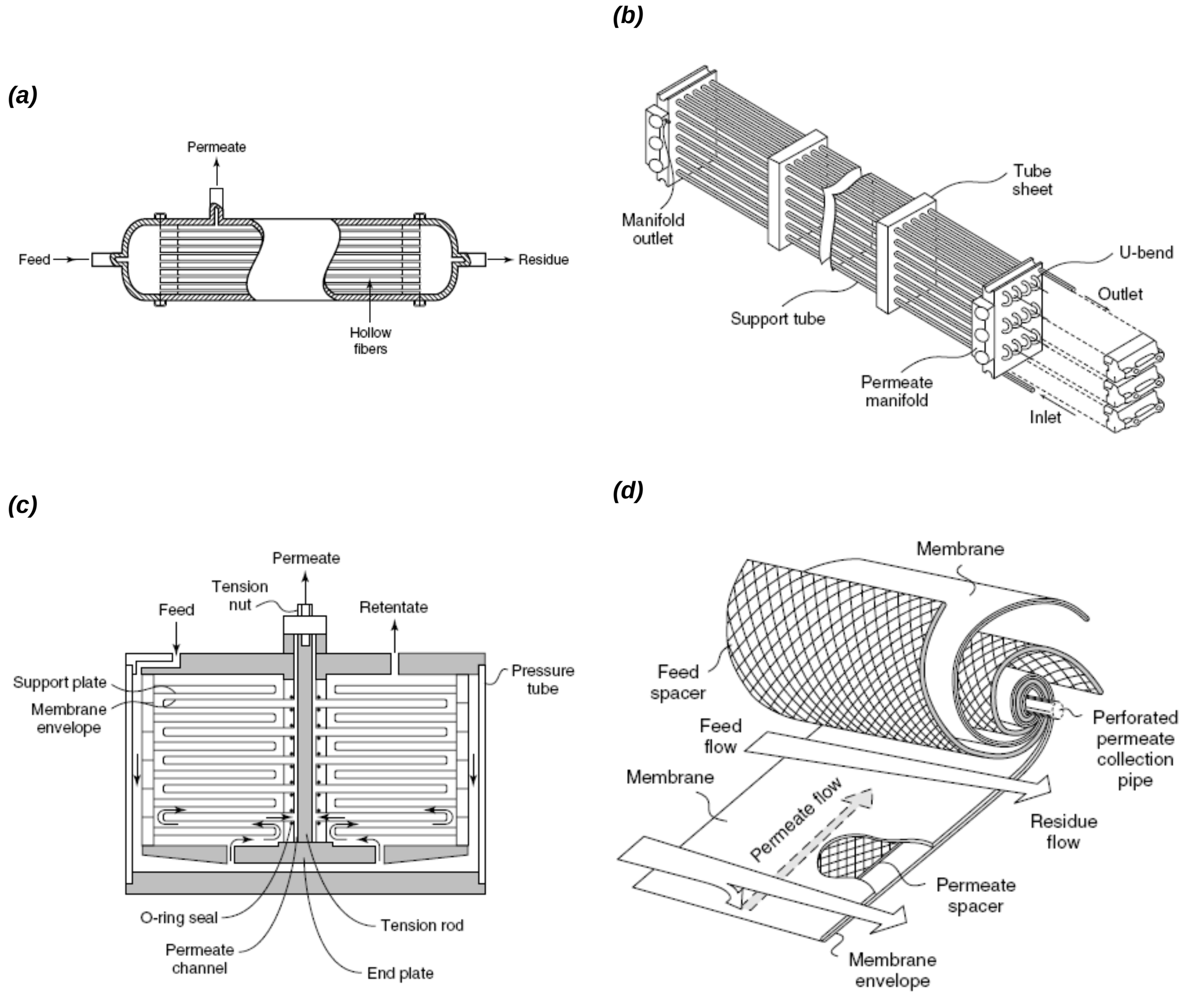
(a)
Permeate
Feed
Residue
Hollow fibers
(b)
Manifold outlet
Tube sheet
U-bend
Outlet
Support tube
Permeate manifold
Inlet
(c)
Permeate
Tension nut
Feed
Retentate
Support plate
Membrane envelope
Pressure tube
O-ring seal
Tension rod
Permeate channel
End plate
(d)
Membrane
Feed spacer
Feed flow
Perforated permeate collection pipe
Membrane
Permeate flow
Residue flow
Permeate spacer
Membrane envelope

Figure 5 - Schematic of (a) Hollow-fiber module, (b) Tubular module, (c) Plant-and-frame modules, (d) Spiral-wound module. Adapted from (Baker, 2004)

Hollow-fiber modules contain membranes of very small external diameter, are self-supported, have high surface area and present the highest relationship between the permeation area and volume of the module against other geometries, which represents a better use of space and a reduction in the cost of the equipment. However they have a low permeate flux per unit area. The tubular modules are pressure vessels with membranes usually drilled or porous, shell and tube type, connected in series or parallel. Generally, are much more expensive, but their use is justified in applications with high fouling tendency, since they promote good control of the operational conditions of the feed flow dynamics and of the cleaning facility. The plate-and-frame type fit flat-sheet membranes and act like the filter-presses, membranes are arranged in parallel intermediated by supports and spacers. The spiral-wound modules, like the name said, are flat sheets spiral-wound membranes (SWM) together with spacers, which prevent the contact of membrane against membrane and allow the build-up of the feed channels. The permeate is collected in a perforated central tube. The feed stream enters on one end of the SWM membranes roll and the concentrate leaves the other, being all together engaged in a housing with sealed ends, to prevent permeate and feed mixing. (Cheryan, 1998) (Wagner, 2000)

The principal module design parameters that enter into the decision are summarized in Table 2.

Table 2 - Parameters for membrane module design

Module type	**Hollow-fiber**	**Tubular**	**Plant-and-frame**	**Spiral-wound**
Manufacturing cost (US$/m^2)	5-20	50-200	50-200	5-100
Concentration polarization/Fouling control	Poor	Very good	Good	Moderate
Permeate-side pressure drop	High	Low	Low	Moderate
High-pressure operation	Yes	Marginal	Yes	Yes
Limited to specific types of membrane material	Yes	No	No	No

Adapted from (Baker, 2004)

2.1.2. Membrane characterization

The characterization of the membranes must contain morphological information, related to the porous structure (pore diameter and pore diameter distribution), chemical (hydrophilicity or hydrophobicity relative) and electrical properties and materials (polymers) that constitute them. More particularly, this characterization of the membrane is carried out mainly as a function of the membrane and not of the circulation regime. In turn, the flow regime is related to the hydrodynamic characterization of the feed flow, the physicochemical composition, the pressure and the operating temperature.

The performance of a membrane filtration process is usually assessed in terms of the magnitude of the permeate fluxes and the separation performance of the membrane.

Permeate flux and Hydraulic permeability

The flux is defined as the flow of permeate per unit area, expressed by equation (2). It represents the capacity of the membrane process and determines the required size of the membrane plant. The flux through the membrane is mainly dependent on the properties of the feed solution and the operating conditions used during filtration. If the solution is pure water, the permeate flux can be expressed by equation (3).

$$J = \frac{V_p}{t \times A_m} \tag{2}$$

$$J = \frac{L_p}{\mu_p} \times TMP \tag{3}$$

Being, J the permeate flux, TMP the transmembrane pressure applied, μ_p is the permeate viscosity and L_p the hydraulic permeability. The membrane resistance R_m is defined by $\frac{1}{L_p}$.

Retention coefficients

The membrane preferential permeation to a given solute is given by the observed retention coefficient, R_{obs}, defined in equation (4). It is distinguished from the true retention coefficient, R_{tr}, defined by equation (5).

$$R_{obs} = 1 - \frac{C_p}{C_b} \tag{4}$$

$$R_{tr} = 1 - \frac{C_p}{C_m} \tag{5}$$

Where C_p, C_b and C_m denote the concentration of the component in the permeate, in the bulk solution and at the membrane surface, respectively. When a solute is retained to a certain extent by the membrane, a concentration profile develops from the membrane surface to the bulk solution. This phenomenon, called concentration polarization is responsible for the fact that the observed retention coefficient is always lower than the true retention coefficient.

Volume reduction factor

The goal of many membrane filtration processes is to concentrate and/or purify a certain component in a feed stream. This goal can be achieved by selecting a membrane that retains the substance of interest, but is permeable to the solvent and the other solutes. In batch mode, the target component can be concentrated by continuously bleeding off the permeate from the membrane process and recirculating the retentate stream. Assuming the retention to be constant, the concentration of the desired product in the retentate stream, C_r, can be determined from the initial concentration in the feed, C_0, the observed retention coefficient of the substance, R_{obs} and the volume reduction, VR, by equations (6) and (8).

$$VR = \frac{V_p}{V_0} \tag{6}$$

$$VRF = \frac{1}{1 - VR} \tag{7}$$

$$C_c = C_0 \times \left(\frac{1}{1 - VR}\right)^{R_{obs}} \Leftrightarrow C_c = C_0 \times VRF^{R_{obs}} \tag{8}$$

Where the volume reduction is defined as the ratio of the permeate volume, V_p, to the initial feed volume, V_0. And the volume reduction factor, VRF is the ratio between the initial feed volume and the volume of the resulting retentate and could be expressed by equation (7).

Molecular weight cut-off

In processes involving MF, UF and NF membranes, there is a parameter that approximately indicates the size of the molecules that will be retained. It is called molecular weight cut-off (MWCO); is individual to each membrane and 90-95% of the molecules having molar mass equal to or greater than the MWCO are retained. Generally, the higher the MWCO of the membranes, the greater the permeate flux. However, other variables should also be taken into account in the evaluation of the permeate fluxes, such as porosity and pore size. (Wagner, 2000)

2.1.3. Polarization phenomena and fouling

It is important to understand some of the ways in which membrane permeate flux is reduced below that of the corresponding pure water flux (or more generally pure solvent flux). The reduction can be due to: First, concentration polarization that is a natural consequence of the selectivity of a membrane. This leads to an accumulation of particles or solutes in a mass transfer boundary layer adjacent to the membrane surface. Dissolved molecules accumulating at the surface increase the osmotic pressure and thus decrease the net driving force. This phenomenon is inevitable, but is reversible with an elimination of TMP and hence the flux. Second, there is fouling, that is to say a buildup of material (e.g., adsorbed macromolecules, gels, or deposited particles on or in the membrane surface). The decrease of the permeate flux has a negative impact on the economic aspect and therefore, measures should be taken to avoid this decrease. The first step is to distinguish between polarization and fouling, but the two phenomena may not be entirely independent of each other; fouling can be the result of polarization, which phenomenon is presented in Figure 6.

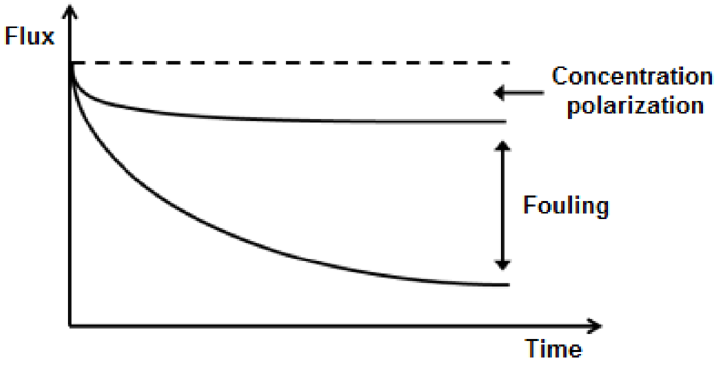

Figure 6 - Typical variation of permeation flux against time, with polarization phenomena and fouling. Adapted from (Mulder, 1996)

Concentration polarization

Concentration polarization as described before is a reversible process and can often be minimized. Changes in some operating parameters, such as recirculation rate, feed flow concentration, temperature, TMP and agitation, may lead to a decrease of the boundary layer adjacent to the membrane surface and accumulating the solutes rejected.

The quantification of concentration polarization is achieved by mass transfer models, which are explained below.

Stagnant film model

The stagnant film model theory, Figure 7, explains that when a driving force acts in the feed flow, the solute is partially retained by the membrane, while the solvent is permeated. Thus a solute concentration profile develops from the concentration C_m at the membrane surface, to the concentration C_b at the core of the feed solution. This phenomenon is called concentration polarization. (Mulder, 1996)

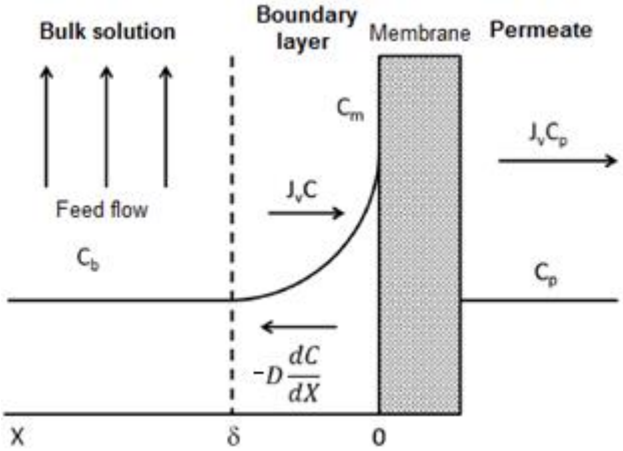

Figure 7 - Concentration profile in the boundary layer in a polarization situation

In steady state, a solute mass balance in the laminar boundary layer can be set up by the next three terms:

1. Convective solute transport towards the membrane in the laminar film layer: J_vC

2. Diffusive transport in the laminar boundary layer from the membrane surface into the bulk (Fick's law): $-D\frac{dC}{dx}$

3. Transport of solutes in the permeate away from the membrane: J_vC_p

And yielding the equation (9), a first order differential equation, that together with the boundary conditions $BC: \begin{cases} x = 0 \rightarrow C = C_m \\ x = \delta \rightarrow C = C_b \end{cases}$ can be integrated to get the equation (10).

$$J_vC = \left(-D\frac{dC}{dx}\right) + J_vC_p \tag{9}$$

$$\frac{C_m - C_p}{C_b - C_p} = e^{\left(\frac{J_v \times \delta}{D}\right)} \tag{10}$$

According to the film theory, the mass transfer coefficient, k, is given by the ratio between the diffusivity, D, and the thickness of the laminar boundary layer, δ. Rearranging the last equation it was obtained the general equation for the concentration polarization, equation (11).

$$\frac{C_m - C_p}{C_b - C_p} = e^{\left(\frac{J_v}{k}\right)} \tag{11}$$

When the concentration on the membrane surface, C_m, reaches a certain level, due to concentration polarization, a gel can be formed with a constant gel concentration, C_g. This gel is then assumed to be impermeable to the macromolecules, it consists of, and thus the permeate concentration, C_p is zero. Modelling this into the film theory model gives the gel layer model, equation (12), which can be used to calculate a limiting flux (J_∞) through the membrane when a gel layer is established.

$$J_\infty = k \times \ln\left(\frac{C_g}{C_b}\right) \tag{12}$$

Osmotic pressure model

The osmotic pressure model assumes that the increase in solute concentration at the membrane surface, due to concentration polarization, leads to a significant increase of osmotic pressure in this region and, consequently, a decrease in both the effective transmembrane pressure, TMP_{eff} and permeate flux. Considering the effect of osmotic pressure on the surface of the membrane and in the absence of any other effects, the permeate flux is given by equation (13).

$$J = \frac{L_p}{\mu_p} \times TMP_{eff} \tag{13}$$

Where,

$$TMP_{eff} = TMP - \Delta\pi \tag{14}$$

$$\Delta\pi = \pi_m - \pi_p \tag{15}$$

The applied TMP, between the feed solution and the permeate has to be larger than the osmotic pressure difference, $\Delta\pi$, between the feed solution immediately adjacent to the membrane surface, π_m, and the permeate, π_p, in order to obtain a flux through the membrane from the bulk side to the permeate side.

The osmotic pressure, π, of a solution can be calculated by use of the van't Hoff equation (16).

$$\pi = \frac{R \times T}{M_i} \times C_i \tag{16}$$

In this equation, R, is the gas constant, T the absolute temperature, M_i the molar mass of component i and C_i the concentration of component i in gL^{-1}. The proportionality between osmotic pressure and concentration given in equation (17) applies at low concentrations and for low molecular-weight molecules. When the osmotic pressure is to be calculated for macromolecular solutions or high concentration solutions, a virial expansion expression can be used as equation (17).

$$\pi = \frac{R \times T}{M_i} \times C_i + B \times C_i^2 + C \times C_i^3 + \cdots \tag{17}$$

It is seen that the van't Hoff equation is the first term of the expanded expression (17). It is also seen that when the concentration is low, almost only the first term contributes to the osmotic pressure. In that way, the equation (17) is reduced to van't Hoff equation (16). The terms B and C are constants for specific molecules. However, virial coefficients for all solutes are not easy to obtain, so usually, the simplification of the last equation to the following expression (18) is used.

$$\pi = A \times C_i^n\,, \quad n > 1 \tag{18}$$

Where A and n are constant characteristics for a given solute i, which are available in literature. (Beier, 2007)

Fouling

Under stationary conditions the concentration polarization gives a constant contribution to the total resistance towards mass transport through the membrane. This corresponds to a constant term, R_{cp} in equation (19). Thus, the flux should be constant when the applied hydrostatic pressure is constant, but in practice the flux often keeps decreasing during filtration. This is due to membrane fouling, which is sketched in Figure 6.

Membrane fouling is a complex phenomenon affected by many factors such as concentration, temperature, pH, ion strength, hydrophilic/hydrophobic interactions etc. Membrane fouling can, for example, consist of adsorption of different molecules, colloids or salts on the membrane surface and on the pore walls inside the membrane. Such adsorption will increase the resistance towards mass transport. Membrane fouling can also be blocking of the pores by different cells, bacteria or aggregated macromolecules, or it can be the build-up of a cake layer on the membrane surface

Resistance in series model

The resistance in series model considers that, in addition to the intrinsic resistance of the membrane, concentration polarization phenomena, adsorption of solutes on the surface or on the pore walls and the formation of gel layer, for example, contribute as additional resistance to permeation. (Cheryan, 1998) The influence of these phenomena types depends on the type of membrane and process fluid feed stream.

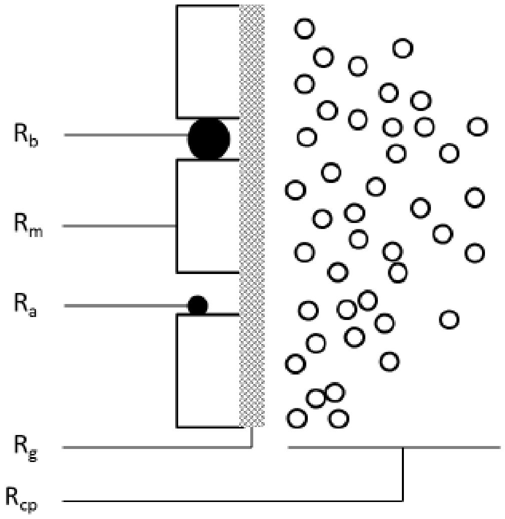

Figure 8 - Resistance types to mass transfer in membrane processes. Adapted from (Mulder, 1996)

In pressure-driven membrane processes, as is the case of MF, UF, NF and RO, the permeate flux according to the resistance in series model assuming that osmotic pressure difference is negligible, could be represented by equation (19).

$$J = \frac{TMP}{\mu_p \times (R_m + R_{cp} + R_a + R_g + R_b)} \tag{19}$$

Where total resistance is the sum of membrane resistance, R_m, resistance by concentration polarization, R_{cp}, resistance by adsorption of solutes, R_a, resistance by a gel layer formation, R_g and resistance by pore blocking, R_b. Schematically presented in Figure 8.

Because of the complex nature of membrane fouling no single equation is able to handle the phenomenon. But in a simplifying point of view it is possible to divide the other terms that reflect the fouling that occurs during operation in two types: the reversible and irreversible fouling, given by equation (20).

$$J = \frac{TMP}{\mu_p \times (R_m + R_{rev} + R_{irrev})} \tag{20}$$

The reversible component, R_{rev}, is the one that occurs during operation but is often removed when the pressure is released or when the membrane is washed with water. The irreversible component, R_{irrev}, is the one that reflects the deposition of material that is only removable (at best) by a cleaning operation with certain chemical cleaning agents. (Field, 2010)

3. Literature review

Membrane processes are being used in the P&P industry since the beginning of 1970s. Energy savings, environmental protection and recovery of valuable sub-products were the first examples of areas where membrane technology were found to be suitable in this industry. (Olsen, 1980)

Since early, industrial applications were studied and applied in the main areas aforementioned. Some of the first examples were presented and discussed by Jönsson and Wimmerstedt in 1985. In the Energy savings context, concentration of the black/brown liquor (from cooking in kraft/sulphite pulping process) by membrane filtration could require less energy than traditional evaporation. On an environmental protection and water recovery perspective, P&P diluted effluents represents a considerable pollution problem by their high COD, BOD, TS and color so one presented example is the treatment of BPE by membrane filtration. Finally, the recovery of valuable sub-products by fractionation and purification of lignin/lignosulphonates by membrane filtration of the black/brown liquor. (Jönsson & Wimmerstedt, 1985)

Almost 25 years later, Adnan, et al., 2009 continued to assert that membrane technology was being commercially applied in the P&P industry often in several areas such as for the treatment of freshwater, chemical recovery, treatment of BPE and complement or improve water recycling and closing the loop in the P&P industry. Even so, the commercial application of membrane technology in the P&P industry consisted of less than 2% of the global membrane market, indicating that there was still a lot of areas to be explored. Much of the R&D was concentrated on the conventional pressure-driven membrane processes (MF, UF, NF, RO) but some more advanced membrane technologies such as the Electrodialysis (ED), Membrane Bioreactor (MBR), Vibratory Shear Enhanced Processing (VSEP) and Membrane Distillation (MD) had been tested. (Adnan, et al., 2009)

3.1. Environmental protection and water recovery

3.1.1. Bleach plant effluents treatment

In efforts to maximize the water system closure and/or minimize the environmental impact, previous studies have explored the possibility of treating very different types of BPE.

An example of continuous improvement attempts is presented with a BPE from a Portuguese eucalyptus kraft pulp mill. UF/NF/ED articles with Portucel Setúbal, concerning the minimization of the environmental impact, UF performance for color removal in the effluents of the first caustic extraction stage, E1C/D, from the bleaching sequence with chlorine/chlorine dioxide (C/D-E1-D-E-D) was studied with polysulfone alkali-resistant membranes. For a membrane of 10kDa cut-off, the color removal was maximal (≈65%) and nearly independent of the feed circulation rate. (Afonso & Pinho, 1990) After some years the effluent of the first caustic extraction stage changed for E1D, now with a bleaching sequence with only chlorine dioxide (D-E1-D-E-D) an ECF process was studied with cellulose acetate UF membranes and one thin film composite NF membrane. The substitution of chlorine/chlorine dioxide by chlorine dioxide was very effective because it reduces 84% of EOX, 82% of TOX and 72% of color in the E1 effluent to be treated. The highest removal of TOX and color achieved by UF was 72 and 92%, respectively, with a tight UF membrane. The total removal of color and more than 90% removal of TOX was achieved by NF and gave a permeate with characteristics close to the requirements for the process water in the P&P industry, TOC=36±8 mgC/L, TOX=0,9±0,2 mgCl^-/L, EOX=0,91±0,07 mgCl^-/L, free of divalent salts and with an NaCl equivalent concentration of 0.6 g/L. (Rosa & Pinho, 1995) In an attempt to improve the UF/NF membrane processes aforementioned, pre-treatment such as flotation and MF was studied. It was found that flotation pre-treatment by dissolved-air or dissolved-CO_2 flotation leads to less membrane fouling, because it helps to remove suspended solids and TOC, makes possible feed circulation through the narrow channels of UF SWM modules, an important asset for the economic feasibility of large-scale applications. (Pinho, et al., 2000)

To further reduce the environmental impact of the discharges, improve the quality of bleached pulps and to facilitate the reuse of the water from the bleaching plants, new bleaching processes/sequences have begun to be further implemented.

Fälth, et al., investigated the treatment of seven alkaline filtrates from ECF and TCF kraft pulp mills with PCI tubular polyethersulphone UF membranes with 4 kDa and 6 kDa cut-off. By conductivity measurements, it was found in the study that the factor with the largest impact on flux is the concentration of the low-molecular-weight inorganic substances. By COD and BOD measurements, it was found that the retention of organic substances varies depending on the type of filtrate and the water management system of the mill and low-molecular-weight substances have a larger influence on the flux than the high-molecular-weight substances. The concentration also seems to be very important for the fouling of the membranes, where a higher concentration means more severe fouling - not only more fouling, but also a fouling that is harder to remove upon cleaning of the membranes. (Fälth, et al., 2001)

Shukla, et al., in an attempt to treat BPE's for system closure, studied the performance of an UF/NF/RO process in series of an Indian integrated paper mill BPE employing conventional CEHH (chlorination, alkaline extraction, hypo-1, hypo-2) sequence for bleaching of hardwood kraft pulp (eucalyptus). Thin film composite SWM modules made-up by polysulphone and polyamide were used with a MWCO of 1000 Da, 300 Da and 50 Da respectively. On the first attempt, only the E-stage BPE was submitted to the treatment, initial inlet pressure was 6,8 bar for UF, NF and 10,3 bar for RO. The initial permeate fluxes were around 82, 65 and 34 $Lh^{-1}m^{-2}$ for UF, NF and RO respectively. After RO treatment TDS and AOX removal was 99,77% and 98,51% respectively and all other pollutants like TSS, COD and color removal was found to be 100%. Water recovery was 86,4%, 95,28% and 95,95% for UF, NF and RO membranes respectively. (Shukla, et al., 2008) At another study, the same process had been applied but for the treatment of combined BPE, i.e. not only the E-stage effluent. At this time, the initial permeate fluxes were 39, 15 and 40 $Lh^{-1}m^{-2}$ for UF (6,8 bar), NF (6,8 bar) and RO (10,3 bar) respectively. Other higher pressures were tested but more water recovery was observed at low initial inlet pressure than at high initial inlet pressure. After RO treatment, COD and AOX removal was 99,3% and 92,5% respectively and all other pollutants like TDS and color removal was found to be 100%. (Shukla, et al., 2010) With the evolution of time the mill changes for an $OCE_{OP}HH$ (oxidation, chlorination, alkali extraction re-enforced by oxygen and peroxide, hypo-1, hypo-2) sequence for the bleaching of hardwood pulp. This time, same authors studied the performance of the UF/NF/RO process aforementioned for separate effluents, C-stage and E-stage BPE. During the study, it was found, that extraction stage effluent was most suitable for membrane filtration. The best membrane performance was obtained at low pressure. Comparatively with the last studies the initial permeate fluxes of the E-stage BPE were around 14 $Lh^{-1}m^{-2}$ for UF (6,8 bar), NF (6,8 bar) and RO (10,3 bar), which represents lower values due to the higher fraction of low molecular weight compounds with the improvement of the bleaching sequence. At a higher pressure, the permeate flux was initially high, but decreased rapidly. During the study, the optimum operating pressures for the UF, NF, and RO membranes for the treatment of both effluent streams were 6,8, 10,3, and 13,7 bar, respectively. (Shukla, et al., 2013)

In most cases when membrane filtration is used, it cannot be used without some kind of pre-treatment of the feed. The reason being that the feed channels in the modules get blocked in most types of elements. Especially SWM modules are very sensitive to this type of blocking. In order to avoid this, before introducing the effluent to the UF membranes, some primary treatments were applied as coagulation followed by bag filtration and MF (pore size 2 μm) to remove suspended particles from the effluent in both studies presented before by Shukla, et al.

Oñate, et. al. used a sequential UF/NF/RO membrane system too to treat an alkaline BPE from a kraft pulp mill featuring oxygen predelignification and ECF bleaching. The studies were preformed on a DSS LabStak® M20 Alfa Laval equipment. It was found that this membrane processes applied over alkaline extraction BPE led to high-quality permeate streams, opening the way to greater water closure because a high-quality permeate could be produced with a view to water reuse, at relatively low energy consumption. In this study it was found too, that most organic fraction in alkaline BPE could be removed by UF membranes of 10 kDa MWCO, and almost complete chloride rejection was obtained by the RO membrane. In all, 78% initial COD and total phenols, 82% AOX and 98% colour were retained above 10 kDa MWCO at 6 bar TMP. (Oñate, et al., 2015)

Different sequences of pressure-driven membrane processes were performed also to treat oxygen and peroxide-reinforced extraction stages (E_{OP}) filtrate from different ECF kraft pulp mills bleach plants. Usually the E_{OP} effluent is clarified and pre-treated through neutralization using acidic effluent streams (from chlorine dioxide stages) and thereafter the resulting effluent is discharged into the environment. Increasingly stringent environmental regulations and increasing input costs negatively affects the sustainability and competitiveness of the P&P industry. As a result, it has become necessary that broader strategies aimed at helping the industry to improve the environment performance whilst also reducing the operation costs are initiated. (Johakimu, et al., 2016)

Quezada, et. al., performed a study with this type of effluent and found that with a tubular tight UF membrane (4 kDa) made by polyether sulfone, it was possible to obtain a COD removal of 79% with a colour reduction of 86% (considered sufficient for the mill requirements) with best conditions for a higher permeate flux (over 200 $Lh^{-1}m^{-2}$) were a cross-flow velocity (CFV) of 3 ms^{-1} and a TMP of 7 bar. They found too that the effluent treatment plant (ETP) was very affected by the treatment of the EPO filtrate because if the UF permeate was recycled to the bleaching plant, the effluent flow rate reduced by approximately 30%, the efficiency of the COD removal in the biological treatment increased by 7% and the generation of biological sludge decreased by 20%. A decrease in the coagulant dosage by 40% in the tertiary treatment and consequently a decrease of tertiary sludge by 45% was also observed. (Quezada, et al., 2014) Johakimu, et al., did a preliminary techno-economic assessment for water and caustic soda recover, from this type of effluent too, using a UF/RO sequence. They report that to be economically viable the E_{OP} effluent flow rates must be higher than 480 m^3day^{-1} and water recovery rate must exceed 70%. At this optimum flow and water recovery rates, the process cost is approximately 1,30 €m^{-3}. Depending on the E_{OP} flowrates, the investment cost is in the range of 342-1720 k€ (between 480 and 2400 m^3day^{-1}) and the payback time is between 3 and 4 years. Caustic soda consumed and that remaining in the E_{OP} effluent is specific to each pulp mill, in this case motivations of caustic recovery s were based on environmental rather than economic benefit due to the very low concentration of caustic soda in E_{OP} effluent. (Anon., s.d.) (Johakimu, et al., 2016)

Less common, but also found in literature were membrane processes for the treatment of BPEs generated during sulphite pulp production.

Ebrahimi, et. al., tested ceramic tubular membranes to treat an alkaline BPE from one german pulp mill. The performance of single-stage and multi-stage cross-flow MF, UF and NF systems was tested in different configurations. It was found that the most suitable membrane configuration was a MF/UF (0,1µm/20kDa) sequence, due to their separation efficiency and performance revealed, reducing the COD concentration by 45% and residual lignin levels by 73%. Using a single UF membrane stage, a significant COD and lignin removal was also possible, but the susceptibility to fouling was higher reducing their performance by up to 80%. NF experiments after UF presented very low fluxes and all stages were performed at a TMP of 2 bar. Efficient chemical cleaning methods (1 h with 1% (w/v) NaOH at 60 °C) for fouled membranes were combined with back flushing to establish a successful cleaning process. (Ebrahimi, et al., 2015)

Nordin & Jönsson articles present some case studies on the largest industrial UF plant treating BPE from a sulphite P&P mill - Stora Enso located in Nymölla, Sweden. The bleaching sequence is TCF working in an OQP sequence (oxygen, chelate and peroxide), where de O-stage is alkaline and the pH is adjusted with sodium hydroxide. The UF plant has been in operation since 1995, with a processing capacity to treat 400 m^3h^{-1} of BPE the plant is equipped with a total area of 4800 m^2 tubular membranes manufactured by ITT Aquious – PCI, UK. The UF plant removes non-biodegradable, high-molecular-mass organic matter from the effluent, reducing their COD by 50%. The low-molecular-mass organic matter remaining in the permeate is decomposed in an activated sludge plant (ASP) before being discharged while the retentate with a TS content of 18% (w/w) is incinerated in the bark boiler of the mill. The plant was divided in two production lines, one for softwood and another for hardwood with the design data presented in Table 3.

Table 3 - Design data for the UF planta t Nymölla mill. Adapted from (Nordin & Jönsson, 2006)

Production line	**Softwood**	**Hardwood**
Total membrane area (m^2)	2900	1900
Membrane type	ES404	EM006
MWCO (kDa)	4	6
Number of stages in series	7	6
Number of modules	1060	720
Number of tubes in series in a module	18	9
Inlet pressure (bar)	7	8
CFV (ms^{-1})	1,8	3,6
VR (%)	98%	
Average flux ($Lh^{-1}m^{-2}$)	90	150
T (°C)	70-80°C	
Installed power (kW)	450	800

Adapted from (Nordin & Jönsson, 2006) (Nordin & Jönsson, 2008)

Tubular modules are used in the UF plant at Nymölla mill since this module design can handle successfully liquids containing fibres or particles without the need for extensive pre-treatment. The high temperature decreases the membrane lifetime, but the reduced fouling problems are considered a more important advantage.

The closed-loop management of process water in the mill has contributed to an increase in the feed concentration from the original 8000 mg/l COD to more than 10 000 mg/l ten years later. At the same time, increased production has resulted in a feed flow increase from 300 to 400 m^3h^{-1} which dealt to an increase of the usual atmospheric pressure in the permeate side into 1 bar and consequently a decrease in TMP. A drastic decrease of flux with axial position in the modules in the last stage was revealed too due to the high frictional pressure drop caused by the high viscosity (7,7 cP) of the solution in the last stages. So the aim of these authors was to evaluate the performance of the UF plant on the hardwood line and try to optimize the operating conditions, membrane area and energy requirements. On the first study, it was found that increasing the inlet pressure in the last stage of the UF plant from 7 to 11 bar would increase the average permeate flux from 13 to 33 $Lh^{-1}m^{-2}$, while decreasing the CFV from 3.6 ms^{-1} to 2 ms^{-1} would increase the average permeate flux in the last stage from 13 to 18 $Lh^{-1}m^{-2}$. However, changing the CFV in only the last stage would disturb the flow balance in the entire UF plant. (Nordin & Jönsson, 2006) In another study, they found that conventional series connection may be satisfactory for non-viscous liquids, but when treating highly viscous solutions a parallel arrangement of the membranes could be the best option. One example is, if an additional stage with VRF of 2 treating the retentate from the UF plant modules with the parallel arrangement would need only 41% of the membrane area and 37% of the energy requirement compared to modules with the arrangement in series. (Nordin & Jönsson, 2008)

3.2. Energy-efficiency and sub-products valorization

In pulp mills where the recovery boiler has become a bottleneck the extraction of lignin by UF is an alternative to increase pulp production. Kraft black liquor lignin is a biofuel that is separated from the cellulose during kraft pulping. Improved technology and energy integration in paper mills have led to an energy surplus at many mills. It was therefore of great interest to extract the lignin from the pulp mills and sell it as fuel to replace fossil fuel in other furnaces. Lignin is the main energy carrier in chemical pulp mills and in the pulping process approximately 90 – 95% of the lignin is removed from the wood in pulping and burnt in the recovery boiler.

It was the aim of Wallberg, et al., studies to fractionate a kraft black liquor with a TS content of about 15%(w/w) (36% was lignin) by UF in a pilot-plant unit equipped with single-tube modules. The purity of the final lignin fuel is of importance as the ash content preferably should be as low as possible. This should be done to such an extent that the resulting fuel has levels of inorganic substances low enough to enable it to be burned in any furnace. It was found that the retention of lignin for the three polymeric membranes with cut-offs of 4, 8 and 20 kDa was 80%, 67% and 45%, respectively. Batch and semi-continuous diafiltration modes were carried out with a 8 kDa membrane, the highest lignin concentration achieved during these experiments was 190 gL^{-1} with a final TS content of 22%(w/w) (78% was lignin) for the semi-continuous diafiltration. The average TMP was 560 kPa at the beginning of these experiments and had risen to 640 kPa by the end. However, the initial flux of the kraft black liquor containing 60 gL^{-1} lignin was 100 $Lh^{-1}m^{-2}$ but it ended up with 6 $Lh^{-1}m^{-2}$, which represents a flux decline of 94%, due to the extremely importance of fouling in UF experiments a cleaning method was performed and the initial PWF was recovered by 90-95% with only an alkaline agent (Ultrasil 11 at 0,5%(w/w)). (Wallberg, et al., 2003)

Holmqvist, et al., made a comparison between lignin extraction by UF of black liquors from one mill that employs batch digestion and other that employs continuous digestion. A ceramic membrane with a MWCO of 15 kDa was used. At 90°C and a TMP of 2 bar it was found that the average flux of kraft black liquor was higher in the batch digestion than the continuous digestion, with 160 and 110 $Lh^{-1}m^{-2}$, respectively due to the lower concentration of lignin in this liquor. The retention of lignin was about the same for both liquors, 35%. The optimal volume reduction was found to be 80–90% and the production cost was in the interval 17–26€ per MWh calorific value of the lignin fuel. (Holmqvist, et al., 2005)

The heat value of lignin is known, however, interest in the extraction of lignin for use as an external biofuel and in specialty chemicals is growing. The lignin is a feasible raw material for many valuable substances such as activated carbon, vanillin, vanillic acid, dispersing agents, ion-exchange agents, polymer fillers, binding agents for the production of fibre boards, artificial fertilisers and complexing agents. (Dafinov, et al., 2005)

Black liquor and/or brown liquor from the P&P industry contains hundreds of different compounds and several high-value organic chemicals are formed and extracted during pulping. Black liquor mainly contains lignin and hemicelluloses, vast amounts of hemicelluloses are discharged from pulp mills all over the world as waste, but these could be isolated and utilized in various applications too. There is a considerable interest in integrated forest biorefineries which, besides pulp produce high-value-added products. Several studies were performed by different authors in this context which are presented below.

Jönsson, et al., did several studies to evaluate the fractionation performance of different membranes at different operating conditions, in different modules, of different liquors and achieve a wide range of results. Hardwood black liquor (TS= 17%, Ash = 0,44 g/g, Lignin = 59 gL^{-1} and Hemicelluloses = 6,9 gL^{-1} which about 80% was xylose)) was used to study the separation of lignin and hemicelluloses during UF. The permeate, which contained most of the lignin and only a minor amount of hemicelluloses, was concentrated by NF. UF was performed at 90°C, CFV of 5 ms^{-1} and TMP of 1 bar with a ceramic membrane with a nominal cut-off of 15kDa, and NF at 60°C CFV of 4 ms^{-1} and TMP of 25 bar with a polymeric membrane with a MWCO of 1kDa. Two alternative processes for the extraction of lignin from hardwood black liquor were studied, UF of black liquor withdrawn from the evaporation unit and before the evaporation unit. The production cost was about the same for both alternatives, 33€ per ton of lignin based on a plant processing 200 m^3h^{-1} of pulping liquor at a 90% VR and a NF plant processing the UF permeate at a 70% VR. The concentration of lignin in the product stream was 100 gL^{-1} after UF of evaporated liquor and 165 gL^{-1} after UF and NF of black liquor. The retention of lignin was about 80% during NF, which means that 92% of the lignin in the UF permeate was recovered in the NF retentate. The total yield of lignin was 75% of the original amount of lignin in the BL. (Jönsson, et al., 2008) (Jönsson & Wallberg, 2009) Another example was focused on isolation of hemicelluloses by UF of thermomechanical pulp mill process water where the retention of hemicelluloses and lignin, and the flux and fouling of three UF membranes (ETNA01, ETNA10 and UFX5) were studied at various operating conditions. One of the membranes (UFX5) was found to have a high hemicellulose retention (≥ 90%) independent of flux and pressure. It has the benefit of high temperature tolerance that can process the water at 75–85°C which is the temperature of the pulp mill water. Studies were performed in SWM modules and permeate fluxes between 150 and 200 $Lh^{-1}m^{-2}h$ could be obtained at low hemicellulose concentrations with both the ETNA10 and UFX5 membranes. (Persson & Jönsson, 2010)

Toledano, et al., employed a technique to obtain different liquors from the black liquor, containing lignins with specific molecular weights by UF using ceramic membranes of different cut-offs (5, 10 and 15 kDa) and compared with lignin fractionated by selective precipitation. Lignin by selective precipitation had higher molecular weight and was more contaminated, while ultra-filtrated lignin fractions (5 and 10kDa fractions) could be used for example as adhesives where low molecular weight and purity are important factors to take into account. (Toledano, et al., 2010) (Toledano, et al., 2010)

UF was tested as a form of pretreatment prior to NF to separate hemicelluloses from lignin. Olsson, et al., concludes that it was possible fractionate lignin and hemicellulose from black liquor and that UF as a pre-treatment has advantages compared to NF alone, based on the concentrating study, done at 4 ms^{-1} and 20 bar until a volume reduction of close to 95 % could be reached. At that point a flux of 50 $Lh^{-1}m^{-2}$ was obtained and was compared to a volume reduction of 80 % with a flux of 30 $Lh^{-1}m^{-2}$ when untreated black liquor was used as feed for the NF. Tubular membranes with 20 kDa and 1 kDa were used for UF and NF, respectively. The concentration of lignin at the end of the concentrating study was a bit lower (210 mg/g when UF was used as a pre-treatment compared to 230 mg/g when untreated black liquor was used as feed) when permeate from UF was used but this is in minor importance since the higher flux leads to greater advantages (increase 100% of the initial NF permeate flux, from 200 to 400 $Lh^{-1}m^{-2}$). (Olsson, 2013) However, in a posterior study by Arkell, et al., the preliminary economic estimation indicated that the MPF-36 (NF polymeric membrane 1kDa) membrane without pretreatment by UF was the most cost-efficient alternative, where the produced liquor with a lignin concentration of 230 gL^{-1} had a cost of 46€ per ton of lignin. The cost of lignin when using the ceramic UF membrane as pre-treatment was about 50% higher but this process configuration could be interesting if a lignin fraction free from high molecular weight hemicelluloses is required or if the hemicellulose rich retentate, obtained from UF, can be utilized elsewhere. (Arkell, et al., 2014)

Lignosulphonates and fermentable sugars are the main components of spent sulphite liquors (SSL) produced in acid sulphite pulping. Some authors focused their attention on fractionate and concentrate these streams for a posterior biorefinery point of view. One example presented by Restolho, et al., which applied UF, NF and RO to filter a hardwood (Eucalyptus globulus) SSL (TS ≈ 170 gL^{-1}, lignosulphonates ≈ 85 gL^{-1}, total sugars ≈ 57 gL^{-1}, pH ≈ 3,5) in order to separate the lignosulphonates from the sugars for subsequent fermentation, fractionate the lignosulphonates to produce valuable products, and concentrate the sugars. More than 15 membranes were characterized and tested in the study, where most of them could not separate the lignosulphonates from the sugars due to the overlap of the molecular weights of both. Microdyn-Nadir UP010 (UF membrane with a MWCO of 10 kDa) membrane displayed the widest gap between the retentions of lignosulphonates (68%) and total sugars (3%). Many NF/RO membranes presented high retentions for the total sugars contained in SSL (>95%) where Alfa Laval RO99 seemed the most suitable to concentrate the sugars (xylose retention over 93%, where the xylose was the main sugar). Unfortunately, the studies were carried out only in total recirculation mode and 25°C, which not allows to conclude anything about technical and economical feasibility of the process. (Restolho, et al., 2009) Another industrial SSL from acid sulphite pulping of Eucalyptus globulus TS ≈ 7%, lignosulphonates ≈ 41 gL^{-1}, total sugars ≈ 23 gL^{-1}, pH ≈ 3,3) too, were studied for the same purpose by Fernández-Rodríguez, et al., this time with ceramic membranes with MWCO of 15, 5 and 1 kDa. The combination of these membranes in four series systems was proposed, where a system formed by 15 kDa and 5 kDa membranes in series offered the lowest sugar rejection (10,57%) while a system constituted by 15 kDa, 5 kDa and 1 kDa membranes in series achieved the highest LS rejection of 71,70%. The 5 kDa membrane was the bottleneck of the process in both cases, but the pre-filtration with the 15 kDa membrane improve the permeate flux of the 5 kDa from 6 to around 10 $Lh^{-1}m^{-2}$. (Fernández-Rodríguez, et al., 2015)

Some other authors focused their studies in minor components which are not yet applicable at industrial levels. Separation and purification of monocarboxylic and dicarboxylic acids by combining membrane filtration, acid precipitation, and crystallization processes where performed by (Niemi, et al., 2011), while (Hellstén, et al., 2013) studied a process which consists of UF to remove most of lignin, size-exclusion chromatography to separate hydroxy acids and NaOH, ion-exchange to convert the sodium salts of acids to protonated form, adsorption to remove residual lignin, and evaporation to concentrate the product fractions and to remove volatile acids.

3.3. Fouling and cleaning

Severe flux decline was observed and evaluated by different authors during membrane filtration of several P&P mill effluents.

Dal-Cin et. al., used a series resistance model based on pure water fluxes, to quantify the relative contributions of adsorption, pore plugging and concentration polarization to flux decline when a waste stream of the plug screw feeder pressate from a semi chemical mechanical pulp digester (pH = 5,7; TS = 14,3 gL^{-1}; TOC = 5,7 gL^{-1}; Sugars = 2,7 gL^{-1}; Lignin = 4,3 gL^{-1}) was submitted to UF. It was found that the selection of an appropriate membrane material would minimize adsorptive fouling while pore plugging is controlled by using membranes with a suitable MWCO. The wide range of molecular-weight materials in this type of effluents requires careful selection of the pore size and operating pressure because pore plugging phenomenon may become more important over high operating times or higher TMP's, resulting in unforeseen flux decline. It was found too that the adsorptive fouling was responsible for a loss of 60-80% of PWF in polyacrylonitrile, polysulfone and polyethersulfone membranes, while regenerated cellulose and thin film composite membranes exhibited very low adsorptive fouling. (Dal-Cin, et al., 1996) Another study which is in accordance that the fouling of hydrophilic membranes made of regenerated cellulose was less severe than the fouling of hydrophobic membranes made of polyethersulphone and a composite fluoropolymer in P&P mill effluents were performed by Persson & Jönsson with a wastewater from a Masonite (type of hardboard formed by pressing a board of long cellulose fibers at elevated temperature) mill. It was already found that a decrease in the pH of the feed solution will lead to an increase of the flux in regenerated cellulose membrane (UC005) but leads to a decrease in a composite fluoropolymer membrane (ETNA10). Activated carbon is known to adsorb both organic molecules, such as phenolic compounds, and various inorganic ions and by pretreatment of the wastewater with activated carbon the permeate flux increased in both type of membranes, although it would be very costly to use this method in larger scale due to the high price of activated carbon (2000 €/m^3). (Persson & Jönsson, 2009)

Wallberg, et al., performed a study to evaluate the cleaning of the hardwood line at the UF plant of the Nymölla paper mill (presented before in section 3.1.1.). The purpose was to find out what the fouling layer consists of and choose the most appropriate cleaning procedure. It was found that the fouling was mainly organic origin and was seen as brown precipitation on the surface of the membranes. Production data showed that the membranes were often cleaned when there was no decline in flux. The cleaning procedure used in the mill was a combination of Berocell 537 (0,25% vol.) and Ultrasil 96 (0,5% vol.), where it was found that using only Ultrasil 96 resulted in the same PWF as the two chemical system. (Wallberg, et al., 2001)

Chen, et al., used different characterization methods, such as scanning electron microscopy, energy-dispersive spectrophotometry, attenuated total reflection-fourier transform infrared spectroscopy and gas chromatography-mass spectrometry to evaluate the membrane foulants from the UF of a super-clear filtrate obtained from a fine paper mill, purified with a polyethersulfone (PES) with a MWCO of 10 kDa membrane. It was found that the reversible foulants during UF accounted for 85,52% of the total foulants, while the irreversible adsorptive foulants (which play a pivotal role in limiting UF technology application) accounted for 14,48% and mostly came from sizing agents, coating chemicals, and others. (Chen, et al., 2015)

3.4. Molar mass of solutes in pulp mill streams

Size-exclusion chromatography (SEC) has been commonly used for the characterization of organic macromolecules such as lignin, and hemicelluloses.

To characterize different types of hemicelluloses, delignified wood and chemical pulps were extracted with dimethyl sulfoxide or alkaline aqueous solutions (on industrial scale is what happens in some bleaching stages). Jacobs & Dahlman employed SEC to characterize the molar masses of hemicelluloses extracted from wood and from chemical pulps. As expected, in most cases the hemicelluloses extracted from wood exhibited higher molar masses than did the corresponding hemicelluloses from chemical pulps. The results also demonstrated that the molar mass of hemicelluloses extracted from kraft pulp were higher than from sulphite pulp, one example is the average molar mass of the hemicelluloses in a non-bleached hardwood magnesium-based sulphite pulp is 6 kDa against 11,6 kDa of the same non-bleached hardwood but in a kraft pulp. It should be also noted that the non-bleached hardwood magnesium-based sulphite pulp presented the relative carbohydrate composition (%w), 84%, 13% and 3% for glucose, xylose and mannose, respectively. (Jacobs & Dahlman, 2001)

Kukkola, et al., used SEC and an UV detector to analyze molecular weights and lignin contents of ECF and TCF bleaching liquors from a laboratory prepared softwood kraft pulp. Determinations of the molecular weight distribution showed that effluents from TCF sequence contained more high-molecular weight material than those from the ECF stage, due to peroxide stages that probably dissolve high-molecular weight lignin effectively. It was found too that molecular weights of ozone stages and chlorine dioxide stages were very low compared to other stages. Values for weight average molecular weights vary from 2,8 to 8 kDa for an ECF effluent, depending on the withdrawn stage, and between 1,2 to 14,3 kDa for a TCF effluent, depending too on the withdrawn stage. (Kukkola, et al., 2011)

4. Materials and methods

4.1. Bleaching plant effluent

The BPE used in this investigation was supplied by the *Caima - Indústria de Celulose, S.A*. pulp mill based in Constância, Portugal. *Caima - Indústria de Celulose, S.A.* has an annual capacity around 125,000 tonnes of bleached TCF hardwood (*eucalyptus globulus*) dissolving sulphite pulp. This mill operates the bleaching sequence E-O-P, where the first step (E) is an extraction stage using sodium hydroxide (NaOH) to continue delignification and to extract hemicelluloses remaining after the cooking. Between the bleaching steps, wash presses are inserted that remove the consumed chemicals and the dissolved reaction products originating from the pulp. This BPE was obtained after this E-stage as shown previous in Figure 1, section 1.1. The first physical and chemical characterization is presented in Table 4.

Table 4 - Some characteristics of the BPE used in this investigation

pH	9,87
ρ (g/L)	1042
TSS (mg/g)	0,44
TS (mg/g)	28,83
Ash (mg/g)	14,23
Total lignin (g/L)	2,88
Acid soluble lignin (mg/g)	1,31
Klason lignin (mg/g)	1,05
Hemicelluloses (mg/g)	0,19
Arabinose (mg/g)	0,00
Galactose (mg/g)	0,00
Glucose (mg/g)	0,03
Mannose (mg/g)	0,03
Xylose (mg/g)	0,13
Others (mg/g)	11,52

4.2. Membranes

4.2.1. Membrane selection by SEC analysis

Molecular mass distribution of hemicelluloses and lignin from the BPE supplied by *Caima - Indústria de Celulose, S.A.* was determined by size exclusion chromatography (SEC), in order to evaluate the order of magnitude of the size of these macromolecules so that it was possible to choose some membranes, based on their manufacturer molecular weight cut-off (MWCO) that were potentially suitable to retain these compounds.

4.2.2. Tested membranes

The performance of six alkali resistant membranes was investigated in a parametric study. Two tight UF flat-sheet polymeric membranes and four NF flat-sheet polymeric membranes. The characteristics of the membranes are given in Table 5.

Table 5 - Data for the polymeric membranes tested in the experiments

Membrane	**Process**	**Material**	**MWCO (kDa)**	**Operating conditions**		
				pH$_{max}$	**TMP$_{max}$ (bar)**	**T$_{max}$ (°C)**
ALFA-LAVAL - ETNA01PP	UF	Composite fluoro polymer	1	11	10	60
ALFA-LAVAL - GR95PP		Polyethersulfone	2	13	10	75
ALFA-LAVAL - NF99HF	NF	Polyamide type thin film composite on polyester	$MgSO_4$ rejection ≥ 98%	10	55	50
KOCH - MPF36		Composite	1	13	35	70
NADIR - NP010		Polyethersulfone	1 – 1,4	14	40	95
NADIR - NP030		Polyethersulfone	0,5 – 0,7	14	40	95

Sources: (Alfa Laval, s.d.), (Koch Membrane Systems, Inc., 2014), (Microdyn-Nadir, 2007), (Arkell, et al., 2013)

4.3. Equipment

Two types of experiments were performed in different modules configurations. However, most of the used equipment was the same in both studies.

The TMP in both studies, was calculated in the same way, following the equation (1).

Since there was no valve on the permeate side of the membranes, it was assumed that it is atmospheric pressure at the permeate side (P_p). The frictional pressure drop (ΔP) was calculated as the difference between the inlet (P_{in}) and outlet pressure (P_{out}).

4.3.1. Parametric studies

The main components of the laboratory equipment used in the experiments were two heat controlled tanks, the feed tank with a capacity of 15 liters and the water tank with a capacity of 5 liters. Two Pt-100 temperature sensors (Pentronic, Gunnebo, Sweden) were immersed in the feed and in the water tank, both connected to temperature regulators (Shinko MCM, Shinko Europe BV, Haarsteeg, the Netherlands) controlling the temperature in the tanks by electrical heaters. A displacement pump (Hydra-cell D25XL, Wanner, Minneapolis, MN, USA) connected to a frequency converter (ELEX 4000, Bergkvist & Co., AB, Gothenburg, Sweden) controlling the CFV. The pressure was regulated by a manual valve on the retentate line, with two pressure transmitters (Trafag DCS40.0AR, Regal Components AB, Uppsala, Sweden) placed at the inlet and the outlet. The permeate flows were measured with electronic balances (PL6001-S, Mettler-Toledo Inc., Columbus, OH, USA). Three stainless steel test sieves in series with 250µm, 180µm and 45µm pores respectively (Endecotts, London, England) were used to pre-filtrate the feed solution.

In this parametric studies four flat-sheet membrane modules were connected in parallel, as shown in Figure 9.

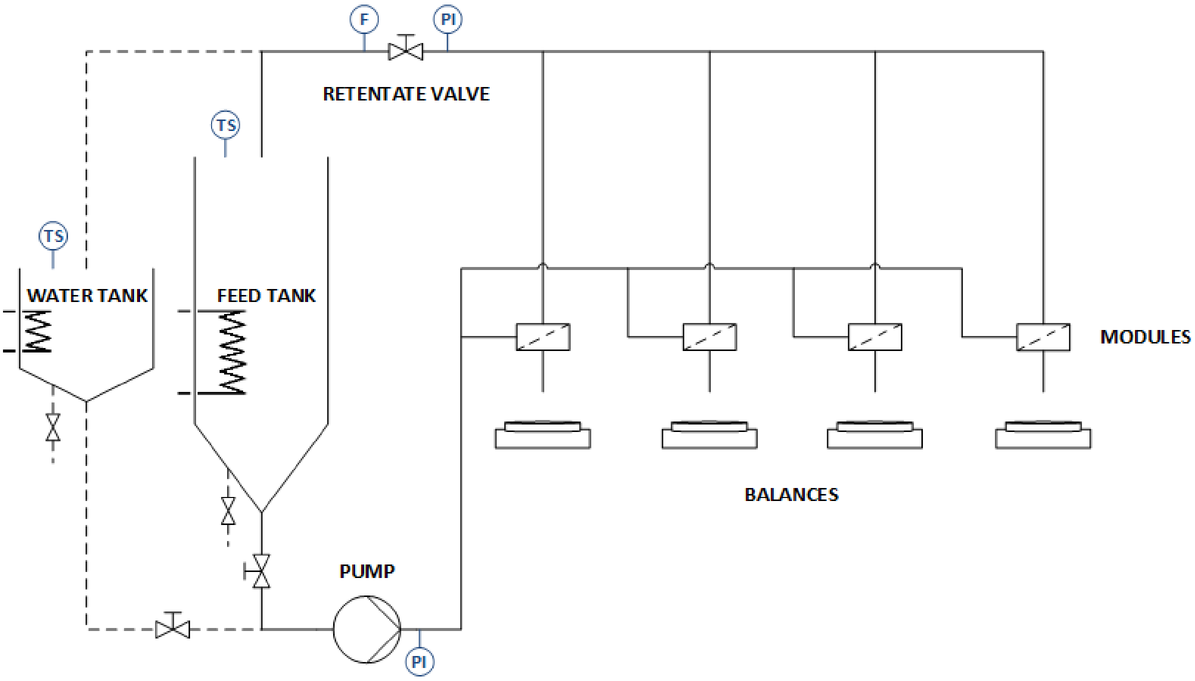

Figure 9 - Flow sheet of the equipment used in the flat-sheet membrane for parametric studies experiments. F = flowmeter, PI = pressure indicator, TS = temperature sensor

Only three of four modules connected in parallel were used simultaneously with different flat-sheet membranes. Each module was equipped with a circular flat membrane with an area of 0,00196 m^2.

4.3.2. Concentration studies

During concentration studies all the equipment aforementioned was used, with the change of the four flat-sheet membrane modules in parallel for one DDS LabStak® M20, as shown in Figure 10. This module was equipped with two double-sided membrane discs with a total membrane area of 0,072 m^2. Instead of one feed thank with 15 liters capacity, one feed tank with 200 liters was used and the temperature was controlled by a steam coil. The 15 liters capacity tank was used as water tank, and the 5 liters water tank was removed.

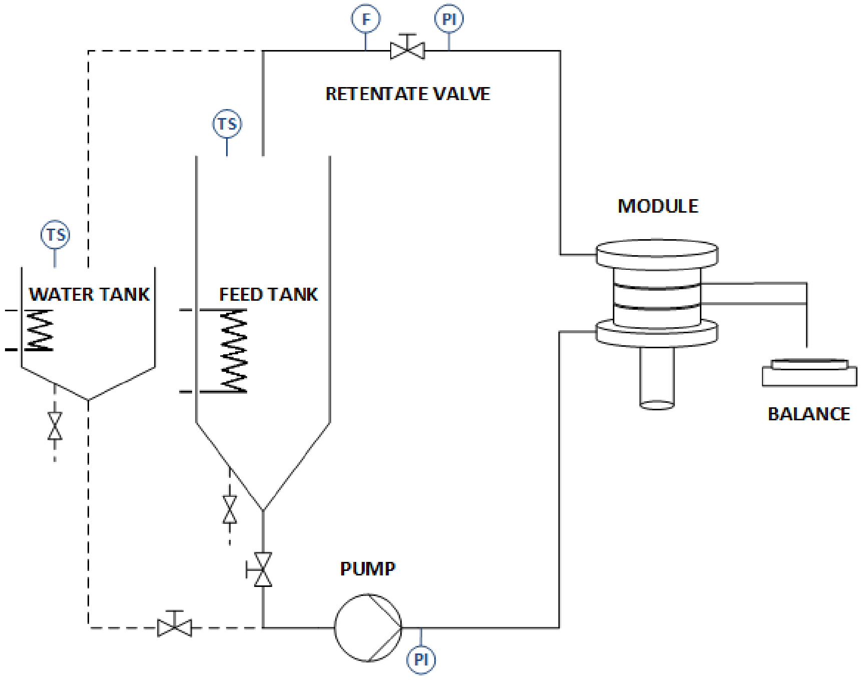

Figure 10 - Flow sheet of the equipment used in the flat-sheet membrane for concentration studies experiments. F = flowmeter, PI = pressure indicator, TS = temperature sensor

In both studies, parametric and concentration, all balances, pressure indicators, temperature sensors and flowmeters were connected to a computer and all the data were recorded using the *LabVIEW® 2009* software (National Instruments Co, Austin, TX, USA).

4.4. Operating procedure

4.4.1. Initial cleaning and PWF of new membranes

The membranes were cleaned with the alkaline cleaning agent Ultrasil 10 (Ecolab AB, Älvsjö, Sweden) for 1 hour at the concentration of 0,5 wt%, the temperature of 50°C, a TMP of 3 bar and a CFV of 0,5 ms^{-1} before the experiments were performed. After this was the system rinsed several times with deionized water. Then the pure water flux (PWF) for the new membranes (J_{wi}) was measured at 30°C and a CFV of 0,3 ms^{-1}, with the TMP range from 2 to 10 bar with a step size of 2. Flux was measured for 5 minutes at each pressure.

4.4.2. Parametric studies

In order to investigate the influence of operating parameters on flux and retention levels, parametric studies were performed in which the CFV and TMP were varied. During the parametric studies, both the retentate and permeate were recycled to the feed tank in order to keep the concentration constant.

Only three membranes could be used simultaneously and there were six membranes to test, then were split in two series. So the first three membranes selected were the MPF36, NP010 and GR95PP. Experiments were performed at maximum temperature of the polymeric membranes, which means that the temperature was 70°C for these first three membranes, where the MPF36 had the lowest value of T_{max} between the first three choices, see Table 5.

For the other three membranes, NP030, NF99HF and ETNA01PP the parametric studies were performed at 50°C, which was the limiting temperature for the NF99HF, see Table 5.

The tested CFVs were 0,4 and 0,8 ms^{-1} during the experiments. To minimize the risk of cake formation at the membrane surface, each experimental series was begun at the highest CFV and lowest TMP. The TMP was increased step-wise to the highest value and permeate samples were taken for each TMP. The TMP was then decreased to the lowest possible value and waited up to half an hour to remove the formed filter cake. After this, the CFV was reduced and then the TMP was increased step-wise again at the new velocity. Measurements were carried out for 15 minutes at each set of experimental conditions.

4.4.3. Concentration studies

The MPF36 and NF99HF membranes were found to be the most suitable in the parametric studies, but only NF99HF was used in the concentration studies due to its higher fluxes, higher retentions and better cleaning performance.

During the concentration studies, two double-sided membrane discs from DDS LabStak® M20 module were stacked by four NF99HF flat-sheet membranes and support paper. Both retentate and permeate were initially recycled to the feed tank, initially charged with approximately 67 liters of sieving BPE. The CFV was set to 0,8 ms^{-1}, and the temperature used was 50°C, that was the maximum operation temperature recommended by the manufacturer and the temperature used on the parametric studies for the selected membrane. Then the TMP was gradually increased to the final operating pressure of 13 bar. The concentration was then increased by withdrawal of permeate while recirculating the retentate. The experiment was interrupted at a volume reduction (VR) of 68%, corresponding to a volume reduction factor (VRF) of 3,125. VR is defined as the ratio between the volume of the permeate (V_p) and the initial volume of the feed (V_0), equation (6). VRF is the ratio between the initial feed volume and the volume of the resulting retentate. VRF and VR are correlated by equation (7).

Samples were taken for the retentate and permeate side with a VR step-size of 0,1 for further analysis.

4.4.4. Membrane regeneration

After each experimental series, in both parametric and concentration experiments, the PWF of fouled membranes (J_{w^*}) was measured, to evaluate the membrane fouling after the experiments. After that the membranes were chemical cleaned as described in section 4.4.1, and the PWF of the regenerated membranes (J_w) was measured again. Both PWFs, for fouled and regenerated membranes, were conducted at 30°C and a CFV of 0,3 ms^{-1} with the TMP range from 2 to 10 bar with a step size of 2. Flux was measured for 5 minutes at each pressure.

4.5. Analysis

4.5.1. Total solids, ash and total suspended solids

Total solids (TS) content was determined by taking 10 ml (5 ml in some cases) of each sample to dry in weighed porcelain crucibles in an oven at 105 °C for 24 h. After this were the porcelain crucibles putted in a desiccator for 30 min before weighed once again.

The dried samples were then put in an oven where they were first heated up to 250°C and maintained this temperature for 30 min and then to 575 °C for 180 min. After this, the samples were cooled down to 200°C in the oven with the door ajar before being placed in a desiccator to cool for another 30 min and then weighed. The weigh difference was the ash content.

For the measurements of Total suspended solids (TSS), 10 ml samples were filtrated through a pre-weighed glass microfiber filter Whatman Grade GF/B with 1,0 µm pores size. Filters with matter were dried in an oven at 105 °C for 24 h. After this were the filters putted in a desiccator for 30 min before weighed once again.

4.5.2. Total lignin

The concentration of lignin was determined by measuring the UV absorbance at a wavelength of 280 nm in a spectrophotometer (UV-160, Shimadzu Corp., Kyoto, Japan). To measure the total lignin content of the samples were they first diluted with deionized water. The extinction coefficient of 24,3 l/g cm was used. (Kukkola, et al., 2011) It should be noted that besides lignin, pectin degradation products have strong UV absorbance at 280 nm. (Arkell, et al., 2013) Thus, the presence of these substances could lead to an overestimation of the lignin concentration.

4.5.3. Acid hydrolysis, acid-insoluble (Klason), acid-soluble lignin and hemicelluloses

In order to measure the content of sugar in the samples and the share of acid-insoluble and acid-soluble lignin, the samples were subjected to acid hydrolysis. The acid hydrolysis was performed by adding 1,5 ml (0,75 ml in some feed samples) of 72% sulphuric acid to 10 ml of the permeates samples (20 ml in the feed samples). The hydrolysis was then performed in an autoclave for around two hours.

Filter crucibles were taken from the oven at 105 °C and put in a desiccator for 30 min before it was weighed. Then is the fluid from acid hydrolysis vacuum filtered through the filter crucible. The filtrate is put in a container before some deionized water is used to rinse the hydrolysis bottle to get the lignin stock in it. This fluid is then vacuum filtered through the filter crucible. Next is the filter crucibles dried in an oven at 105 °C for 24 h and after being in a desiccator for 30 min is they weighed. The weigh difference was the content of Klason lignin.

The fluid from the vacuum filtration is used for the analysis for acid-soluble lignin. The content of acid-soluble lignin is measured by the UV absorbance at a wavelength of 320 nm of the fluid in a spectrophotometer (UV-160, Shimadzu Corp., Kyoto, Japan). The extinction coefficient of 15,0 l/g cm was used. (National Institute of Standards & Technology, 2014)

The filtrate from the acid hydrolysis was also used to determine the sugar content in the samples. Before the analysis, the samples were filtrated through a 0,20 µm syringe filter. The samples were analyzed by high-performance liquid chromatography coupled with pulsed amperometric detection (HPLC-PAD) in order to find the concentration of monomeric sugars in the samples. The chromatography system (ICS-3000, Dionex Corp., Sunnyvale, CA) was equipped with a Carbo Pac PA1 analytical column (Dionex Corp.). The used eluent was deionized water at a flow rate of 1 ml/min and a solution of 200 mM NaOH dissolved in 170 mM sodium acetate was used to clean the column. The volume of the sample injection was 10 µl. The sum of the monomeric sugars after anhydro corrections of 0,88 and 0,90 for pentoses and hexoses, respectively, was used to define the concentration of hemicelluloses.

4.5.4. Total carbon, organic carbon and inorganic carbon

For determination of the total organic carbon (TOC) content of the samples, a TOC-5050A analyzer (Shimadzu Corp., Kyoto, Japan), consisting of an ASI-5000A autosampler (Shimadzu), a combustion tube, a reaction vessel and a non-dispersive infrared gas (NDIR) detector was used. The total carbon (TC) content and the inorganic carbon (IC) content were measured in the system and the TOC content determined by subtracting the IC content from the TC content.

The temperature in the combustion tube during TC measurement was 680°C and high-purity air was used as carrier gas, passing through the system at a constant flow of 150 ml/min. The sample volume injected into the combustion tube was 32 µl. Standard solutions of potassium hydrogen phthalate in deionized water at concentrations of 500, 250, 125, and 50 mg C/l were used for calibration. During IC measurement, the carrier gas was flowing in form of tiny bubbles through the reaction vessel, filled with water acidified with IC reagent (phosphoric acid). A sample volume of 40 µl was injected into the reaction vessel. Standard solutions of sodium hydrogen carbonate and sodium carbonate in deionized water at concentrations of 500, 250, 125, and 50 mg C/l were used for calibration.

4.5.5. Molecular mass distribution of hemicelluloses and lignin

The molecular mass distribution of hemicelluloses and lignin was determined by SEC using a Waters 600E chromatography system (Waters, Milford, MA, USA) equipped with a refractive index detector (model 2414, Waters) and an ultraviolet detector operating at 280 nm (486, Waters). The analytical column was packed with 30 cm Superdex 30 and 30 cm Superdex 200 (GE Healthcare, Uppsala, Sweden). A 125 mM NaOH solution was used as eluent at a flow rate of 1 ml/ min. The system was calibrated with polyethylene glycol (PEG) standards with peak molecular masses of 0,4, 4, 10 and 35 kDa (Merck Schuchardt OHG, Hohenbrunn, Germany). Both the feed and the permeate samples were filtrated through a 0,20 µm syringe filter before the analysis.

5. Results and discussion

5.1. Size exclusion chromatography of the BPE

Molecular mass distribution of hemicelluloses and lignin was measured by SEC, described in section 4.5.5. The SEC diagram of the untreated BPE, as shown in Figure 11, shows that lignin and hemicelluloses in the BPE have low and similar molecular masses, which makes the separation between these two components almost impossible.

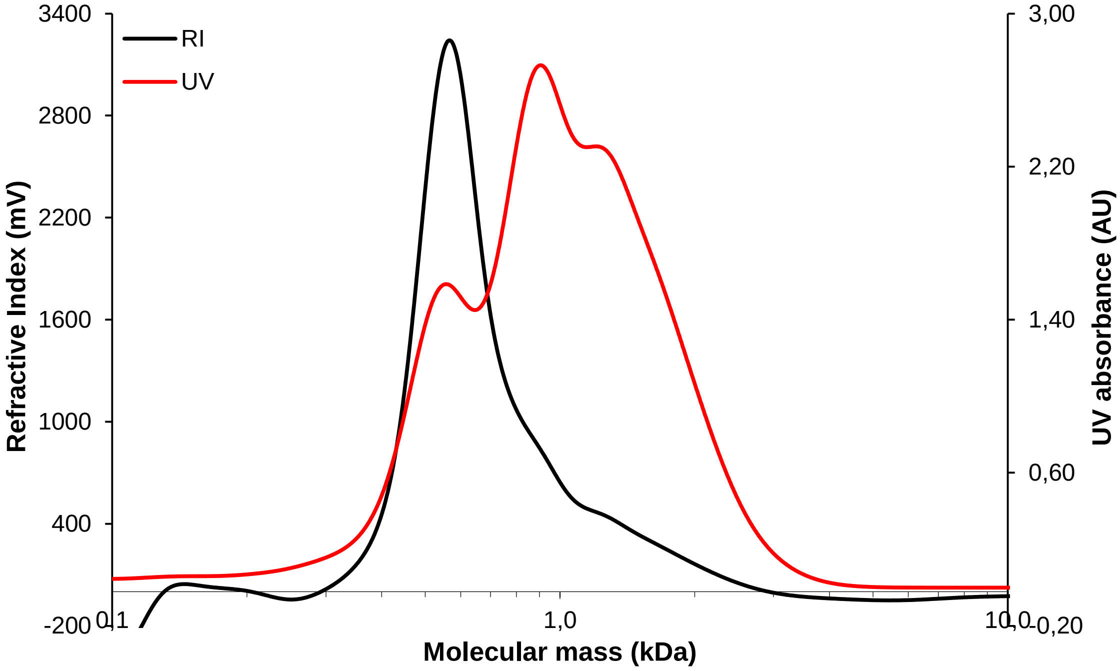

Figure 11 - Molecular mass distribution of lignin (measured as UV absorbance at 280 nm) and hemicelluloses (measured as refractive index) of untreated BPE.

Since it seems impossible to separate the hemicelluloses and the lignin presents in the BPE, the aim changes to concentrate the BPE by membrane filtration. Thus, mass average molecular masses ($\bar{M}_w$) were calculated, by Equation (21) in order to facilitate the choice of the membranes that would be tested.

$$\bar{M}_w = \frac{\sum_i N_i M_i^2}{\sum_i N_i M_i} \tag{21}$$

Where N_i is the value of refractive index or UV absorbance for hemicelluloses and lignin respectively of molecular mass M_i. The mass average molecular masses are found in Table 6.

Table 6 - Mass average molecular mass of lignin and hemicelluloses of untreated BPE.

	Hemicelluloses by RI	**Lignin by UV**
Highest peak (kDa)	0,57	0,91
$\overline{M}_w$ (kDa)	0,88	1,32

Based on the values obtained, was chosen to test some tight UF membranes (MWCO ≤ 2 kDa) and NF membranes (MWCO ≤ 1 kDa), already mentioned in the Table 5.

5.2. Hydraulic permeability of the membranes

After being cleaned and rinsed several times, it was determined the hydraulic permeability with deionized water for all membranes. This determination is important because it serves as a reference to evaluate the fouling and cleaning performance after the experiments. Initial cleaning and PWF measurement technique was described in section 4.4.1. The influence of the TMP applied in the pure water flux (J_{wi}) for each new membrane tested is shown in Figure 12.

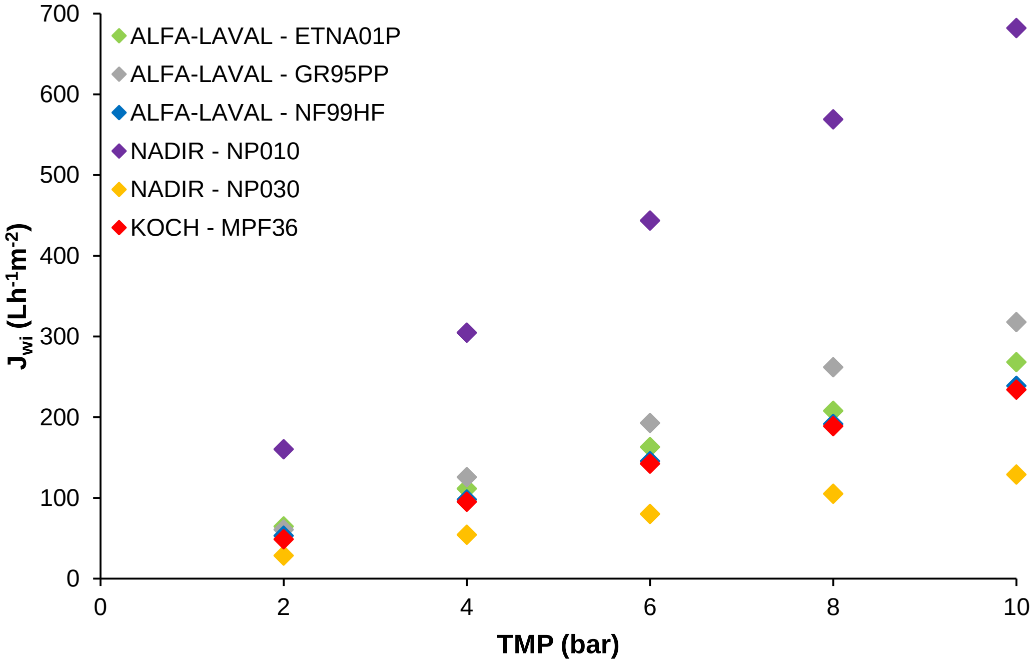

Figure 12 - Pure water fluxes (J_{wi}) in function of TMP for the new membranes tested (before 1st usage).
T = 30°C, CFV = 0,3 ms^{-1}

Hydraulic permeability (L_p) is the line slope of pure water flux (J_{wi}) as a function of TMP applied.

$$J_{wi} = L_p \times TMP \tag{22}$$

Since different temperatures were used along this work, to be able to discuss the results, all the permeability values were adjusted to a standard temperature of 25°C. The correlation (23) used takes into account the pure water viscosity changes with temperature, which influences the flux and consequently the hydraulic permeability.

$$L_{p\ 25°C} = \left(\frac{L_p}{0{,}901}\right) e^{\left(-6{,}96+\frac{2044}{273{,}15+T}\right)} \tag{23}$$

Where L_p is the hydraulic permeability at the temperature T in °C. Values for the hydraulic permeability for each tested membrane at corrected temperature are shown in Table 7.

Table 7 - Hydraulic permeability (L_p) of the membranes tested (1st usage).

Membrane	**Linear regression**	L_p **(Lh^{-1}m^{-2}bar^{-1})**	$L_{p\ 25°C}$ **(Lh^{-1}m^{-2}bar^{-1})**
ETNA01P	$J_{wi} = 26{,}80 \times \text{TMP}$ $R^2 = 0{,}992$	26,8	23,9
GR95PP	$J_{wi} = 32{,}07 \times \text{TMP}$ $R^2 = 0{,}999$	32,1	28,6
NF99HF	$J_{wi} = 24{,}07 \times \text{TMP}$ $R^2 = 0{,}998$	24,1	21,5
NP010	$J_{wi} = 70{,}77 \times \text{TMP}$ $R^2 = 0{,}989$	70,8	63,2
NP030	$J_{wi} = 13{,}13 \times \text{TMP}$ $R^2 = 0{,}997$	13,1	11,7
MPF36	$J_{wi} = 23{,}57 \times \text{TMP}$ $R^2 = 1{,}00$	23,6	21,1

Since we are talking only about PWFs, we are in absence of fouling and able to take some simple modeling. When the structure of the membrane can be assumed to be uniform capillaries the appropriate approach is to use the Hagen-Poiseuille equation.

$$J_{wi} = \frac{\varepsilon \times d_{pore}^2}{32 \times \mu_w \times \tau} \times \frac{TMP}{l_{pore}} \tag{24}$$

Where ε is porosity, μ_w is dynamic viscosity of the water, l_{pore} is the thickness of the porous layer, τ is the tortuosity of the capillaries and d_{pore} is the diameter of the capillaries.

Combining equations (22) and (24),

$$L_p = \frac{\varepsilon \times d_{pore}^2}{32 \times \mu_w \times \tau \times l_{pore}} \tag{25}$$

The hydraulic permeability, L_p, of the NP030 membrane was expected to be one of the lowest face to their low manufacturer MWCO (low d_{pore}), aforementioned in Table 5. With tighter pores, the passage of water through the membrane is made more difficult, decreasing their L_p.

It should also be mentioned that the NF99HF membrane, despite being one of the tightest membranes, features a considerable L_p. This is due to being a very thin membrane (low l_{pore}), which also has some influence in the PWF thru the membrane.

The least expected value occurs in the NP010 membrane. Since the material is the same of the GR95PP, their thickness is not so different from the other ones (except NF99HF) and their manufacturer MWCO was not the highest, it was not expected that it will get the highest (by far) hydraulic permeability value. However, it can be justified by “non visible” parameters, such as the porosity (ε) and tortuosity of the capillaries (τ), shown in equation (25).

5.3. Parametric studies

5.3.1. Permeate fluxes vs TMP with BPE

Parametric tests are performed in a closed loop and are aimed to determine the CFV and the TMP which provides greater flux and selectivity. The parametric studies technique was described in section 4.4.2. The influence of the TMP applied in the permeate flux (J_v) at different CFVs for each membrane tested are shown in Figure 13 and Figure 14.

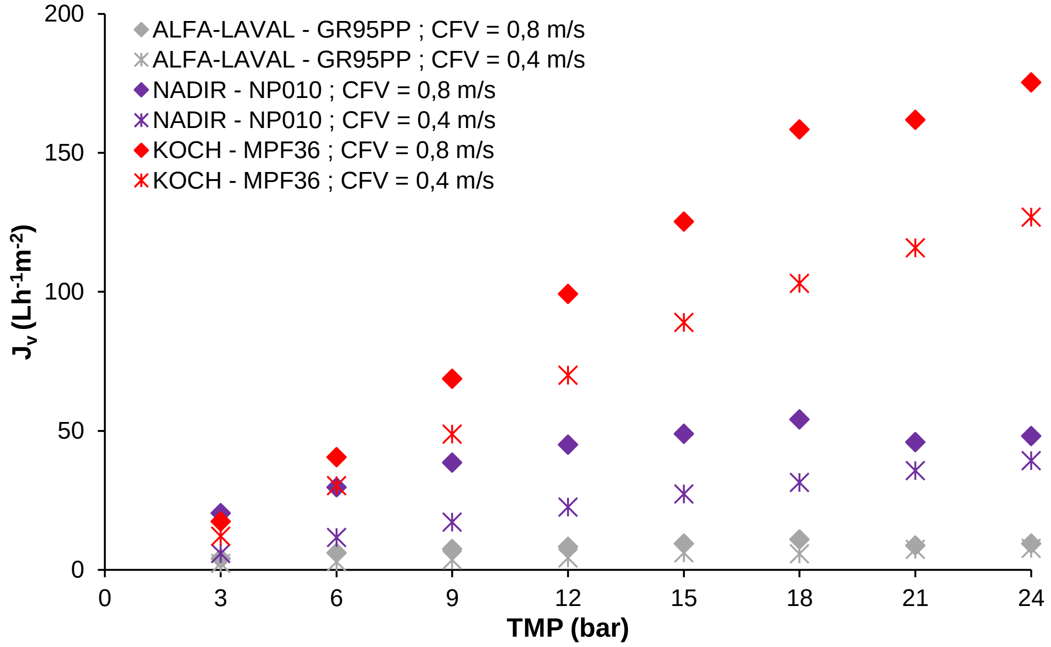

Figure 13 - Influence of the TMP and CFV on the permeate fluxes (J_v) for the first membrane series. T = 70°C

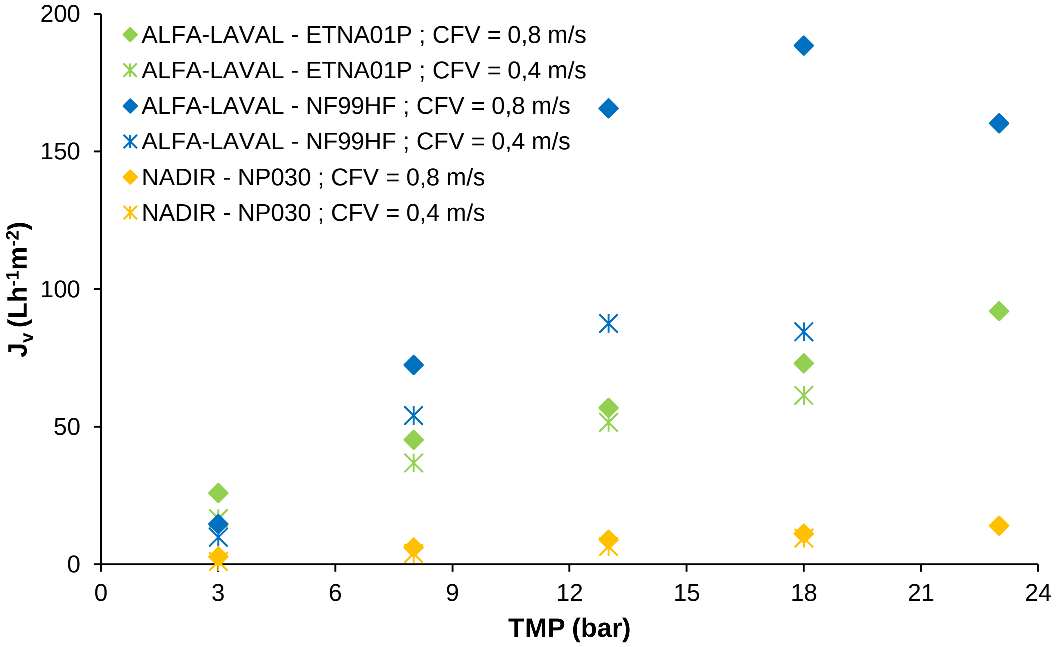

Figure 14 - Influence of the TMP and CFV on the permeate fluxes (J_v) for the second membrane series. T = 50°C

The figures above allows us to conclude that at the higher CFV tested, 0,8 ms^{-1}, lead consistently a higher permeate flux. Thus, all the values presented hereafter are related to this CFV.

For some membranes, at higher pressures the permeate flux (J_v) is no longer significantly affected by the TMP, it levels off to almost constant values. This constant flux is called "limiting flux" and is independent of membrane resistance. For other membranes, we had more than one linear region till we got the "limiting flux", but we will only consider the first one.

5.3.2. Lignin retention

The performance of a membrane filtration process is usually assessed in terms of the magnitude of the permeate flux and the separation performance of the membrane. The ability of the process to separate components from each other can be assessed by comparing the retention of the individual components. In membrane processes the apparent retention (R_{obs}) was given by equation (4).

Assuming as main goal the retention of total lignin ($R_{total\ lignin}$), Figure 15 and Figure 16 presents the different retentions for all the membranes tested at different conditions. Measure of total lignin technique was described in 4.5.2.

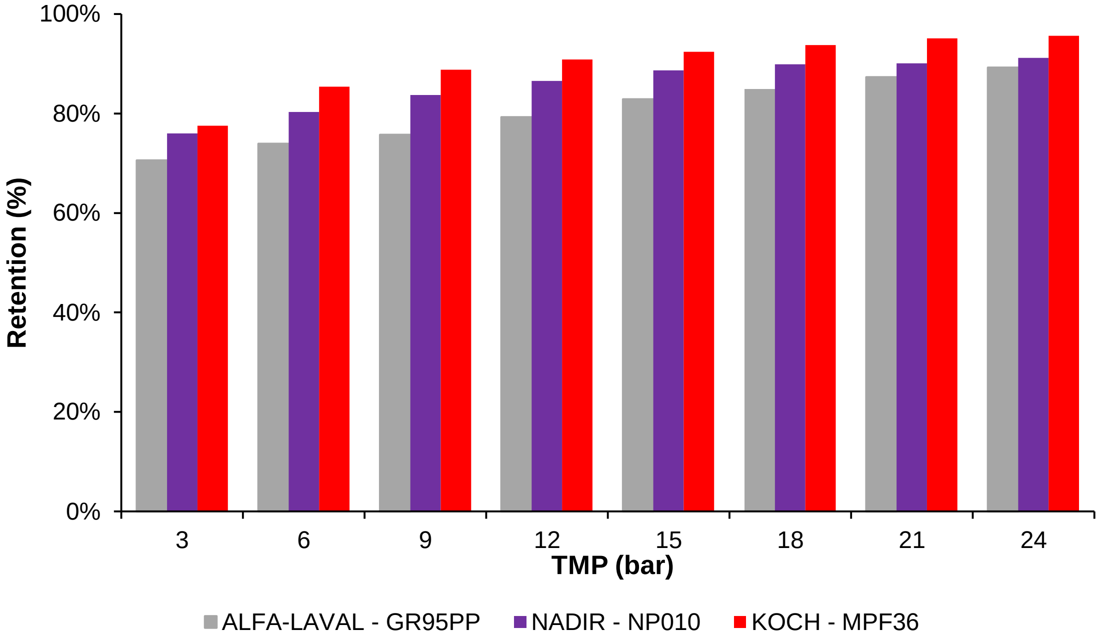

Figure 15 - Influence of the TMP on total lignin retention for the 1st membrane series tested in the parametric studies. T = 70°C, CFV = 0,8 ms-1

The increase of the TMP leads constantly with the increase of $R_{total\ lignin}$ on every membranes tested. This can be due to the concentration polarization phenomenon which explains the increase of solutes content near to the membrane surface, thus creating an additional resistance to lignin macromolecules permeation.

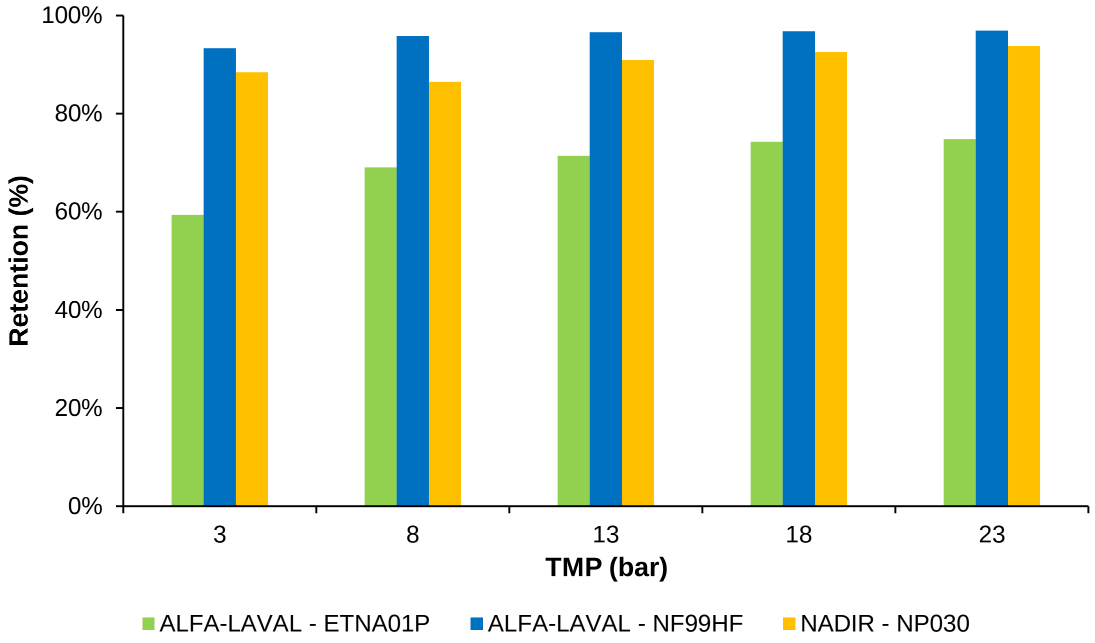

Figure 16 - Influence of the TMP on total lignin retention for the 2^{nd} membrane series tested in the parametric studies. T = 50°C, CFV = 0,8 ms^{-1}

To conclude, Table 8 has been added with values for the chosen optimal conditions, within their linear regions, for each membrane tested. Where the MPF36 and NF99HF membranes were found to be the most suitable in these parametric studies, due to their higher permeate fluxes and total lignin retentions.

Table 8 - Permeate flux (J_v) and total lignin retention ($R_{total\ lignin}$) at the maximum TMP within the linear region, for membranes tested at CFV = 0,8 ms^{-1}.

Membrane	**GR95PP**	**NP010**	**MPF36**	**ETNA01P**	**NF99HF**	**NP030**
Temperature		70°C			50°C	
TMP_{max} (bar)	9	9	15	8	13	23
J_v (L $h^{-1}m^{-2}$)	8	39	125	45	166	14
$R_{total\ lignin}$	76%	84%	92%	69%	97%	94%

5.3.3. Other retentions

In addition to lignin retention, focused on the most suitable membranes, the same equation (4) was used to calculate the hemicelluloses (based on total sugars), TS and ash retentions. The measurement techniques were described in sections 4.5.1 and 4.5.3.

As the objective of NF was to concentrate the BPE and retain most of lignin and hemicelluloses, Figure 17 and Figure 18 present us the influence of the TMP on hemicelluloses, TS and ash retentions.

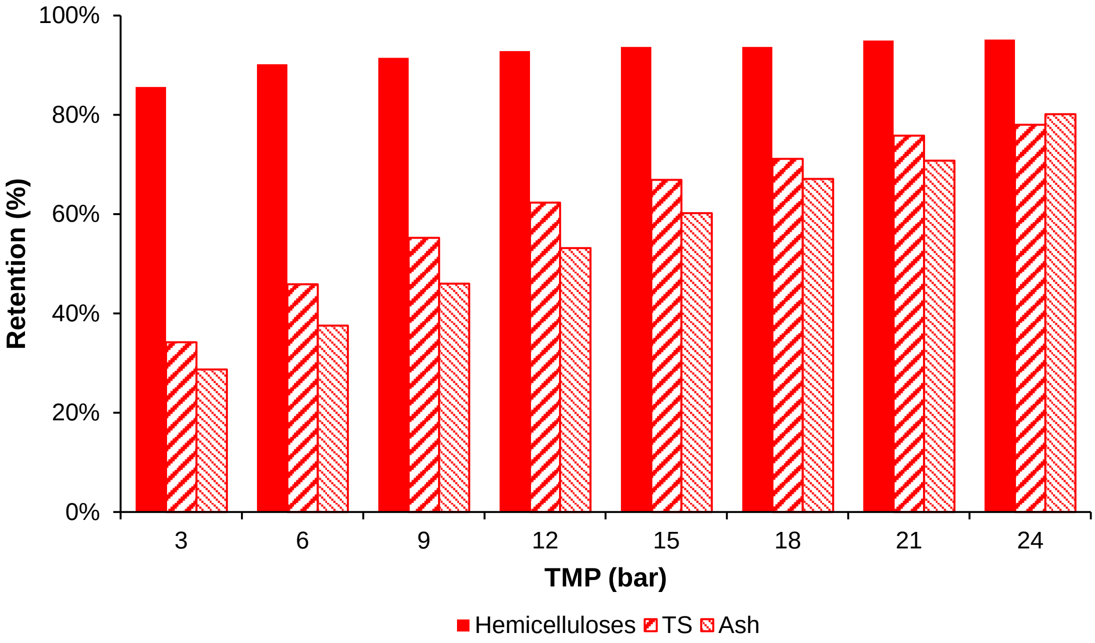

Figure 17 - Influence of the TMP on hemicelluloses, TS and ash retention for the MPF36 membrane. T = 70°C, CFV = 0,8 ms^{-1}

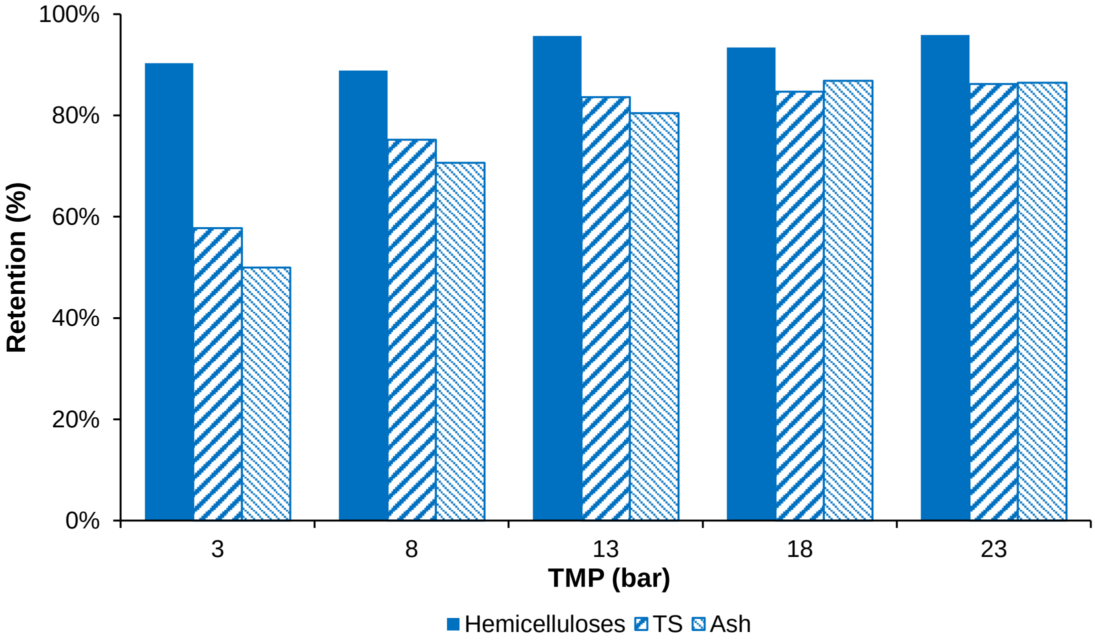

Figure 18 - Influence of the TMP on hemicelluloses, TS and ash retention for the NF99HF membrane. T = 50°C, CFV = 0,8 ms^{-1}

It was possible to achieve high retentions of hemicelluloses (based on total sugars retentions) in both membranes. However, ash retentions and consequently TS retention were higher on the NF99HF membrane according to their manufacturer rejection of $MgSO_4 \geq 98\%$, which is an indication that this membrane has better characteristics to retain inorganic salts.

5.3.4. SEC of permeates

Permeates from NF experiments conducted at the optimal conditions for the two most suitable membranes were analyzed by SEC, described in section 4.5.5.

The comparison between permeates and feed solution, pre and after sieves filtration are shown in Figure 19 and Figure 20. Before and after sieves filtration, to remove fibers, we have the peaks in the same molecular masses but with lower intensity. It works like a duplicate and confirms that we have the same compounds before and after sieves filtration, but a little bit more diluted due to the fact that the installation was cleaned and rinsed between this pre-treatment, as described in section 4.4.2,

Once we have higher retentions for total lignin and hemicelluloses (based on total sugars) for NF99HF membrane in comparison with MPF36 (values presented before in sections 5.3.2 and 5.3.3.) it was expected that the SEC diagrams could support that. In Figure 20, the SEC diagram for permeate of NF99HF membrane, shows really low peaks for total lignin and hemicelluloses content, which agrees with the higher retentions, between 95 and 97%, of these compounds in this membrane in such operating conditions.

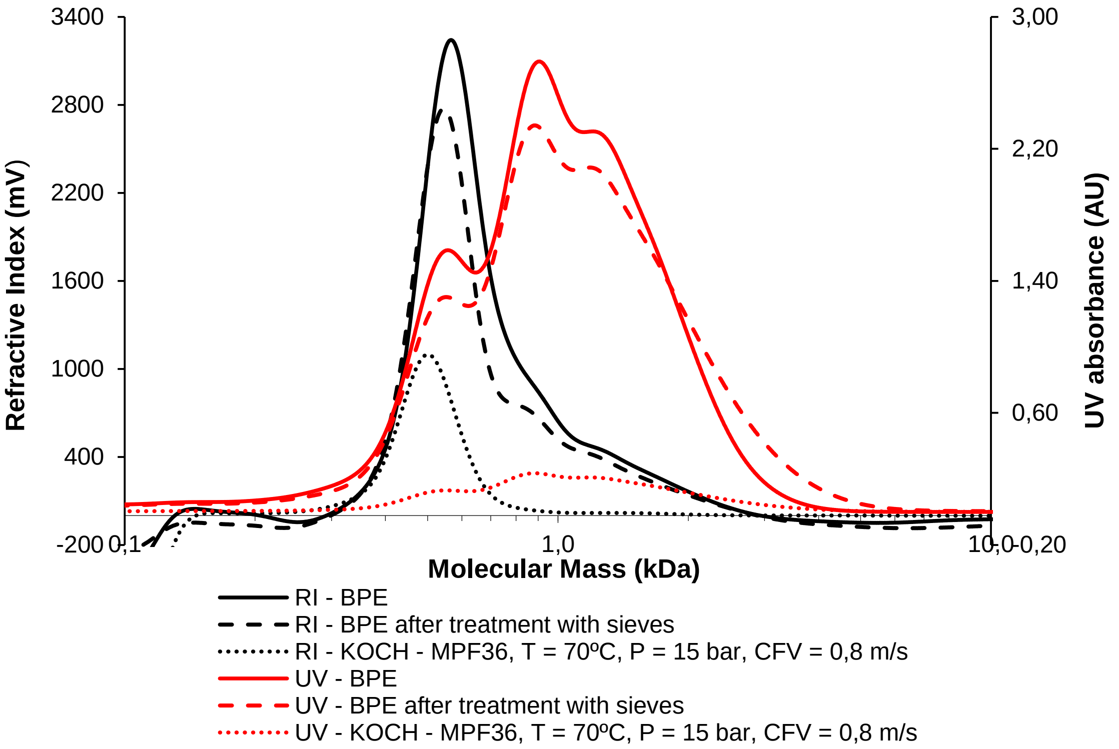

Figure 19 - Molecular mass distribution of lignin (measured as UV absorbance at 280 nm) and hemicelluloses (measured as refractive index) in the BPE, BPE after sieving and permeate of MPF36 membrane. T = 70°C, P = 15 bar, CFV = 0,8 ms^{-1}

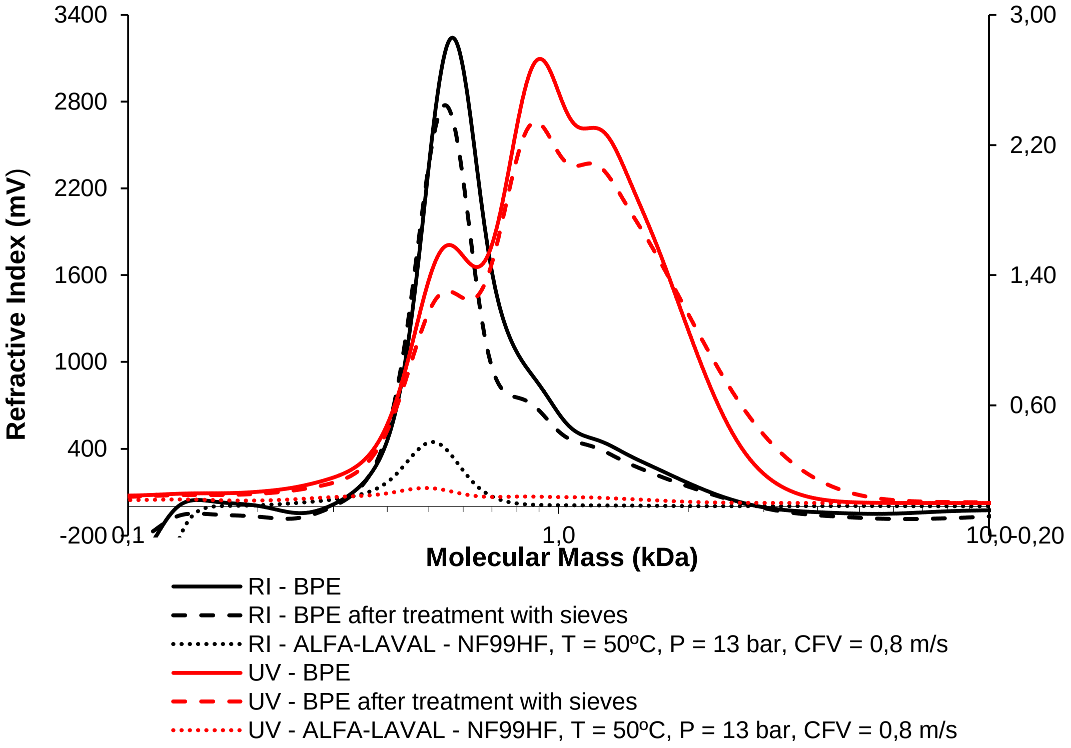

Figure 20 - Molecular mass distribution of lignin (measured as UV absorbance at 280 nm) and hemicelluloses (measured as refractive index) in the BPE, BPE after sieving and permeate of NF99HF membrane. T = 50°C, P = 13 bar, CFV = 0,8 ms^{-1}

In order to evaluate the molecular masses that permeate thru each membrane, equation (21) was used to calculate the mass average molecular mass of lignin and hemicelluloses for the feed after sieving and permeates for each membrane, values shown in Table 9.

Table 9 - Mass average molecular mass of lignin and hemicelluloses for feed BPE, MPF36 (T = 70°C, P = 15 bar, CFV = 0,8 ms^{-1}) and NF99HF (T = 50°C, P = 13 bar, CFV = 0,8 ms^{-1}) permeates.

	BPE feed after sieving	**MPF36 permeate**	**NF99HF permeate**
Hemicelluloses $\bar{M}_w$ (kDa)	0,88	0,52	0,52
Lignin $\bar{M}_w$ (kDa)	1,60	1,60	0,88

Mass average molecular mass for the hemicelluloses were the same in the two different membrane permeates, and lower than the feed. However, for the lignin, MPF36 membrane permeate present the same mass average molecular mass than the feed, but NF99HF have lower value. It could be to the fact that NF99HF have tightest pores in comparison with MPF36, which only smaller lignins were permeable.

5.3.5. Membrane resistances

Focused on the most suitable membranes it is observed that the BPE permeate fluxes (J_v) are always lower, in the examined TMP range, and deviate increasingly from the corresponding pure water fluxes for new membranes (J_{wi}) as the TMP increases. Indicating there are resistances to mass transfer beyond the intrinsic resistance of the membranes (R_m).

That way, the deviation from the PWFs is a result of concentration polarization phenomenon and other phenomena that provides resistance to mass transfer. The following Figure 21 focusing on the linear region for the MPF36 and NF99HF membranes provide some necessary results for the study of membrane resistances.

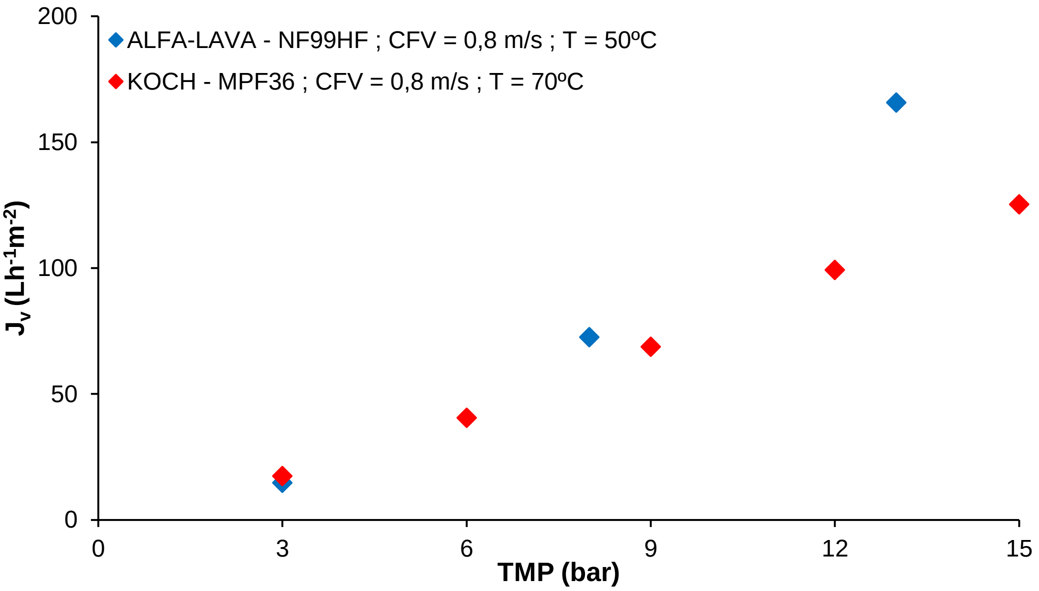

Figure 21 - Permeate fluxes (J_v) in the linear region.

As the hydraulic permeability (L_p), the permeability of the membrane to the BPE (L_v) is the line slope of BPE permeate flux (J_v) as a function of TMP applied in the linear region since it should be avoid to work in the "limiting fluxes".

It was assumed that the permeate viscosity (μ_p) changes is similar to pure water viscosity changes with temperature, since the solutions are very diluted, which influences the permeate flux (J_v) and consequently the permeability (L_v), so following the equation (23) permeability values for the BPE (L_v) were corrected to 25°C for posterior comparison and the values are shown in Table 10.

Table 10 - BPE permeability values. CFV = 0,8 ms-^{1}

Membrane	Linear regression	L_v (Lh^{-1}m^{-2}bar^{-1})	$L_{v\,25°C}$ (Lh^{-1}m^{-2}bar^{-1})
NF99HF	$J_v = 11{,}48 \times \mathrm{TMP}$ $R^2 = 0{,}911$	11,48	6,75
MPF36	$J_v = 8{,}05 \times \mathrm{TMP}$ $R^2 = 0{,}980$	8,05	3,28

To be able to analyze the resistance of the membranes one more parameter is necessary, the hydraulic permeability of fouled membranes after the parametric studies (J_{w^*}). The technique was described in section 4.4.4, and the results were treated as in section 5.2, the values are presented in Figure 22 and the results exposed in the Table 11.

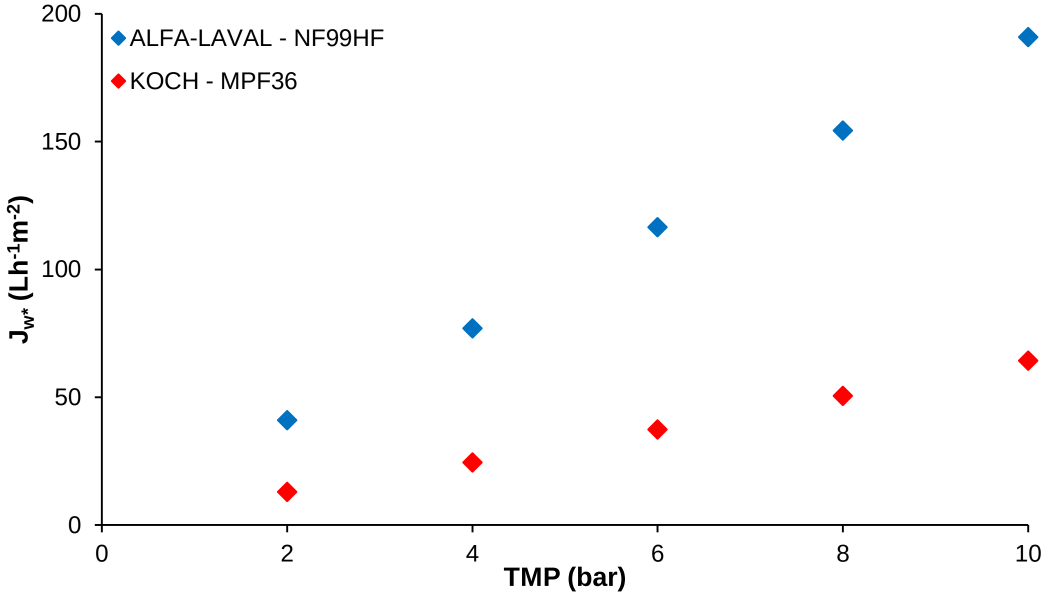

Figure 22 - Pure water fluxes (J_{w^*}) in function of TMP after parametric studies (fouled membranes). T = 30°C, CFV = 0,3 ms^{-1}

Table 11 - Hydraulic permeability (L_{w^*}) after parametric experiments (fouled membranes).

Membrane	**Linear regression**	L_{w^*} **(Lh^{-1}m^{-2}bar^{-1})**	$L_{w^*\,25°C}$ **(Lh^{-1}m^{-2}bar^{-1})**
NF99HF	$J_{w^*} = 19{,}24 \times \mathrm{TMP}$ $R^2 = 0{,}999$	19,24	17,18
MPF36	$J_{w^*} = 6{,}34 \times \mathrm{TMP}$ $R^2 = 0{,}999$	6,34	5,66

The study of resistance to mass transfer were analyzed by the resistance in series model. This model is based on the following equations

$$J = \frac{TMP}{\mu \times R_t} \tag{26}$$

$$R_t = R_m + R_{rev} + R_{irrev} \tag{27}$$

Where R_t represents the total resistance to the membrane permeation. It was considered that the total resistance results from a series of resistances, equation (27). Constituted by the membrane resistance

(R_m) and the resistance caused by fouling divided into two contributions, the reversible resistance by fouling (R_{rev}) and irreversible resistance by adsorption (R_{irrev}).

The membrane resistance (R_m) corresponds to the resistance that the membrane offers to the passage of pure water. The value of this parameter is derived from the hydraulic permeability (L_p) presented previously in Table 7.

$$J_{wi} = \frac{TMP}{\mu_w \times R_m} \Leftrightarrow R_m = \frac{1}{\mu_w \times L_p} \tag{28}$$

The total resistance (R_t) is obtained by the BPE permeability (L_v) presented previously in Table 10.

$$J_v = \frac{TMP}{\mu_p \times R_t} \Leftrightarrow R_t = \frac{1}{\mu_w \times L_v} \tag{29}$$

The value of R_{t^*} is the sum of intrinsic resistance of the membrane (R_m) and its irreversible resistance (R_{irrev}) which was not removed by water circulation. Its value is calculated from the hydraulic permeability values after the parametric studies (fouled membranes) (L_{w^*}) presented in Table 11.

$$J_{w^*} = \frac{TMP}{\mu_w \times R_{t^*}} \Leftrightarrow R_{t^*} = \frac{1}{\mu_w \times L_{w^*}} \tag{30}$$

$$R_{irrev} = R_{t^*} - R_m \tag{31}$$

The irreversible resistance (R_{irrev}) corresponds to the fouling caused by compounds adsorbed on the surface or within the pores of the membrane. This resistance cannot be eliminated only by passage of water, as the compounds are chemically bound to the membrane material.

Reversible resistance by fouling (R_{rev}) is the resistance due to concentration polarization and accumulation of solutes on the surface of the membrane, but not chemically bound thereto. This resistance disappears when it ceases to apply pressure in the system and only water passes, removing material existing on the surface of the membrane. Their value is obtained by equation (32).

$$R_{rev} = R_t - (R_m + R_{irrev}) \tag{32}$$

Table 12 presents the results of the different resistances to the permeation of BPE, for two most suitable membranes in the parametric studies.

Table 12 - Different resistance types to permeation of BPE.

Resistance type	Membrane	
	NF99HF	MPF36
$R_m \times 10^{13}(m^{-1})$	1,67	1,71
$R_{rev} \times 10^{13}(m^{-1})$	3,23	4,62
$R_{irrev} \times 10^{13}(m^{-1})$	0,42	4,64
$R_t \times 10^{13}(m^{-1})$	5,32	10,97

It is noted that the resistance associated with irreversible adsorption material in the membrane is that it has less contribution to the total resistance in the NF99HF and the higher contribution in the MPF36 membrane. This resistance could be related to the pore size of the membrane, while the larger the pore size the greater the access of high molecular weight solutes to its interior, resulting in higher internal adsorption phenomena with consequent reduction of the permeate flux. This is in accordance with both manufacturer MWCO of the membranes.

5.3.6. Membranes regeneration

One of the most important concerns for the application of the membranes is fouling, and chemical cleaning is therefore an integral operation for membrane filtration systems during effluents treatment.

As an attempt to recover the initial hydraulic permeability (L_p), cleaning procedure presented in section 4.4.1 was followed and pure water flux (J_w) versus TMP is presented in the Figure 23. The hydraulic permeability after cleaning the membranes (L_w) was then calculated as described in section 4.4.4 and the values are shown in Table 13.

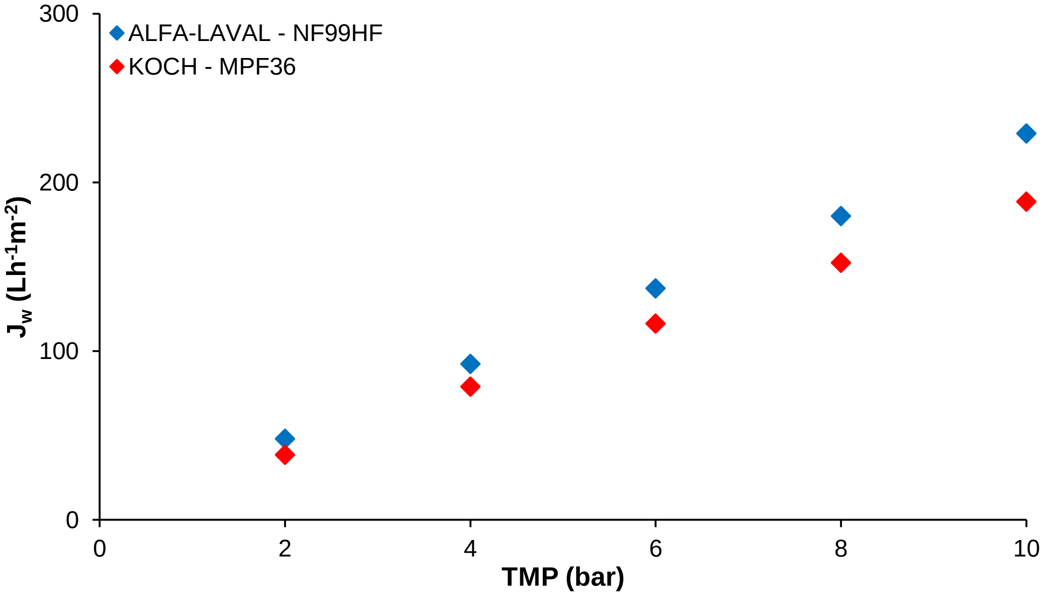

Figure 23 - Pure water fluxes (J_w) in function of TMP after cleaning the membranes. T = 30°C, CFV = 0,3 ms^{-1}

Table 13 - Hydraulic permeability (L_w) after cleaning the membranes.

Membrane	Linear regression	L_w ($Lh^{-1}m^{-2}bar^{-1}$)	$L_{w\,25°C}$ ($Lh^{-1}m^{-2}bar^{-1}$)
NF99HF	$J_w = 22{,}81 \times \text{TMP}$ $R^2 = 0{,}999$	22,81	20,37
MPF36	$J_w = 19{,}07 \times \text{TMP}$ $R^2 = 0{,}999$	19,07	17,03

It is shown in Table 14 according to membrane resistances that MPF36 membrane only recovers 27% of their pure water permeability when only washed with water, due to their high value for the irreversible resistance corresponding to the fouling caused by compounds adsorbed on the surface or within the pores of the membrane that can only remove by cleaning agents. After membrane cleaning with an alkaline agent, technique exposed in section 4.4.4, it was possible to recover 81% of the initial pure water permeability.

With NF99HF, it was possible to recover 80% of their initial pure water permeability only with water washing, which is in accordance to their low irreversible resistance. After cleaning with alkaline agent, 95% recovery of the initial permeate water flux was achieved.

Table 14 - Permeability recovery after washing and after cleaning.

Membrane	$\frac{L_{v\,25°C}}{L_{p\,25°C}}$ (%)	$\frac{L_{w^*\,25°C}}{L_{p\,25°C}}$ (%)	$\frac{L_{w\,25°C}}{L_{p\,25°C}}$ (%)
NF99HF	31%	80%	95%
MPF36	16%	27%	81%

5.4. Concentration studies

In addition to the recirculation mode tests, one trial was carried out in concentration mode, i.e., with collection of the permeate and recirculation of retentate to the tank. These experiment is intended for study the evolution of permeate fluxes with the volume reduction factor, as well as the analysis of the apparent rejection coefficients.

5.4.1. Permeate fluxes vs VR

The influence of the volume reduction (VR) on permeate fluxes was studied by conducting an experiment in concentration mode, as described in section 4.4.3.

This concentration study was realized only with NF99HF membrane at the optimal conditions (T = 50°C, P = 13 bar, CFV = 0,8 ms^{-1}) that was found to be the most suitable for the aim of the project, due to their lowest membrane resistances, highest lignin and sugars retentions, higher permeate fluxes, and good cleaning conditions. As demonstrated before with parametric studies in section 5.3.

The evolution of permeate fluxes during concentration of the BPE is presented in Figure 24.

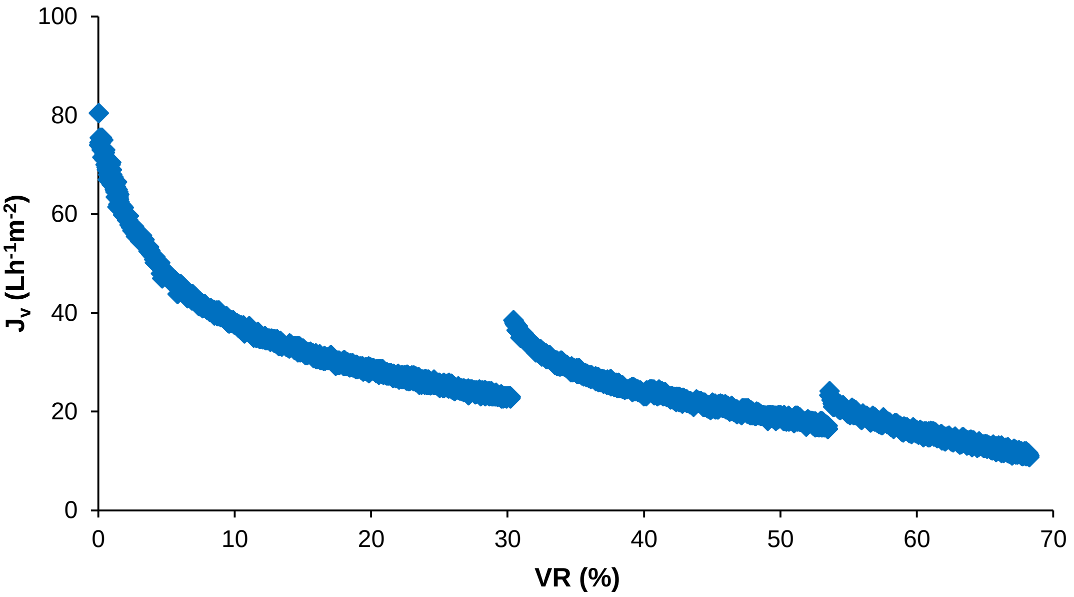

Figure 24 - Flux during concentration of process solution with NF99HF membrane.
T = 50°C, TMP = 13 bar, CFV = 0,8 ms^{-1}

The initial flux of the NF99HF membrane was too much lower in the concentration study, 81 Lh^{-1}m^{-2}, compared with the parametric studies at the same operating conditions, 166 Lh^{-1}m^{-2}. This almost half initial permeate flux value could be justified for some reasons, a) very distinct modules configuration, parametric studies with a single circular flat membrane with 0,00196 m^2 against two double-sided membrane discs and support paper with a total membrane area of 0,072 m^2 in the concentration study. b) NF99HF membrane used in parametric studies was manufactured in 1997 and for the concentration study was manufactured in 2015. c) differences in CFV when changing the modules.

This concentration study was made in three consecutive days, for around 8h per day. During the nights, the system was left in total recirculation with the minimum TMP advised by manufacturer of the used module (around 3 bar) to keep the concentration levels until restart the work in the next day, at the same conditions. So, Figure 24 shows two discontinuity points around 30% and 53,5% VR, which were the points that the system was left in total recirculation during the nights. At the first night the flux recovery was 19% and in the second night was 9%, this values shows that it was removed some of the accumulated solutes on the surface of the membrane, but not chemically bound thereto. This reversible resistances usually disappears when it ceases to apply pressure in the system and only water passes, however it was shown that it is possible to remove some of this cake layer by using total recirculation of the effluent and lower the TMP of the system.

During the days, the permeate fluxes decrease with the volume reduction factor, as a consequence of concentration polarization and membrane fouling, with a higher intensity of these phenomena when the concentration increases (higher volume reduction). Concentration study started with a flux of 81 Lh^{-1}m^{-}

^{2} and ended up with 11 $Lh^{-1}m^{-2}$, which represents a flux decline of 86,5%, till achieve 68% of volume reduction (VR), without any type of chemical cleaning.

During concentration studies, the increase of concentration leads with a slightly increase of a moving average of friction pressure drop (ΔP, the loss of pressure from the feed end to the concentrate end of a module) from 0,5 bar till around 0,7 bar, as shown in Figure 25.

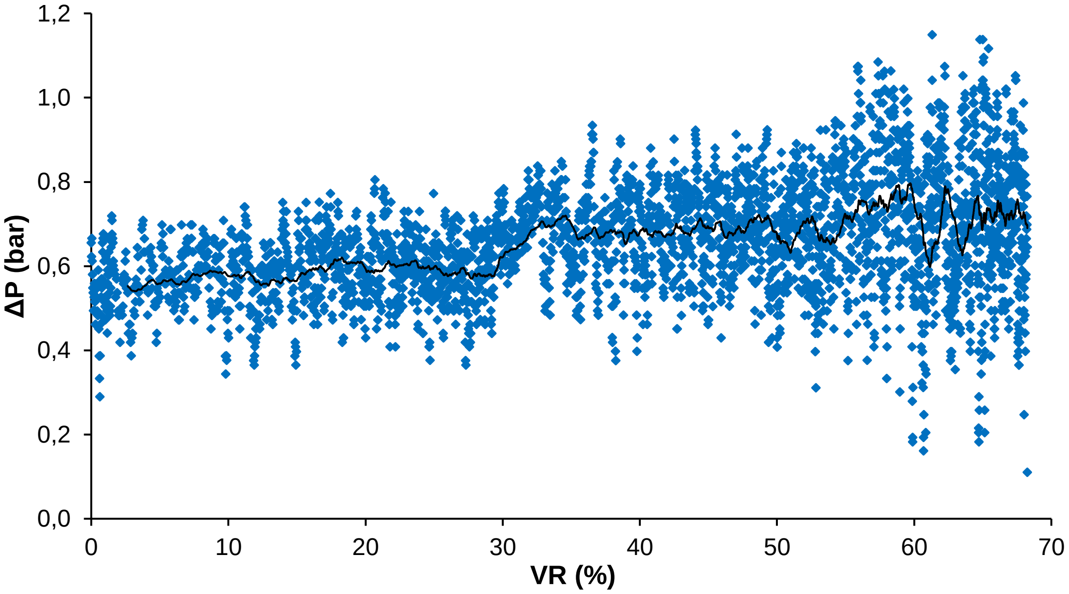

Figure 25 - Moving average of frictional pressure drop during the concentration studies of the BPE. NF99HF, T = 50°C, TMP = 13 bar, CFV = 0,8 ms^{-1}

Some studies about frictional pressure drop with this kind of effluent were performed and usually pressure drop increases with the extent of fouling. A high pressure drop is problematic because it may lead to telescoping and inefficient operation, and thus a decline in system performance. (Nordin & Jönsson, 2006) It might be have an additional cause for the flux decline presented and discussed before in Figure 24.

5.4.2. Characterization of fractionated streams

Quantification of the concentration of BPE was analyzed by physicochemical characterization of concentrates and permeates. To this end, samples were taken for the retentate and permeate side with a VR step-size of 10%, which all values are presented in Annex A – Physicochemical characterization of fractionated streams.

Experimental results for the feed (VR of 0%), concentrate and permeate at the end of the experiment (VR of 68%) are presented in Table 15.

Table 15 - Physicochemical characterization of the feed (retentate at VR of 0%), concentrate and permeate for a VR of 68%

	Feed	Retentate	Permeate
pH	9,75	9,44	9,29
ρ (g/L)	1022	1031	1022
TS (mg/g)	28,31	68,25	26,96
Ash (mg/g)	14,35	32,53	14,58
Total lignin (g/L)	3,22	9,40	0,42
Acid soluble lignin (mg/g)	1,20	3,25	0,18
Klason lignin (mg/g)	1,51	6,09	0,06
Hemicelluloses (mg/g)	0,18	0,69	0,018
Arabinose (mg/g)	0,00	0,00	0,001
Galactose (mg/g)	0,00	0,00	0,000
Glucose (mg/g)	0,03	0,09	0,005
Mannose (mg/g)	0,02	0,09	0,004
Xylose (mg/g)	0,13	0,51	0,008
Others (mg/g)	10,56	25,62	11,95
Total carbon (g/L)	7,80	20,72	6,57
Inorganic carbon (g/L)	0,23	0,35	0,40
Total organic carbon (g/L)	7,57	20,36	6,17

The main goal of this experiment was to promote the concentration of the effluent and retain valuable compounds such as lignin and hemicelluloses (measured in total sugars). Increasing TS from 28,31 mg/g to 68,25 mg/g (from ≈3% to ≈7% (w/w)) it was achieved with a BPE volume reduction of 68%, this increase in TS concentration happened because permeable components were being removed and total lignin and hemicelluloses started to have a higher contribution in TS.

Values of concentrations for each VR step-size are presented in Figure 26 and Figure 27. Based on that compositions and using equation **Erro! A origem da referência não foi encontrada.** for the different components it was possible to evaluate the evolution of the apparent retention levels for each compound, as shown in Figure 28.

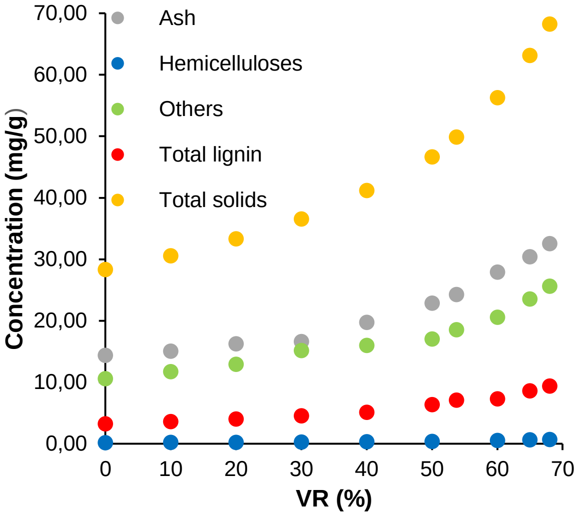

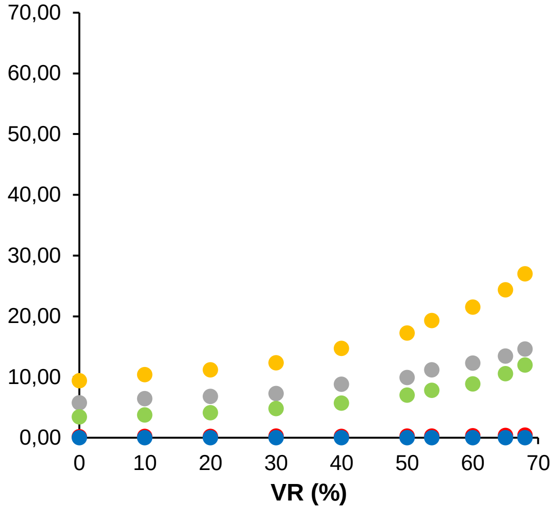

Figure 26 - Concentration values for retentate streams

Figure 27 - Concentration values for permeate streams

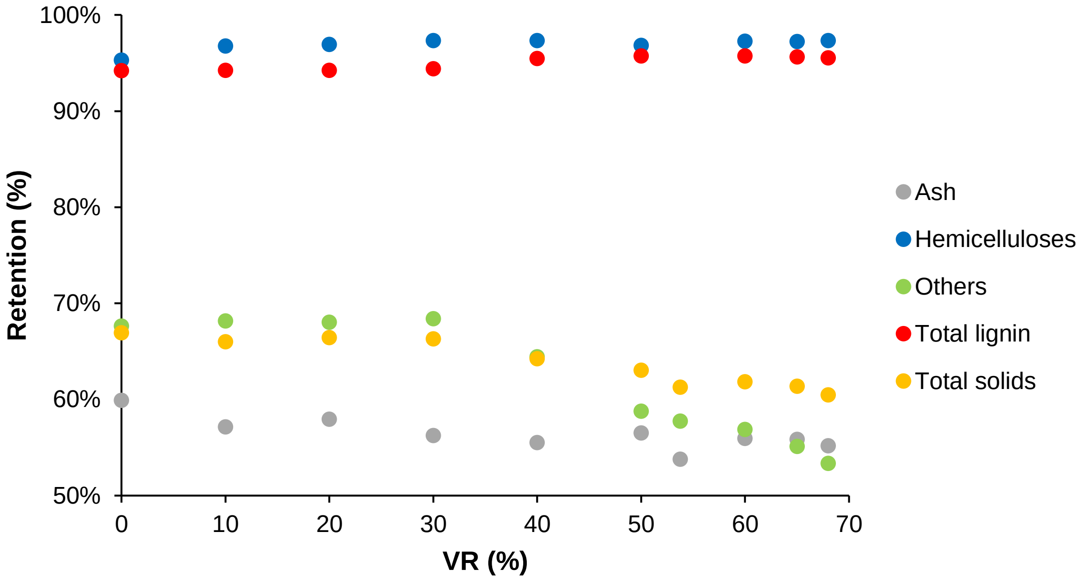

Figure 28 - Variation of apparent retentions with volume reduction (VR) for each component

Concentrations close to zero, for the total lignin and hemicelluloses on the permeate streams were expected, since NF99HF was chosen for their high retentions on these compounds in the parametric studies presented before in section 5.3. Retention values remained almost constant between 94-97% with the increase of concentration. Which allows to say that NF99HF membrane, operating at 50°C a TMP of 13 bar and a CFV of 0,8 ms^{-1}, have a really impressive selectivity for these components, until a VR of 68%.

On the other hand, ash and consequently TS retention, in the beginning of experiments, were almost 20% lower than in the parametric studies. Furthermore, apparent retentions for these components were decreasing with the concentration. In the end of the experiment (VR = 68%) the retention for ash and TS were 55,2% and 60,5% respectively.

Content of “Others”, is the difference between TS and ash, hemicelluloses and total lignin. As shown in Figure 28, their retention decrease around 15% between the beginning and the final of the study and it contributes to the decrease in TS retention. So, it starts to have higher contribution in TS content on the permeate side. In order to confirm that the “Others” could be organic matter, TOC analysis, described in section 4.5.4, were performed in the fractionated streams, as shown in Figure 29. Based on it, apparent retention evolution for TOC with VR is presented in Figure 30.

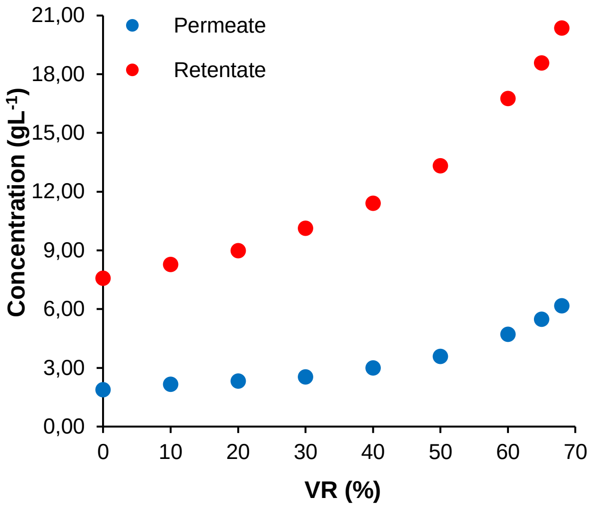

Figure 29 - TOC concentrations for retentate and permeate streams

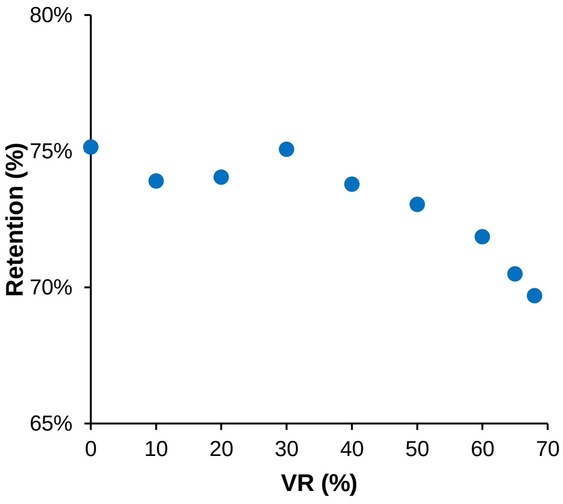

Figure 30 - Variation of TOC retention with volume reduction (VR)

The fall in TOC retention after the VR of 30% is in accordance with the fall in “Others” retention after the same VR. Besides the confirmation that “Others” is organic matter, it starts to have more contribution in the permeate streams with the increase of concentration, it arouses some curiosity in what type of compounds it could be. For that purpose, high performance liquid chromatography (HPLC) was employed with some standards, where acetic and formic acid had the higher contribution and credibility since the samples were complex, multicomponent mixture, as shown in Annex B – HPLC Analysis: Standards and fractionated streams.

5.4.3. SEC of fractionated streams

Permeates and retentate streams from concentration experiments were analyzed by SEC, as described in section 4.5.5. SEC diagrams for molecular mass distribution of hemicelluloses, and lignin in the beginning and in the end of the experiments are presented in Figure 31 and Figure 32, respectively. SEC diagrams for the intermediate step-sizes are presented in the Annex C – SEC diagrams of fractionated streams.

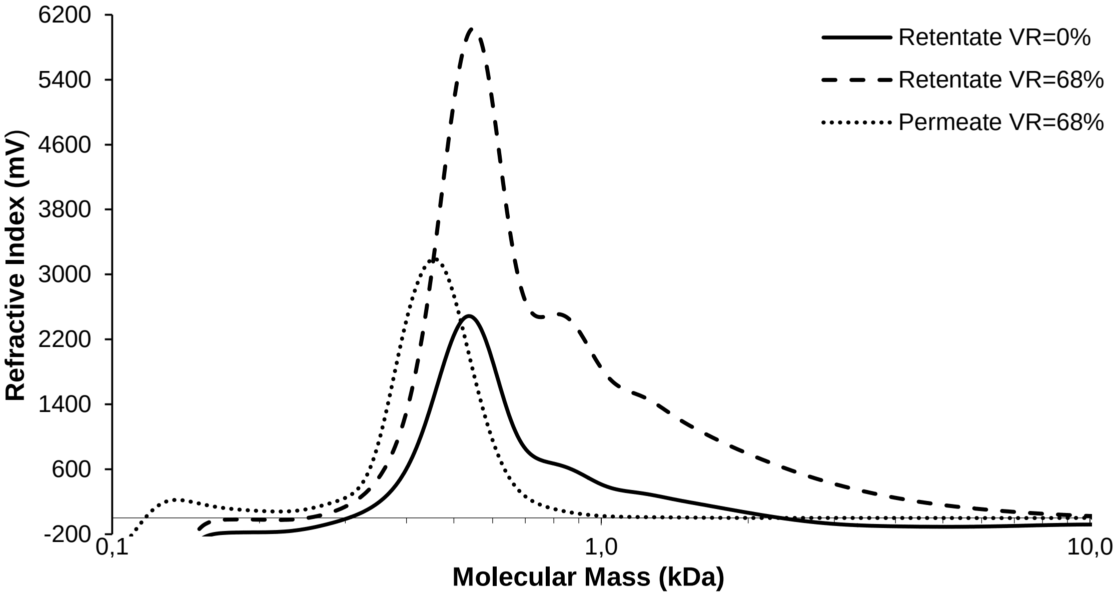

Figure 31 - Molecular mass distribution of hemicelluloses (measured as refractive index) for the feed (retentate at VR of 0%), concentrate and permeate for a VR of 68%

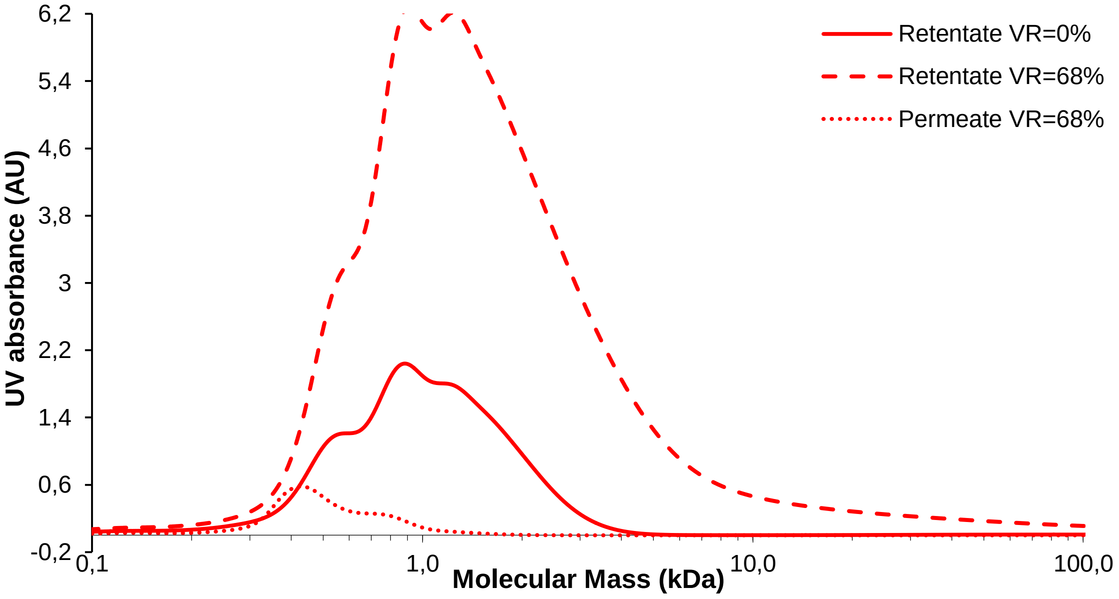

Figure 32 - Molecular mass distribution of lignin (measured as UV absorbance at 280 nm) for the feed (retentate at VR of 0%), concentrate and permeate for a VR of 68%

It was expected that the peaks in the final retentate stream would be higher than in the feed stream (Retentate at VR=0%), i.e. by Table 15 the concentrations of hemicelluloses and lignin in the final retentate are around three and four times higher, respectively, in comparison with the feed stream due to the extremely high retentions of these compounds. Which are in accordance with the SEC diagrams presented above. However, for the final permeate stream it was not expected that the RI peak for hemicelluloses analysis would be higher than in the feed, i.e. by Table 15 the concentration of hemicelluloses in the final permeate is around ten times lower than in the feed. Which is not in accordance with Figure 31. So, it should be noted that, in the final permeate stream, some unknown compound is sensitive to the RI analysis beside hemicelluloses, which turns less credible the measurements of hemicelluloses by RI.

In order to evaluate the molecular masses that permeates the membrane during concentration studies, equation (21) was used to calculate the mass average molecular mass of lignin and hemicelluloses for the feed, final retentate and final permeate, values are shown in Table 16.

Table 16 - Mass average molecular mass of lignin and hemicelluloses for the feed (retentate at VR of 0%), concentrate and permeate for a VR of 68%

	Feed	**Retentate**	**Permeate**
Hemicelluloses $\overline{M}_w$ (kDa)	0,79	1,77	0,48
Lignin $\overline{M}_w$ (kDa)	1,48	19,08	0,64

Since the rejection was not 100%, a very low quantity of some hemicelluloses and lignin are presented in the permeate side. However, their mass average molecular mass are lower than in feed, which proves that only the lowest molecular weight hemicelluloses and lignin are permeable. On the contrary, in the final retentate stream, high molecular weight components start to have higher contribution, which turns the mass average molecular mass of hemicelluloses and lignin higher.

5.4.4. Membrane regeneration

After around 27 hours of concentrating the BPE in batch mode, membrane regeneration performance was evaluated as described in section 4.4.4. The PWF's of new membranes, fouled membranes and after cleaning are presented Figure 33.

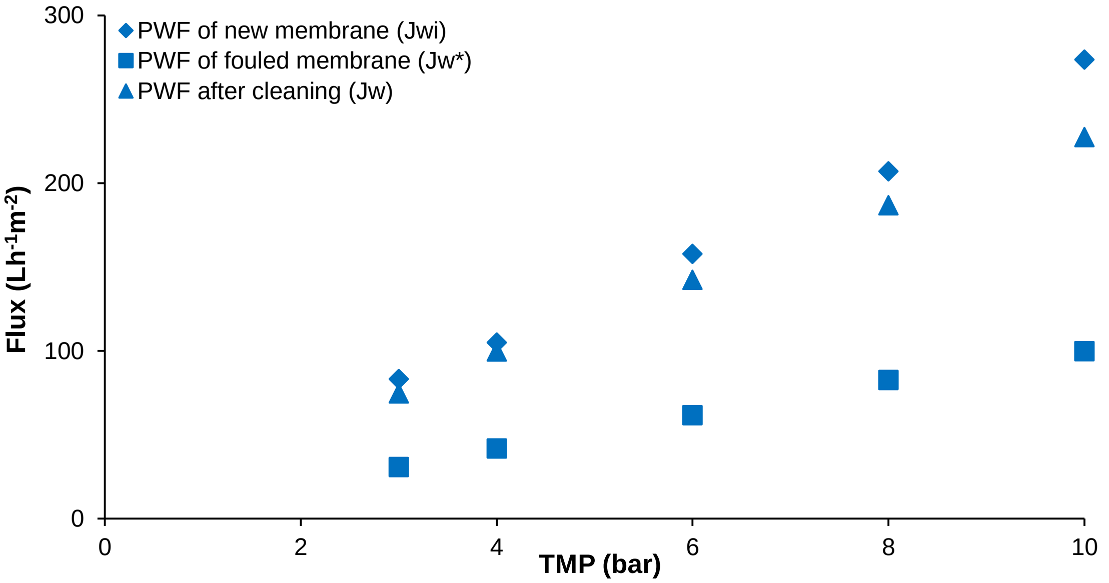

Figure 33 - Pure water fluxes (PWF) in function of TMP for the new, fouled and cleaned membranes after the concentration experiment

Linear regressions of each PWF against TMP are presented in Table 17, as well as the permeability recoveries after washing and after chemical cleaning with the alkaline agent.

Table 17 - Hydraulic permeability values and permeability recovery after washing and after cleaning

Linear regression	**L_p (Lh^{-1}m^{-2}bar^{-1})**	$\frac{L_{w^*}}{L_p}$ (%)	$\frac{L_w}{L_p}$ (%)
$J_{wi} = 26{,}71 \times \mathrm{TMP}$ $R^2 = 0{,}996$	26,7	38%	87%
	L_{w^*} (Lh^{-1}m^{-2}bar^{-1})		
$J_{w^*} = 10{,}18 \times \mathrm{TMP}$ $R^2 = 0{,}998$	10,2		
	L_w (Lh^{-1}m^{-2}bar^{-1})		
$J_w = 23{,}32 \times \mathrm{TMP}$ $R^2 = 0{,}993$	23,3		

The initial hydraulic permeability (L_p) of the NF99HF membrane is around 10% higher when compared with the measurements before the parametric studies, considering the big differences in modules configuration and membrane areas used, these values are not so misfits, which confirms the hydraulic permeability values for this membrane.

It was possible to recover 38% of their initial hydraulic permeability only with water washing after the concentration studies, this value is 42% lower than the value achieved after parametric studies. This value should be expected due to the higher operation time in concentration studies where the membrane get more fouled and leads with higher concentrations of compounds, in this case with more irreversible fouling, which is the one caused by compounds adsorbed on the surface or within the pores of the membrane and cannot be eliminated only by water circulation, as the compounds are chemically bound to the membrane material.

Finally, after cleaning with an alkaline agent the hydraulic permeability recovery was 87%, which reveals again, as in parametric studies, that the chemical cleaning performed as described in section 4.4.4 seems suitable for the process.

5.5. Cost estimates

The cost of a NF plant treating 70 m^3h^{-1} process solution was estimated based on the results of the concentration studies shown in Table 18, and technico-economical data used in calculations are shown in Table 19.

Table 18 - Experimental data used in the cost estimates

Feed flow, Q_{feed} (m^3h^{-1})	70
VR (%)	68%
CFV (ms^{-1})	0,8
TMP (bar)	13
Average flux, J_{av} ($Lh^{-1}m^{-2}$)	24,2
ΔP in each module (bar)	0,7

Table 19 - Technico-economical data

Investment cost (€.m^{-2})	2000[a]
Electricity price (€.kWh^{-1})	0,10[c]
Membrane replacement cost (€m^{-2})	95[a]
Membrane lifetime (year)	1,5[b]
Cleaning cost (€.m^{-2}year-^{1})	50[b]
Operating time (h.$year^{-1}$)	8000[b]
Pump efficiency (η)	0,8
Maintenance and labor (% of investment cost.$year^{-1}$)	5%[a]
Annuity factor (%)	10%[a]

[a] (Jönsson, et al., 2008), [b] (Arkell, et al., 2013), [c] (YLCE, s.d.)

Continuous processes may be single-stage (feed and bleed) or multistage processes, depending upon the processing capacity required. The feed-and-bleed design is used in most large-scale commercial applications. As shown in Figure 34, a part of the concentrate is recycled. The flow rate in the recirculation loop is 5–10 times the feed solution rate. (Cui & Muralidhara, 2010)

It was assumed that the plant will work in a single-stage feed and bleed process and will be equipped with a feed pump, a recirculation pump and Alfa Laval Flat Sheet Membrane Modules M38L/H (Alfa Laval, s.d.) (Plate-and-frame configuration) equipped with NF99HF membranes.

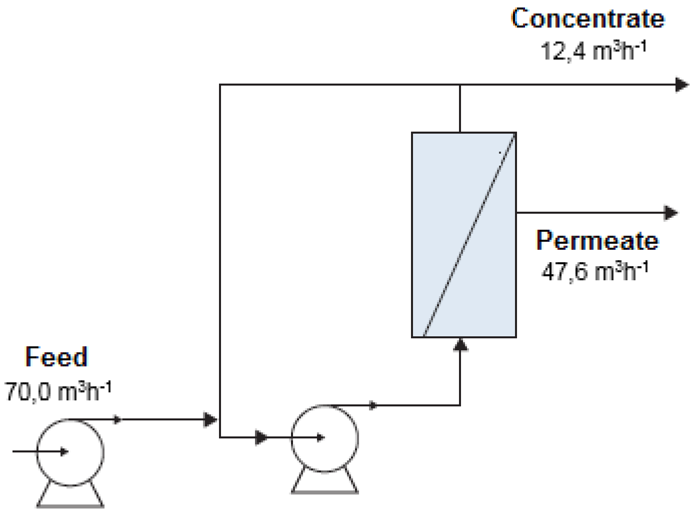

Figure 34 - Single-stage feed and bleed system for the industrial scale-up process. Adapted from (Cui & Muralidhara, 2010)

Since the plant will operate close to the temperature limits given by the manufacturer (50 °C), the membranes lifetime was assumed to be 18 months if the plant is operated continuously. It was assumed that the membranes will be cleaned every day for one hour and the cost of cleaning with a commercial alkaline cleaning agent was assumed to be 50 €.$m^{-2}year^{-1}$. (Arkell, et al., 2013) Maintenance and labour costs were estimated to be 5% of the investment cost. (Jönsson, et al., 2008)

5.5.1. Investment cost

The investment cost is composed of the cost of the plant and the cost of the membrane elements. For a first estimate of a large scale unit with a 20% safety factor the calculation of the membrane area is given by equation (33).

$$Membrane\ area = \frac{Q_{feed} \times VR}{J_{av}} \times 1{,}2 \tag{33}$$

The membrane area required by equation (33), based on the obtained conditions in the concentration study, Table 18, is 2360 m^2. Since each M38L/H module from Alfa Laval could have a maximum membrane area of 60 m^2, 40 modules would be needed and arranged in parallel/series.

Jönsson, et al., used an investment cost of 2000 € per m^2 of membrane area for an alkali resistant tubular polymeric NF membrane. (Jönsson, et al., 2008) According to Table 2, tubular and plate-and-frame modules have both highly costs, so it should be reasonable use the same value to calculate the investment cost for this process. By this way, a total investment cost of 4,72M€ was predictable.

Another way to predict the investment cost was proposed by Nilsson, et al., where it was assumed that in the economic evaluation, the investment cost of the plant is divided into the costs of the three main sections:

1. The feed section including feed tank, Cleaning in place (CIP) tank, feed pump and feed heat exchanger
2. The membrane section with the recirculation loops, including recirculation pumps, heat exchangers, pipes, frames, membranes and housings
3. The automation section, including the control panel, frequency inverters, etc.

Based on the following three equations (34), (35) and (36), the investment cost could be estimated.

$$Total\ invesment\ cost = \left(Cost_{feed\ section} + Cost_{membrane\ section}\right) \times factor_{automation} \tag{34}$$

$$Cost_{feed\ section} = 5000€ \times Q_{feed}\ (m^3h^{-1}) \tag{35}$$

$$Cost_{membrane\ section} = 1000€ \times Membrane\ area\ (m^2) \times factor_{module} \tag{36}$$

Where the module factor ($factor_{module}$) depends on the module configuration and should be 1,3 for plate-and-frame modules. And the factors for automation ($factor_{automation}$) are 1,0 for manual operation, 1,3 for semi-automatic operation and 1,5 for fully automatic operation. (Nilsson, et al., s.d.)

According to Nilsson, et al., assumptions, this industrial scale process will have an investment cost of 4,44M€ if semi-automatic or 5,13M€ with fully automatic operation. Value predictable by Jönsson, et al., assumptions is in the middle of this range and could be used, which with an annuity factor of 0,1 corresponds to a capital cost of 472 k€.year^{-1}.

5.5.2. Operating costs

The operating costs consist of electricity, replacement of membranes, cleaning, maintenance and labour costs. Electricity is needed mostly for pumping. A feed pump will be needed to deliver the inlet pressure of the plant and a recirculation pump will be needed to compensate for the frictional pressure drop and to maintain the circulation flow in the membrane plant. The energy required per m^3 of permeate in the feed pump is given by equation (37), and in the recirculation pump by equation (38).

$$W_{feed} = \frac{TMP \times Q_{feed}}{\eta \times (VR \times Q_{feed})} = \frac{TMP}{\eta \times VR} \tag{37}$$

$$W_{recirc} = \frac{\Delta P \times Q_{feed^*}}{\eta \times (J_{av} \times Membrane\ area)} \tag{38}$$

The energy required by the feed pump is thus 0,66 kWh.m^{-3} of permeate and by the recirculation pump, 0,22 kWh.m^{-3}. Where, Q_{feed^*}, is the feed flow in the inlet of the modules. It was assumed that the $Q_{feed^*} = 7{,}5 \times Q_{feed}$. (Baker, 2004) The annual electricity cost could be estimated by equation (39).

$$Electricity\ cost_{annual} = \left(W_{feed} + W_{recirc}\right) \times \left(Q_{feed} \times VR\right) \times Operating\ time \times Electricity\ price \tag{39}$$

Membrane replacement and cleaning annual costs can be calculated by equations (40) and (41) respectively.

$$Membrane\ replacement\ cost_{annual} = \frac{(Membrane\ replacement\ cost\ per\ m^2) \times Membrane\ area}{Membrane\ lifetime} \tag{40}$$

$$Cleaning\ cost_{annual} = (Cleaning\ cost\ per\ year\ per\ m^2) \times Membrane\ area \tag{41}$$

Additional costs should be evaluated, one example is the cooling required for the feed stream since the E-stage BPE leaves the plant at 90 °C and should be cooled till 50 °C.

To summarize, both capital and operating costs are presented in Table 20.

Table 20 - Cost estimates for NF installation with full-time use (8000h.year^{-1})

Membrane area (m^2)	2360
Membrane modules	40
Investment cost (M€)	4,72
Capital cost (k€.year^{-1})	**472**
Electricity required (kWh m^{-3} of permeate)	0,88
Electricity cost (k€ year^{-1})	34
Membrane replacement cost (k€.year^{-1})	150
Cleaning cost (k€.year^{-1})	118
Maintenance and labor costs (k€.year^{-1})	24
Operating costs (k€.year^{-1})	**326**
Total cost (k€.year^{-1})	**798**

Guiding principles for the energy requirement for a single stage evaporation is 30-40 kWh per m^3 water removed. (IETS, 2016) If it was considered an average of 35 kWh per m^3 of water removed with a price of 0,10 € per kWh, a cost of 3,5 € per m^3 of water removed in the case of a single stage evaporation was needed. However, in the NF process presented before 2,14 € per m^3 of permeate was achieved with capital costs included.

6. Conclusion and future work

6.1. Contributions

The literature review presented before shows that in the P&P industry each case is different due to the different ways of production (i.e. infinite type of raw materials, different chemical agents used, different operating conditions, etc.), different specifications on the final product (i.e. pulp for different paper grades, dissolving pulp for the textile industry, speciality pulp for chemical applications, etc.) and due to the constant environmental restrictions and evolution of the processes (i.e. new technologies, internal recirculation of the effluents, new bleaching sequences, etc.). A lot of studies were performed by different authors to treat BPE from kraft pulp mills in an environmental context and water reuse for a closed loop approach. However, very few studies about BPE treatment for energy-efficiency improvement, water recovery and sub-products valorization from sulphite pulp mills were found.

The use of UF/NF processes for the treatment of the E-stage BPE filtrate in a TCF sulphite pulp mill with an E-O-P bleaching sequence was evaluated.

Firstly, the BPE used in this investigation was submitted to a physicochemical analysis where it was found that is extremely diluted with around 3% (w/w) of TS, of which 50% was ash (inorganics) content due to the high quantity of caustic soda impregnated in the E-stage; the pH of the effluent is around 10.

The organic matter existing in the other half of the TS composition, is of high interest. In the P&P industries and biorefineries point of view, two compounds deserved our special attention: lignin and hemicelluloses. A concentration of 2,88 g/L for lignin and 0,19 mg/g for hemicelluloses was measured, in which xylans were the main polysaccharide (≈68%), with the raw material processed in the mill being hardwood (*eucalyptus globulus)*. By SEC analysis mass average molecular mass for both compounds was calculated being 1,32 kDa for lignins and 0,88 kDa for hemicelluloses. The fractionation of them looked hard due to the overlap and the very small difference between each one. With this being said, the aim of the project focused into concentrate both compounds.

For the pH and molecular masses of lignins and hemicelluloses presented before, two tight UF membranes (MWCO ≤ 2 kDa) and four NF membranes (MWCO ≤ 1 kDa), were chosen to test six alkali resistant membranes. Two of the NF membranes were found to be the most suitable for the process due to their high fluxes and high apparent retention levels for lignin and hemicelluloses, NF99HF and MPF36.

The best operating conditions tested for MPF36 were found to be at T=70°C, a CFV=0,8 ms^{-1} and a TMP=15 bar which gives a permeate flux (J_v) of 125 L.h^{-1}m^{-2} with apparent retention levels of 92%, 94%, 67% and 60% for lignin, hemicelluloses, TS and ash, respectively. For the - NF99HF, the best operating conditions were found to be at T=50°C, a CFV=0,8 ms^{-1} and a TMP=13 bar, giving a permeate flux (J_v) of 166 L.h^{-1}m^{-2} with apparent retention levels of 97%, 96%, 84% and 81% for lignin, hemicelluloses, TS and ash, respectively.

By evaluation of the membrane resistances, it was found that MPF36 has more than twice of NF99HF due to its higher irreversible resistance (R_{irrev}), which corresponds to the fouling caused by compounds adsorbed on the surface or within the pores of the membrane. This resistance cannot be eliminated only by passage of water, as the compounds are chemically bound to the membrane material; indeed, the performance of membrane regeneration by a chemical cleaning with an alkaline agent was evaluated, in which 81% and 95% of PWF were recovered for the MPF36 and NF99HF membrane, respectively.

Due to its higher fluxes, retentions, less resistances and higher membrane regeneration performance, the NF99HF was found to be the most suitable for the process; using that membrane, concentration studies in a batch mode were also performed.

During almost 27 hours, 68% of volume reduction (VR) was achieved, in which the permeate flux decreased 87% from the beginning until the end of the experience, caused by a concentration polarization and fouling phenomena. An average flux (J_{av}) of 24,2 $L.h^{-1}m^{-2}$ was obtained and the frictional pressure drop (ΔP) had slightly increased from 0,5 to 0,7 bar.

With a VR of 68%, the TS concentration increased from 3% to 7% (w/w) in the retentate stream. The apparent retention levels for lignin and hemicelluloses remained almost constant between 94 and 97% which highlights the great selectivity of this membrane for these compounds. Lignin content increased from 3,2 g/L to 9,4 g/L and hemicelluloses content increased from 0,2 mg/g to 0,7 mg/g.

TOC measurements were performed and for a VR of 68%, the permeate stream had a concentration of 6,2 g/L, having the feed stream started with 7,6 g/L. These results led to know which types of organic matter can be permeable; for that reason HPLC analysis was performed and it was detected the presence of acetic and formic acids.

Finally, cost estimation for an internal process modification of *Caima - Indústria de Celulose, S.A.*, which enables to concentrate their 70 m^3/h of the E-stage BPE until 68% of VR, leads to a necessary investment between 4,44M€ and 5,13M€. The NF plant would need a total membrane area of 2360 m^2, equipped with 40 Alfa Laval M38L/H modules (Plate-and-frame configuration).

The operating costs would be 326k€ per year which represents 0,87€ per m^3 of permeate or 2,14€ per m^3 of permeate if capital costs are included with an annuity factor of 10%.

6.2. Future work

Following the above-described work, it would be interesting, in future terms, to develop a more in-depth study at various levels, such as:

- Evaluate a wider range of CFVs and their advantages/disadvantages on the process;
- Study and evaluate the impact of different types of pre-treatments, like pH changes;
- Perform concentration studies until a TS concentration around 50% (w/w), which is the concentration achieved after the traditional evaporation process;
- Study the feasibility of the process with SWM and compare with the traditional evaporation;

- Study design configurations in parallel/series and to check which one will be better for an industrial scale;
- Evaluate the possibility of reusing the permeate, for example in pulp washing;
- Evaluate the possibility of fractionation the valuable sub-products, such as lignin, hemicelluloses, acetic and formic acid.

7. References

Adnan, S., Hoang, M. & Wang, H., 2009. *Research, development and application of membrane technology in the pulp and paper industry.* s.l., APPITA.

Afonso, M. D. & Pinho, M. N. d., 1990. Ultrafiltration of Bleach Effluents in Cellulose Production. *Desalination,* Volume 79, pp. 115-124.

Alfa Laval, n.d. *Flat Sheet Membranes - Nanofiltration and Reverse Osmosis Membranes.* s.l.:s.n.

Alfa Laval, n.d. *Membrane Filtration System - Alfa Laval Flat Sheet Membrane Module M38L/H.* s.l.:s.n.

Anon., n.d. [Online] Available at: http://pt.loobiz.com/conversion/rand+euro [Accessed November 2016].

Arkell, A., Krawczyk, H., Thuvander, J. & Jönsson, A.-S., 2013. Evaluation of membrane performance and cost estimates during recovery of sodium hydroxide in a hemicellulose extraction process by nanofiltration. *Separation and Purification Technology,* p. 387–393.

Arkell, A., Olsson, J. & Wallberg, O., 2014. Process performance in lignin separation from softwood black liquor by membrane filtration. *Chemical Engineering Research and Design,* Volume 92, pp. 1792-1800.

Baker, R. W., 2004. *Membrane Technology and Applications.* 2nd ed. USA: John Wiley & Sons, Ltd..

Beier, S. P., 2007. *Pressure driven membrane processes.* s.l.:s.n.

Chen, C. et al., 2015. Application of Ultrafiltration in a Paper Mill: Process Water Reuse and Membrane Fouling Analysis. *BioResources,* Volume 10, pp. 2376-2391.

Cheryan, M., 1998. *Ultrafiltration and Microfiltration Handbook.* s.l.: Taylor & Francis Routledge.

Cui, Z. F. & Muralidhara, H., 2010. *Membrane Technology - A Practical Guide to Membrane Technology and Applications in Food and Bioprocessing.* 1st ed. s.l.:Elsevier Ltd..

Dafinov, A., Font, J. & Departament, R. G.-V., 2005. Processing of black liquors by UF/NF ceramic membranes. *Desalination,* Volume 173, pp. 83-90.

Dal-Cin, M. et al., 1996. Membrane performance with a pulp mill effluent: Relative contributions of fouling mechanisms. *Journal of Membrane Science,* Volume 120, pp. 273-285.

Ebrahimi, M. et al., 2015. Treatment of the Bleaching Effluent from Sulfite Pulp Production by Ceramic Membrane Filtration. *Membranes,* Volume 6, pp. 1-15.

Fälth, F., Jönsson, A.-S. & Wimmerstedt, R., 2001. Ultrafiltration of effluents from chlorine-free, bleach plants. *Desalination,* Volume 133, pp. 155-165.

Fernández-Rodríguez, J., García, A., Coz, A. & Labidi, J., 2015. Spent sulphite liquor fractionation into lignosulphonates and fermentable sugars by ultrafiltration. *Separation and Purification Technology,* Volume 152, pp. 172-179.

Field, R., 2010. Fundamentals of Fouling. In: K. Peinemann & S. P. Nunes, eds. *Membranes for Water Treatment: Volume 4.* s.l.:WILEY-VCH Verlag GmbH & Co. KGaA.

Hellstén, S. et al., 2013. Purification process for recovering hydroxy acids from soda black liquor. *Chemical Engineering Research and Design,* Volume 91, pp. 2765-2774.

He, Y. et al., 2012. Recent advances in membrane technologies for biorefining and bioenergy production. *Biotechnology Advances,* pp. 817-858.

Holmqvist, A., Wallberg, O. & Jönsson, A.-S., 2005. Ultrafiltration of kraft black liquor from two swedish pulp mills. *Chemical Engineering Research and Design,* Volume 83, pp. 994-999.

IETS, 2016. Annex XVII - Membrane filtration for Energy-Efficient separation of lignocellulosic biomass components. In: *IETS Annual report 2015.* s.l.:s.n.

Jacobs, A. & Dahlman, O., 2001. Characterization of the Molar Masses of Hemicelluloses from Wood and Pulps Employing Size Exclusion Chromatography and Matrix-Assisted Laser Desorption Ionization Time-of-Flight Mass Spectrometry. *Biomacromolecules,* Volume 2, pp. 894-905.

Johakimu, J. K., Andrew, J., Sithole, B. B. & Syphus, E., 2016. Preliminary techno-economic assessment of recovering water and caustic soda from alkaline bleach plant effluent. *Journal of Cleaner Production,* Volume 139, pp. 914-921.

Jönsson, A.-S., 2016. Membranes for lignin and hemicellulose recovery in pulp mills. In: *Membrane Technologies for Biorefining.* UK: Elsevier, pp. 105-133.

Jönsson, A.-S., Nordin, A.-K. & Wallberg, O., 2008. Concentration and purification of lignin in hardwood kraft pulping liquor by ultrafiltration and nanofiltration. *Chemical Engineering Research and Design,* Volume 86, pp. 1271-1280.

Jönsson, A.-S. & Wallberg, O., 2009. Cost estimates of kraft lignin recovery by ultrafiltration. *Desalination,* Volume 237, pp. 254-267.

Jönsson, A.-S. & Wimmerstedt, R., 1985. The application of membrane technology in the pulp and paper industry. *Desalination,* pp. 181-196.

Koch Membrane Systems, Inc., 2014. *Kms flat sheet membrane samples.* s.l.:s.n.

Kukkola, J. et al., 2011. Size-exclusion chromatographic study of ECF and TCF softwood kraft pulp bleaching liquors. *Environmental Science and Pollution Research,* pp. 1049-1056.

Microdyn-Nadir, 2007. *The art to clear solutions.* s.l.:s.n.

Mulder, M., 1996. *Basic Principles of Membrane Technology.* 2nd ed. Netherlands: Kluwer Academic Publishers.

National Institute of Standards & Technology, 2014. *Reference Material 8494 - Wheat Straw Whole Biomass Feedstock,* Gaithersburg, MD 20899: NIST.

Niemi, H. et al., 2011. Fractionation of Organic and Inorganic Compounds from Black Liquor by Combining Membrane Separation and Crystallization. *Chemical Engineering and Technology,* Volume 34, pp. 593-598.

Nilsson, M., Lipnizki, F., Trägårdh, G. & Östergren, K., n.d. *Energy evaluation of a nanofiltration plant operated at elevated temperatures,* Lund, Sweden: Lund University.

Nordin, A.-K. & Jönsson, A.-S., 2006. Case study of an ultrafiltration plant treating bleach plant effluent from a pulp and paper mill. *Desalination 201,* p. 277–289.

Nordin, A.-K. & Jönsson, A.-S., 2008. Optimisation of membrane area and energy requirement in tubular membrane modules. *Chemical Engineering and Processing 47,* p. 1090–1097.

Olsen, O., 1980. Membrane technology in the pulp and paper industry. *Desalination,* pp. 291-302.

Olsson, J., 2013. *Separation of lignin and hemicelluloses from black liquor and pre-treated black liquor by nanofiltration,* Lund University: Department of Chemical Engineering.

Oñate, E., Rodríguez, E., Bórquez, R. & Zaror, C., 2015. Membrane treatment of alkaline bleaching effluents from elementary chlorine free kraft softwood cellulose production. *Environmental Technology,* Volume 36, pp. 890-900.

Persson, T. & Jönsson, A.-S., 2009. Fouling of Ultrafiltration Membranes during Isolation of Hemicelluloses in the Forest Industry. *Scholarly Research Exchange,* pp. 1-7.

Persson, T. & Jönsson, A.-S., 2010. Isolation of hemicelluloses by ultrafiltration of thermomechanical pulp mill process water - Influence of operating conditions. *Chemical Engineering Research and Design,* Volume 2010, pp. 1548-1554.

Pinho, M. d., Minhalma, M., Rosa, M. & Taborda, F., 2000. Integration of flotation/ultrafiltration for treatment of bleached pulp effluent. *Pulp & Paper Canada,* Volume 101, pp. 50-54.

Quezada, R. et al., 2014. Membrane treatment of the bleaching plant (EPO) filtrate of a kraft pulp mill. *Water Science & Technology,* pp. 843-850.

Restolho, J. A., Prates, A., Pinho, M. N. d. & Afonso, M. D., 2009. Sugars and lignosulphonates recovery from eucalyptus spent sulphite liquor by membrane processes. *Biomass and Bioenergy,* Volume 33, pp. 1558-1566.

Rosa, M. J. & Pinho, M. N. d., 1995. The role of ultrafiltration and nanofiltration on the minimisation of the environmental impact of bleached pulp effluents. *Journal of Membrane Science,* Volume 102, pp. 155-161.

Scott, K., 1998. *Handbook of Industrial Membranes.* 2nd ed. s.l.:Elsevier Science Limited.

Shukla, S. K., Kumar, V. & Bansal, M. C., 2008. *Application of Membrane Filtration for Reuse of Bleaching Plant Effluent in the Process.* Malta, WSEAS.

Shukla, S. K., Kumar, V. & Bansal, M. C., 2010. Treatment of combined bleaching effluent by membrane filtration technology for system closure in paper industry. *Desalination and Water Treatment,* Volume 13, pp. 464-470.

Shukla, S. K., Kumar, V., Kim, T. & Bansal, M. C., 2013. Membrane filtration of chlorination and extraction stage bleach plant effluent in Indian paper Industry. *Clean Technologies and Environmental Policy,* Volume 15, pp. 235-243.

Strathmann, H., 1986. Synthetic Membranes and Their Preparation. In: P. Bungay, H. Lonsdale & M. d. Pinho, eds. *Synthetic Membranes: Science, Engineering and Applications.* s.l.:Springer Netherlands, pp. 1-37.

Suhr, M. et al., 2015. *Best Available Techniques (BAT) Reference Document for the Production of Pulp, Paper and Board.* Luxembourg: Publications Office of the European Union.

Toledano, A., García, A., Mondragon, I. & Labidi, J., 2010. Lignin separation and fractionation by ultrafiltration. *Separation and Purification Technology,* Volume 71, pp. 38-43.

Toledano, A. et al., 2010. Comparative study of lignin fractionation by ultrafiltration and selective precipitation. *Chemical Engineering Journal,* Volume 157, pp. 93-99.

Wagner, J., 2000. *Membrane Filtration Handbook: Practical Tips and Hints.* 2nd ed. s.l.:Osmonics, Inc..

Wallberg, O., Jönsson, A.-S. & Wickström, P., 2001. Membrane cleaning - a case study in a sulphite pulp mill bleach plant. *Desalination,* Volume 141, pp. 259-268.

Wallberg, O., Jönsson, A.-S. & Wimmerstedt, R., 2003. Fractionation and concentration of kraft black liquor lignin with ultrafiltration. *Desalination,* Volume 154, pp. 187-199.

YLCE, n.d. [Online] Available at: https://www.ylce.pt/UsefullInformation/PriceTable [Accessed Novembro 2016].

8. Annexes

Annex A – Physicochemical characterization of fractionated streams

Table 21 - Physicochemical characterization of retentates and permeates for a VR of 0%, 10% and 20%

	VR=0%		**VR=10%**		**VR=20%**	
	Retentate	**Permeate**	**Retentate**	**Permeate**	**Retentate**	**Permeate**
pH	9,75	9,42	9,74	9,48	9,71	9,45
ρ (g/L)	1022	1016	1015	1009	1017	1012
TS (mg/g)	28,31	9,36	30,55	10,39	33,34	11,18
Ash (mg/g)	14,35	5,75	15,06	6,45	16,23	6,83
Total lignin (g/L)	3,22	0,19	3,60	0,21	3,99	0,23
Acid soluble lignin (mg/g)	1,20	0,08	1,25	0,09	1,45	0,10
Klason lignin (mg/g)	1,51	n.a.	1,78	n.a.	2,04	n.a.
Hemicelluloses (mg/g)	0,18	0,009	0,21	0,007	0,23	0,007
Arabinose (mg/g)	0,00	0,001	0,00	0,001	0,00	0,001
Galactose (mg/g)	0,00	0,000	0,00	0,000	0,00	0,000
Glucose (mg/g)	0,03	0,003	0,03	0,003	0,03	0,003
Mannose (mg/g)	0,02	0,003	0,03	0,000	0,03	0,000
Xylose (mg/g)	0,13	0,003	0,14	0,003	0,16	0,003
Others (mg/g)	10,56	3,42	11,69	3,72	12,89	4,12
Total carbon (g/L)	7,80	2,05	8,54	2,34	9,24	2,53
Inorganic carbon (g/L)	0,23	0,17	0,25	0,18	0,27	0,20
Total organic carbon (g/L)	7,57	1,88	8,28	2,16	8,98	2,33

Table 22 - Physicochemical characterization of retentates and permeates for a VR of 30%, 40% and 50%

	VR=30%		**VR=40%**		**VR=50%**	
	Retentate	**Permeate**	**Retentate**	**Permeate**	**Retentate**	**Permeate**
pH	9,70	9,39	9,46	9,10	9,49	9,16
ρ (g/L)	1020	1013	1019	1013	1023	1014
TS (mg/g)	36,57	12,32	41,17	14,71	46,62	17,24
Ash (mg/g)	16,59	6,26	19,75	8,78	22,84	9,93
Total lignin (g/L)	4,54	0,25	5,10	0,23	6,35	0,27
Acid soluble lignin (mg/g)	1,56	0,11	1,74	0,11	2,06	0,13
Klason lignin (mg/g)	2,25	n.a.	2,65	n.a.	3,35	n.a.
Hemicelluloses (mg/g)	0,27	0,007	0,31	0,008	0,39	0,012
Arabinose (mg/g)	0,01	0,001	0,01	0,001	0,01	0,001
Galactose (mg/g)	0,00	0,000	0,00	0,000	0,00	0,000
Glucose (mg/g)	0,04	0,003	0,04	0,003	0,05	0,004
Mannose (mg/g)	0,03	0,000	0,04	0,000	0,05	0,003
Xylose (mg/g)	0,19	0,003	0,23	0,004	0,28	0,005
Others (mg/g)	15,17	4,80	16,01	5,69	17,04	7,03
Total carbon (g/L)	10,42	2,74	11,70	3,26	13,62	3,89
Inorganic carbon (g/L)	0,29	0,21	0,30	0,28	0,31	0,30
Total organic carbon (g/L)	10,13	2,53	11,40	2,99	13,32	3,59

Table 23 - Physicochemical characterization of retentates and permeates for a VR of 60%, 65% and 68%

	VR=60%		**VR=65%**		**VR=68%**	
	Retentate	**Permeate**	**Retentate**	**Permeate**	**Retentate**	**Permeate**
pH	9,41	9,22	9,39	9,11	9,44	9,29
ρ (g/L)	1028	1012	1030	1011	1031	1022
TS (mg/g)	56,29	21,48	63,12	24,38	68,25	26,96
Ash (mg/g)	27,89	12,29	30,41	13,43	32,53	14,58
Total lignin (g/L)	7,30	0,31	8,58	0,37	9,40	0,42
Acid soluble lignin (mg/g)	2,62	0,14	2,89	0,16	3,25	0,18
Klason lignin (mg/g)	4,51	n.a.	5,53	n.a.	6,09	0,06
Hemicelluloses (mg/g)	0,52	0,014	0,61	0,017	0,70	0,018
Arabinose (mg/g)	0,01	0,001	0,00	0,001	0,00	0,001
Galactose (mg/g)	0,00	0,000	0,00	0,000	0,00	0,000
Glucose (mg/g)	0,07	0,004	0,09	0,005	0,09	0,005
Mannose (mg/g)	0,07	0,003	0,08	0,004	0,09	0,004
Xylose (mg/g)	0,37	0,006	0,44	0,007	0,51	0,008
Others (mg/g)	20,58	8,87	23,52	10,56	25,62	11,95
Total carbon (g/L)	17,09	5,08	18,89	5,86	20,72	6,57
Inorganic carbon (g/L)	0,32	0,36	0,32	0,39	0,35	0,40
Total organic carbon (g/L)	16,76	4,72	18,57	5,48	20,36	6,17

Annex B – HPLC Analysis: Standards and fractionated streams

==== Shimadzu LCsolution Browser Report ====

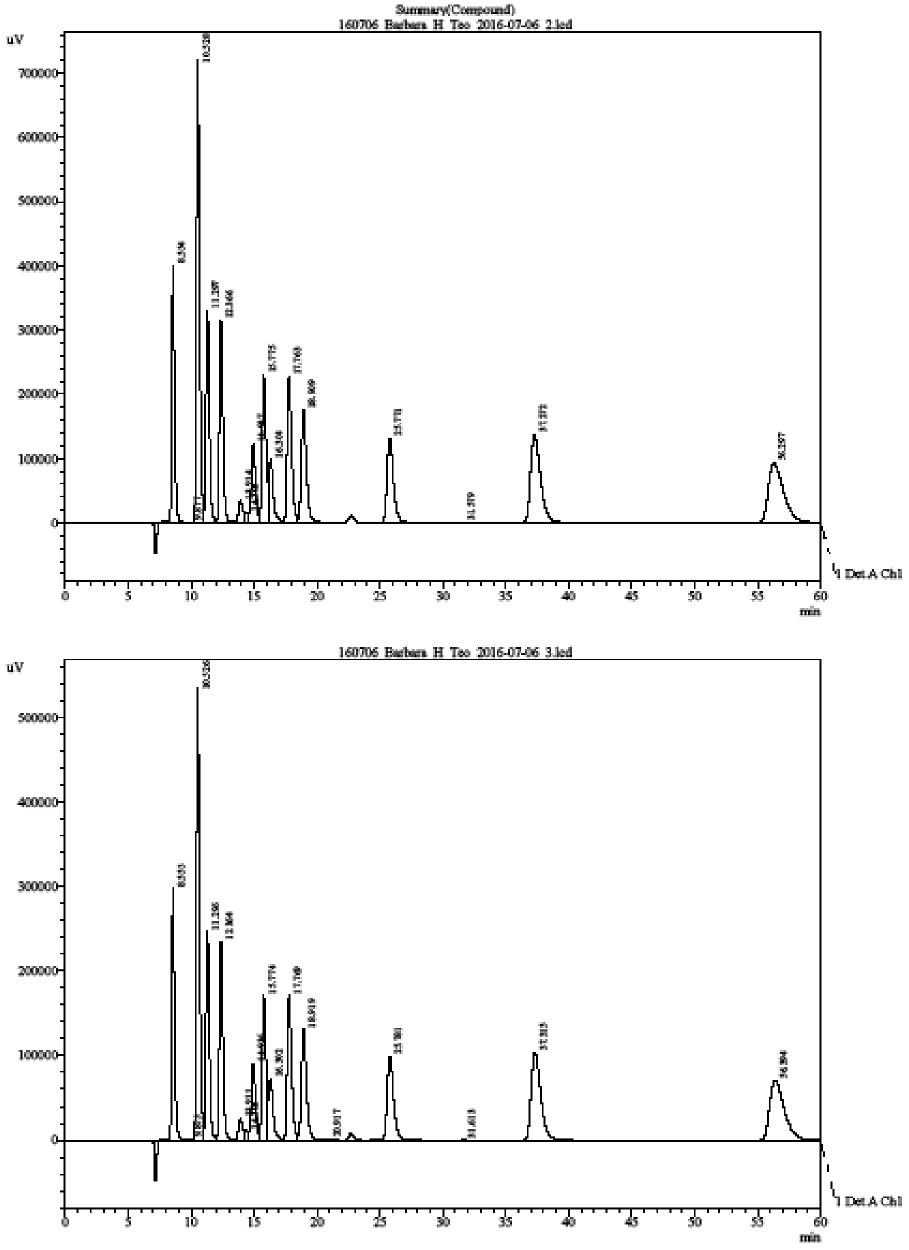

Figure 35 - HPLC standards concentrations 1 and 2

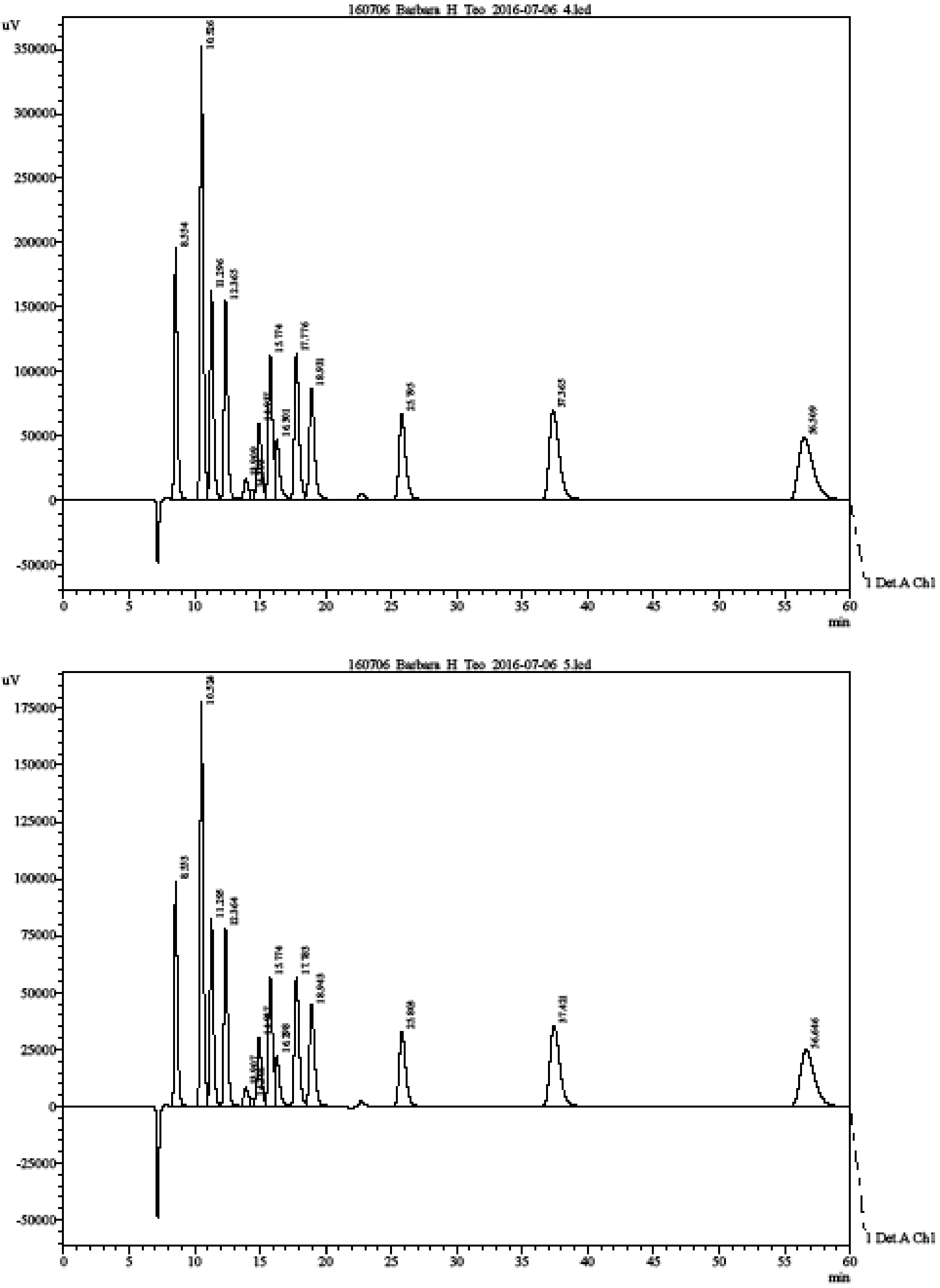

Figure 36 - HPLC standards concentrations 3 and 4

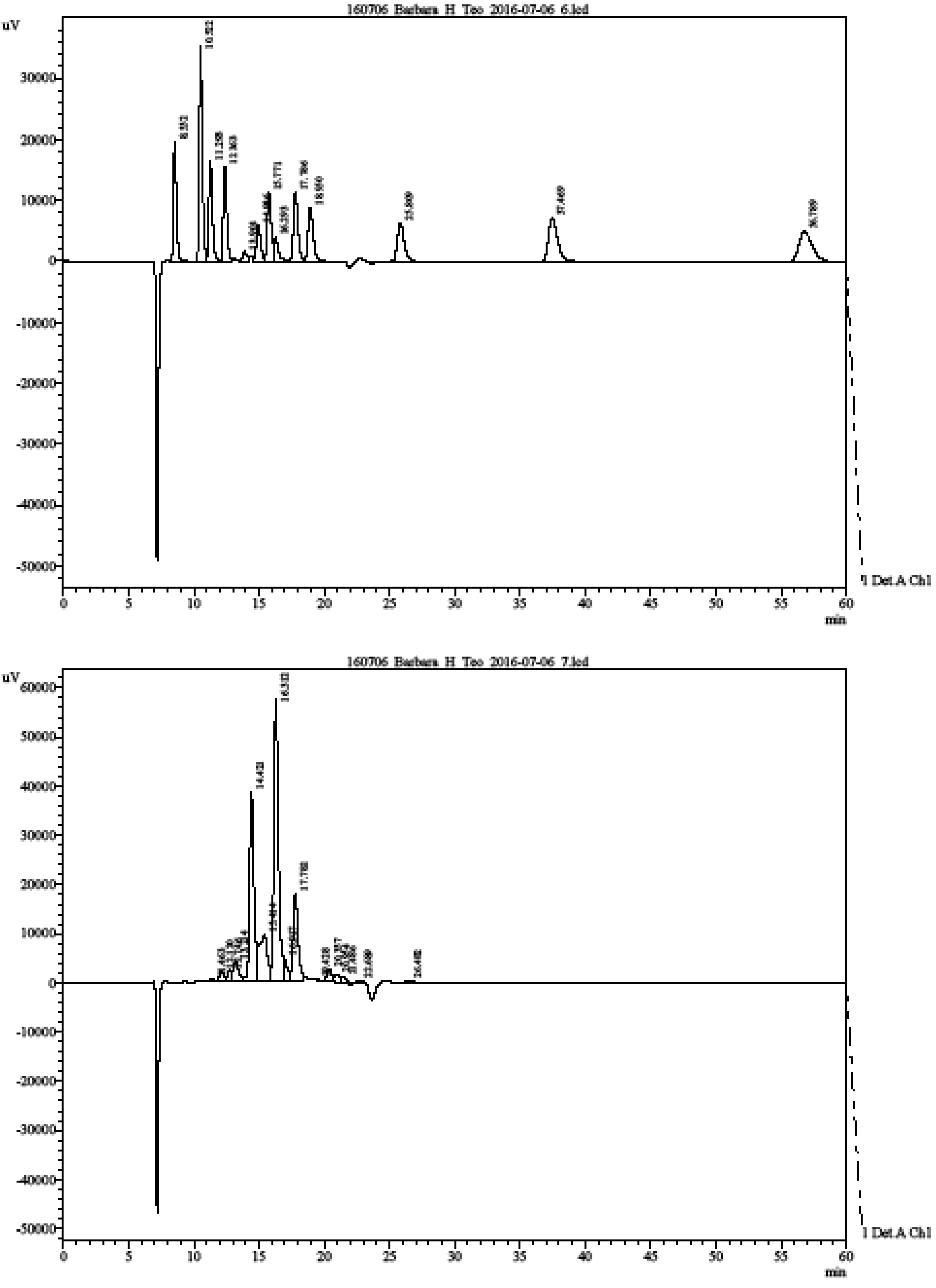

Figure 37 - HPLC standard concentration 5 and Permeate VR=0%

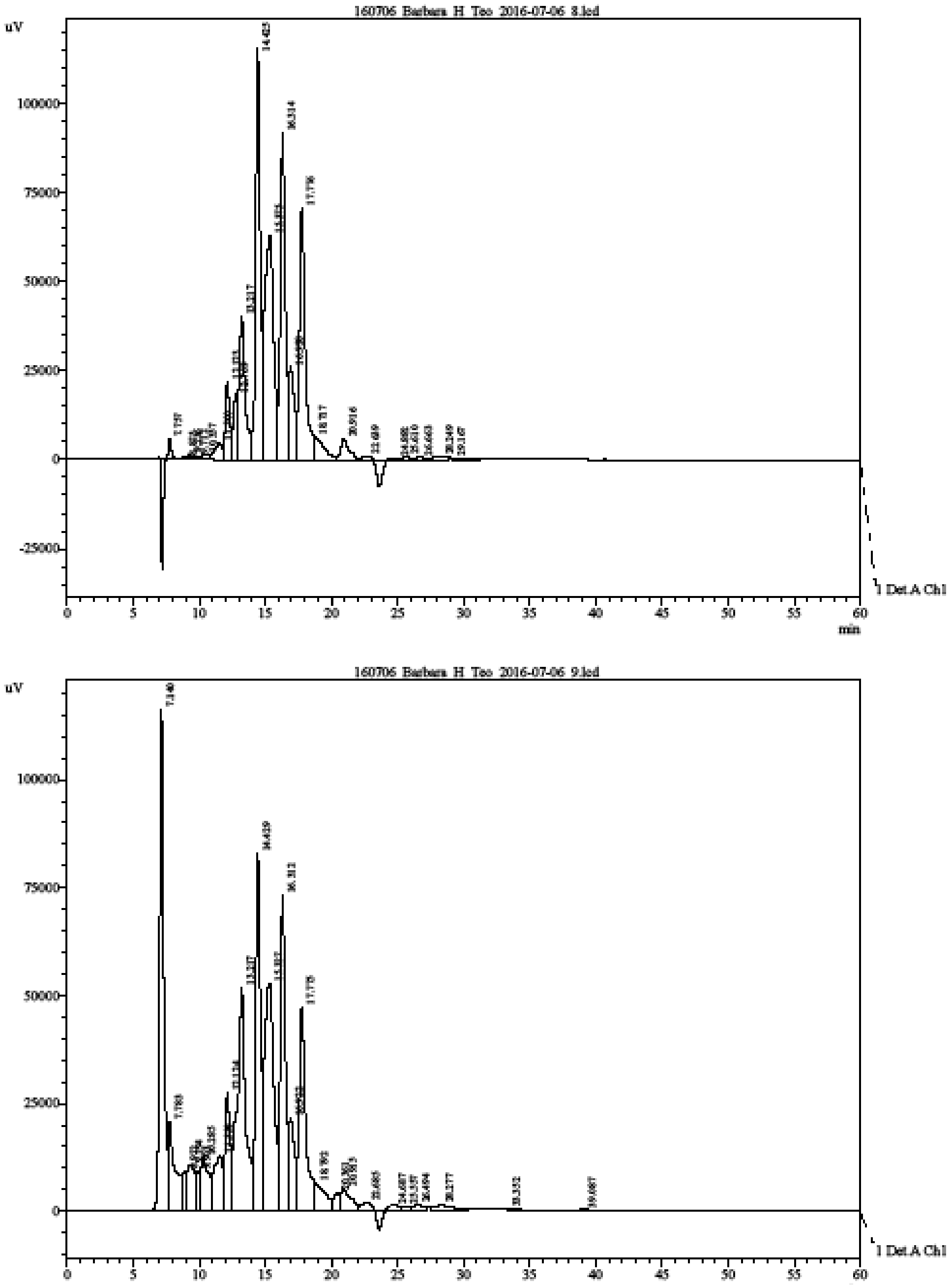

Figure 38 - HPLC Permeate VR=68% and Retentate VR=0%

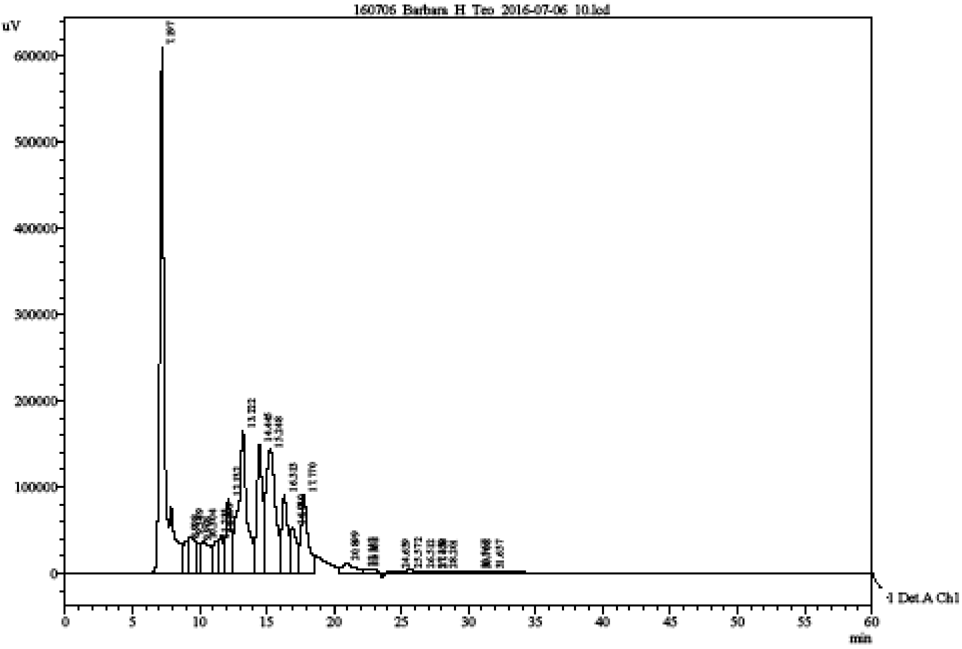

<< Detector A >>

ID#1 Compound Name: Cellobiose

Title	Sample Name	Sample ID	Ret. Time	Area	Height	Conc.
160706 Barbara H Teo 2016-07-06 2.l	Standard Sampl	STD-0001	8.554	6547379	399700	5.038
160706 Barbara H Teo 2016-07-06 3.l	Standard Sampl	STD-0002	8.553	4891113	297536	3.763
160706 Barbara H Teo 2016-07-06 4.l	Standard Sampl	STD-0003	8.554	3151829	195224	2.425
160706 Barbara H Teo 2016-07-06 5.l	Standard Sampl	STD-0004	8.553	1615272	99125	1.243
160706 Barbara H Teo 2016-07-06 6.l	Standard Sampl	STD-0005	8.552	321915	19676	0.248
160706 Barbara H Teo 2016-07-06 7.l	P0	UNK-0001	0.000	0	0	0.000
160706 Barbara H Teo 2016-07-06 8.l	P68	UNK-0002	8.875	20513	641	0.016
160706 Barbara H Teo 2016-07-06 9.l	C0	UNK-0003	8.922	199074	9294	0.153
160706 Barbara H Teo 2016-07-06 10	C68	UNK-0004	8.998	712622	37075	0.548
Average			8.695	2182465	132284	1.679
%RSD			2.283	112.075	113.602	112.075
Maximum			8.998	6547379	399700	5.038
Minimum			8.552	20513	641	0.016
Standard Deviation			0.198	2446005	150277	1.882

ID#2 Compound Name: Glucose

Title	Sample Name	Sample ID	Ret. Time	Area	Height	Conc.
160706 Barbara H Teo 2016-07-06 2.l	Standard Sampl	STD-0001	10.528	12548469	721890	10.044
160706 Barbara H Teo 2016-07-06 3.l	Standard Sampl	STD-0002	10.526	9365807	536641	7.497
160706 Barbara H Teo 2016-07-06 4.l	Standard Sampl	STD-0003	10.526	6173902	352321	4.942
160706 Barbara H Teo 2016-07-06 5.l	Standard Sampl	STD-0004	10.524	3132321	178020	2.507
160706 Barbara H Teo 2016-07-06 6.l	Standard Sampl	STD-0005	10.522	624618	35357	0.500
160706 Barbara H Teo 2016-07-06 7.l	P0	UNK-0001	0.000	0	0	0.000
160706 Barbara H Teo 2016-07-06 8.l	P68	UNK-0002	10.357	58960	1464	0.047
160706 Barbara H Teo 2016-07-06 9.l	C0	UNK-0003	10.285	513451	12419	0.411
160706 Barbara H Teo 2016-07-06 10	C68	UNK-0004	10.304	1722906	36688	1.379
Average			10.446	4267554	234350	3.416
%RSD			1.059	108.848	117.229	108.848
Maximum			10.528	12548469	721890	10.044
Minimum			10.285	58960	1464	0.047
Standard Deviation			0.111	4645127	274727	3.718

ID#3 Compound Name: XyGaMa

Title	Sample Name	Sample ID	Ret. Time	Area	Height	Conc.
160706 Barbara H Teo 2016-07-06 2.l	Standard Sampl	STD-0001	11.297	6160260	330980	5.031
160706 Barbara H Teo 2016-07-06 3.l	Standard Sampl	STD-0002	11.296	4593361	246633	3.752
160706 Barbara H Teo 2016-07-06 4.l	Standard Sampl	STD-0003	11.296	3018917	162253	2.466
160706 Barbara H Teo 2016-07-06 5.l	Standard Sampl	STD-0004	11.295	1538076	82259	1.256
160706 Barbara H Teo 2016-07-06 6.l	Standard Sampl	STD-0005	11.293	306328	16364	0.250
160706 Barbara H Teo 2016-07-06 7.l	P0	UNK-0001	11.463	13829	477	0.011
160706 Barbara H Teo 2016-07-06 8.l	P68	UNK-0002	11.500	191496	4909	0.156
160706_Barbara_H_Teo_2016-07-06_9.l	C0	UNK-0003	11.558	604121	13064	0.493

Figure 39 - HPLC Retentate VR=68% and summarized tables 1

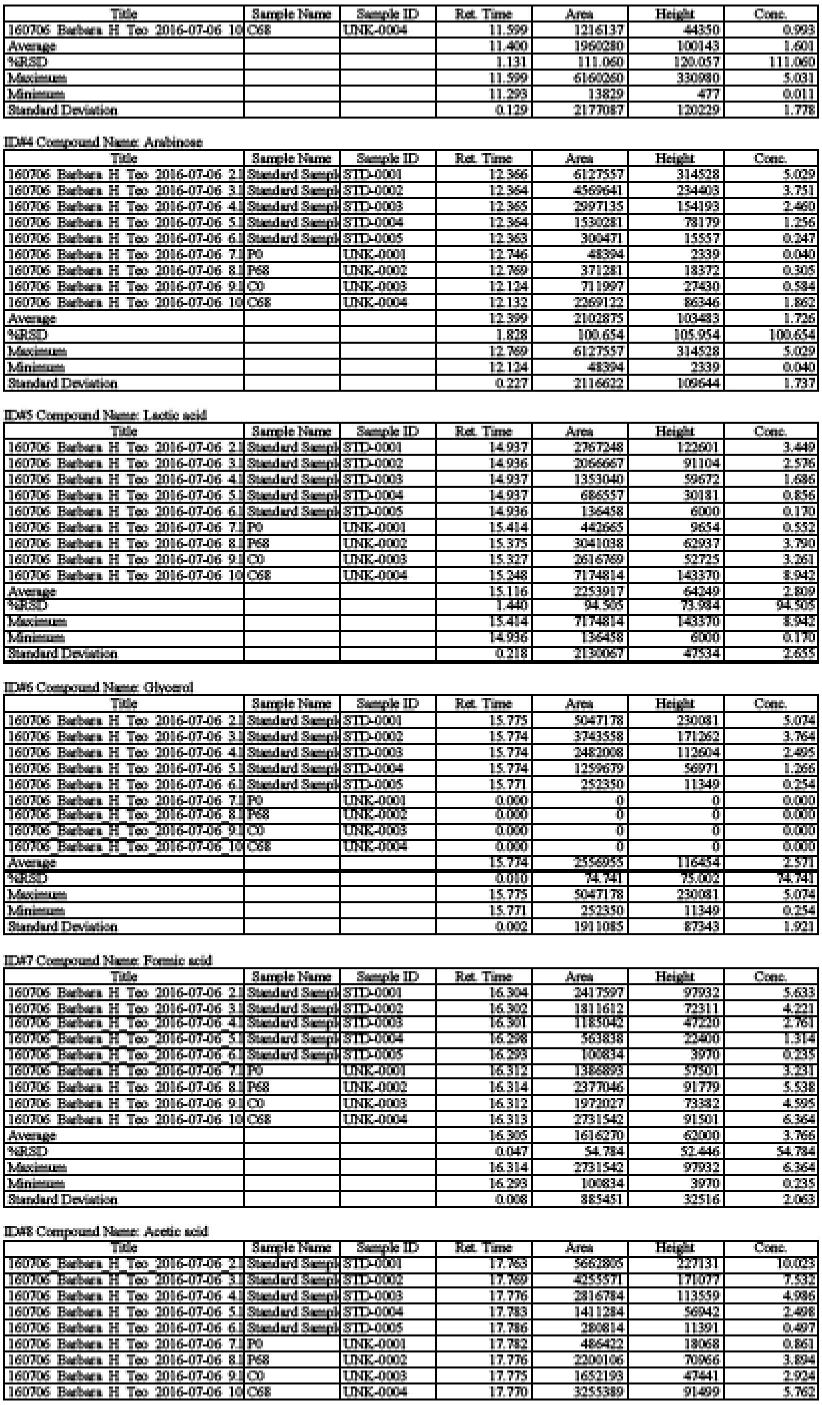

Title	Sample Name	Sample ID	Ret. Time	Area	Height	Conc.
160706_Barbara_H_Teo_2016-07-06_10	C68	UNK-0004	11.599	1216137	44350	0.993
Average			11.400	1960280	100143	1.601
%RSD			1.131	111.060	120.057	111.060
Maximum			11.599	6160260	330980	5.031
Minimum			11.293	13829	477	0.011
Standard Deviation			0.129	2177087	120229	1.778

ID#4 Compound Name: Arabinose

Title	Sample Name	Sample ID	Ret. Time	Area	Height	Conc.
160706_Barbara_H_Teo_2016-07-06_2.l	Standard Sampl	STD-0001	12.366	6127557	314528	5.029
160706_Barbara_H_Teo_2016-07-06_3.l	Standard Sampl	STD-0002	12.364	4569641	234403	3.751
160706_Barbara_H_Teo_2016-07-06_4.l	Standard Sampl	STD-0003	12.365	2997135	154193	2.460
160706_Barbara_H_Teo_2016-07-06_5.l	Standard Sampl	STD-0004	12.364	1530281	78179	1.256
160706_Barbara_H_Teo_2016-07-06_6.l	Standard Sampl	STD-0005	12.363	300471	15557	0.247
160706_Barbara_H_Teo_2016-07-06_7.l	P0	UNK-0001	12.746	48394	2339	0.040
160706_Barbara_H_Teo_2016-07-06_8.l	P68	UNK-0002	12.769	371281	18372	0.305
160706_Barbara_H_Teo_2016-07-06_9.l	C0	UNK-0003	12.124	711997	27430	0.584
160706_Barbara_H_Teo_2016-07-06_10	C68	UNK-0004	12.132	2269122	86346	1.862
Average			12.399	2102875	103483	1.726
%RSD			1.828	100.654	105.954	100.654
Maximum			12.769	6127557	314528	5.029
Minimum			12.124	48394	2339	0.040
Standard Deviation			0.227	2116622	109644	1.737

ID#5 Compound Name: Lactic acid

Title	Sample Name	Sample ID	Ret. Time	Area	Height	Conc.
160706_Barbara_H_Teo_2016-07-06_2.l	Standard Sampl	STD-0001	14.937	2767248	122601	3.449
160706_Barbara_H_Teo_2016-07-06_3.l	Standard Sampl	STD-0002	14.936	2066667	91104	2.576
160706_Barbara_H_Teo_2016-07-06_4.l	Standard Sampl	STD-0003	14.937	1353040	59672	1.686
160706_Barbara_H_Teo_2016-07-06_5.l	Standard Sampl	STD-0004	14.937	686557	30181	0.856
160706_Barbara_H_Teo_2016-07-06_6.l	Standard Sampl	STD-0005	14.936	136458	6000	0.170
160706_Barbara_H_Teo_2016-07-06_7.l	P0	UNK-0001	15.414	442665	9654	0.552
160706_Barbara_H_Teo_2016-07-06_8.l	P68	UNK-0002	15.375	3041038	62937	3.790
160706_Barbara_H_Teo_2016-07-06_9.l	C0	UNK-0003	15.327	2616769	52725	3.261
160706_Barbara_H_Teo_2016-07-06_10	C68	UNK-0004	15.248	7174814	143370	8.942
Average			15.116	2253917	64249	2.809
%RSD			1.440	94.505	73.984	94.505
Maximum			15.414	7174814	143370	8.942
Minimum			14.936	136458	6000	0.170
Standard Deviation			0.218	2130067	47534	2.655

ID#6 Compound Name: Glycerol

Title	Sample Name	Sample ID	Ret. Time	Area	Height	Conc.
160706_Barbara_H_Teo_2016-07-06_2.l	Standard Sampl	STD-0001	15.775	5047178	230081	5.074
160706_Barbara_H_Teo_2016-07-06_3.l	Standard Sampl	STD-0002	15.774	3743558	171262	3.764
160706_Barbara_H_Teo_2016-07-06_4.l	Standard Sampl	STD-0003	15.774	2482008	112604	2.495
160706_Barbara_H_Teo_2016-07-06_5.l	Standard Sampl	STD-0004	15.774	1259679	56971	1.266
160706_Barbara_H_Teo_2016-07-06_6.l	Standard Sampl	STD-0005	15.771	252350	11349	0.254
160706_Barbara_H_Teo_2016-07-06_7.l	P0	UNK-0001	0.000	0	0	0.000
160706_Barbara_H_Teo_2016-07-06_8.l	P68	UNK-0002	0.000	0	0	0.000
160706_Barbara_H_Teo_2016-07-06_9.l	C0	UNK-0003	0.000	0	0	0.000
160706_Barbara_H_Teo_2016-07-06_10	C68	UNK-0004	0.000	0	0	0.000
Average			15.774	2556955	116454	2.571
%RSD			0.010	74.741	75.002	74.741
Maximum			15.775	5047178	230081	5.074
Minimum			15.771	252350	11349	0.254
Standard Deviation			0.002	1911085	87343	1.921

ID#7 Compound Name: Formic acid

Title	Sample Name	Sample ID	Ret. Time	Area	Height	Conc.
160706_Barbara_H_Teo_2016-07-06_2.l	Standard Sampl	STD-0001	16.304	2417597	97932	5.633
160706_Barbara_H_Teo_2016-07-06_3.l	Standard Sampl	STD-0002	16.302	1811612	72311	4.221
160706_Barbara_H_Teo_2016-07-06_4.l	Standard Sampl	STD-0003	16.301	1185042	47220	2.761
160706_Barbara_H_Teo_2016-07-06_5.l	Standard Sampl	STD-0004	16.298	563838	22400	1.314
160706_Barbara_H_Teo_2016-07-06_6.l	Standard Sampl	STD-0005	16.293	100834	3970	0.235
160706_Barbara_H_Teo_2016-07-06_7.l	P0	UNK-0001	16.312	1386893	57501	3.231
160706_Barbara_H_Teo_2016-07-06_8.l	P68	UNK-0002	16.314	2377046	91779	5.538
160706_Barbara_H_Teo_2016-07-06_9.l	C0	UNK-0003	16.312	1972027	73382	4.595
160706_Barbara_H_Teo_2016-07-06_10	C68	UNK-0004	16.313	2731542	91501	6.364
Average			16.305	1616270	62000	3.766
%RSD			0.047	54.784	52.446	54.784
Maximum			16.314	2731542	97932	6.364
Minimum			16.293	100834	3970	0.235
Standard Deviation			0.008	885451	32516	2.063

ID#8 Compound Name: Acetic acid

Title	Sample Name	Sample ID	Ret. Time	Area	Height	Conc.
160706_Barbara_H_Teo_2016-07-06_2.l	Standard Sampl	STD-0001	17.763	5662805	227131	10.023
160706_Barbara_H_Teo_2016-07-06_3.l	Standard Sampl	STD-0002	17.769	4255571	171077	7.532
160706_Barbara_H_Teo_2016-07-06_4.l	Standard Sampl	STD-0003	17.776	2816784	113559	4.986
160706_Barbara_H_Teo_2016-07-06_5.l	Standard Sampl	STD-0004	17.783	1411284	56942	2.498
160706_Barbara_H_Teo_2016-07-06_6.l	Standard Sampl	STD-0005	17.786	280814	11391	0.497
160706_Barbara_H_Teo_2016-07-06_7.l	P0	UNK-0001	17.782	486422	18068	0.861
160706_Barbara_H_Teo_2016-07-06_8.l	P68	UNK-0002	17.776	2200106	70966	3.894
160706_Barbara_H_Teo_2016-07-06_9.l	C0	UNK-0003	17.775	1652193	47441	2.924
160706_Barbara_H_Teo_2016-07-06_10	C68	UNK-0004	17.770	3255389	91499	5.762

Figure 40 - HPLC summarized tables 2

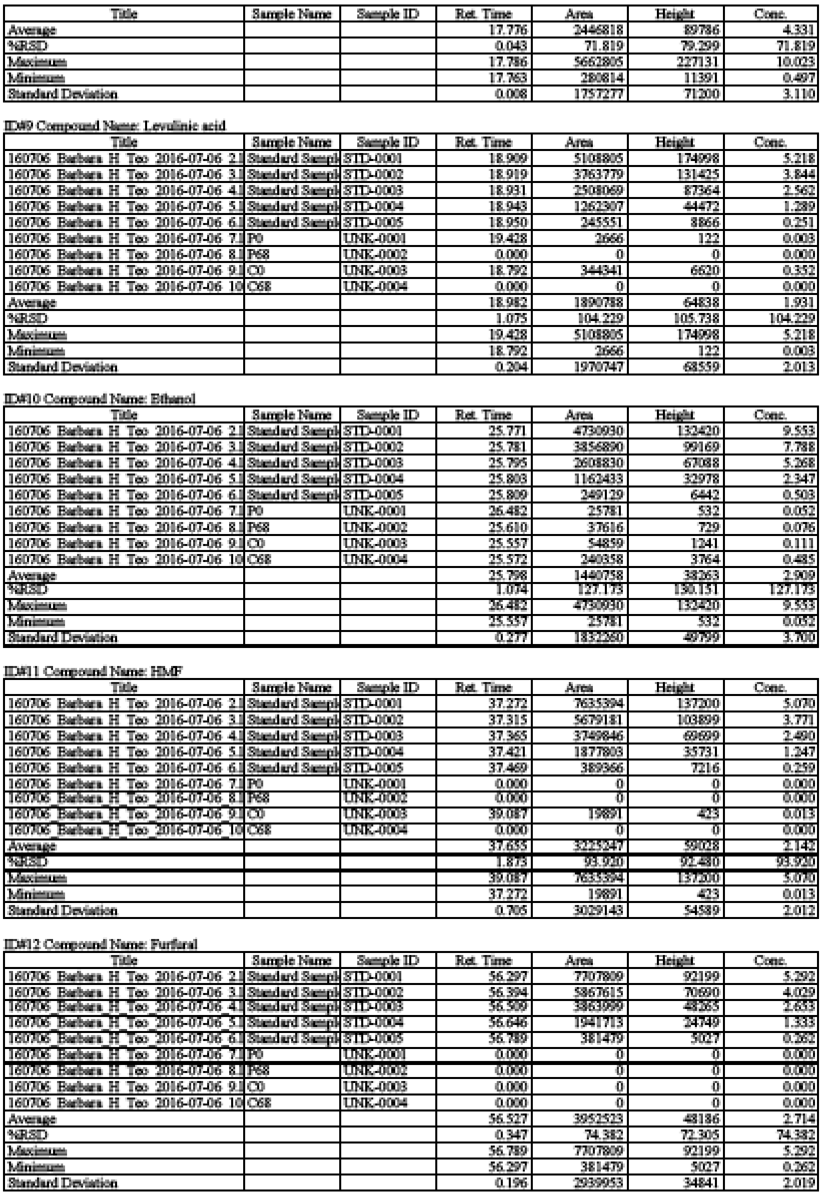

Title	Sample Name	Sample ID	Ret. Time	Area	Height	Conc.
Average			17.776	2446818	89786	4.331
%RSD			0.043	71.819	79.299	71.819
Maximum			17.786	5662805	227131	10.023
Minimum			17.763	280814	11391	0.497
Standard Deviation			0.008	1757277	71200	3.110

ID#9 Compound Name: Levulinic acid

Title	Sample Name	Sample ID	Ret. Time	Area	Height	Conc.
160706_Barbara_H_Teo_2016-07-06_2.l	Standard Sampl	STD-0001	18.909	5108805	174998	5.218
160706_Barbara_H_Teo_2016-07-06_3.l	Standard Sampl	STD-0002	18.919	3763779	131425	3.844
160706_Barbara_H_Teo_2016-07-06_4.l	Standard Sampl	STD-0003	18.931	2508069	87364	2.562
160706_Barbara_H_Teo_2016-07-06_5.l	Standard Sampl	STD-0004	18.943	1262307	44472	1.289
160706_Barbara_H_Teo_2016-07-06_6.l	Standard Sampl	STD-0005	18.950	245551	8866	0.251
160706_Barbara_H_Teo_2016-07-06_7.l	P0	UNK-0001	19.428	2666	122	0.003
160706_Barbara_H_Teo_2016-07-06_8.l	P68	UNK-0002	0.000	0	0	0.000
160706_Barbara_H_Teo_2016-07-06_9.l	C0	UNK-0003	18.792	344341	6620	0.352
160706_Barbara_H_Teo_2016-07-06_10	C68	UNK-0004	0.000	0	0	0.000
Average			18.982	1890788	64838	1.931
%RSD			1.075	104.229	105.738	104.229
Maximum			19.428	5108805	174998	5.218
Minimum			18.792	2666	122	0.003
Standard Deviation			0.204	1970747	68559	2.013

ID#10 Compound Name: Ethanol

Title	Sample Name	Sample ID	Ret. Time	Area	Height	Conc.
160706_Barbara_H_Teo_2016-07-06_2.l	Standard Sampl	STD-0001	25.771	4730930	132420	9.553
160706_Barbara_H_Teo_2016-07-06_3.l	Standard Sampl	STD-0002	25.781	3856890	99169	7.788
160706_Barbara_H_Teo_2016-07-06_4.l	Standard Sampl	STD-0003	25.795	2608830	67088	5.268
160706_Barbara_H_Teo_2016-07-06_5.l	Standard Sampl	STD-0004	25.803	1162433	32978	2.347
160706_Barbara_H_Teo_2016-07-06_6.l	Standard Sampl	STD-0005	25.809	249129	6442	0.503
160706_Barbara_H_Teo_2016-07-06_7.l	P0	UNK-0001	26.482	25781	532	0.052
160706_Barbara_H_Teo_2016-07-06_8.l	P68	UNK-0002	25.610	37616	729	0.076
160706_Barbara_H_Teo_2016-07-06_9.l	C0	UNK-0003	25.557	54859	1241	0.111
160706_Barbara_H_Teo_2016-07-06_10	C68	UNK-0004	25.572	240358	3764	0.485
Average			25.798	1440758	38263	2.909
%RSD			1.074	127.173	130.151	127.173
Maximum			26.482	4730930	132420	9.553
Minimum			25.557	25781	532	0.052
Standard Deviation			0.277	1832260	49799	3.700

ID#11 Compound Name: HMF

Title	Sample Name	Sample ID	Ret. Time	Area	Height	Conc.
160706_Barbara_H_Teo_2016-07-06_2.l	Standard Sampl	STD-0001	37.272	7635394	137200	5.070
160706_Barbara_H_Teo_2016-07-06_3.l	Standard Sampl	STD-0002	37.315	5679181	103899	3.771
160706_Barbara_H_Teo_2016-07-06_4.l	Standard Sampl	STD-0003	37.365	3749846	69699	2.490
160706_Barbara_H_Teo_2016-07-06_5.l	Standard Sampl	STD-0004	37.421	1877803	35731	1.247
160706_Barbara_H_Teo_2016-07-06_6.l	Standard Sampl	STD-0005	37.469	389366	7216	0.259
160706_Barbara_H_Teo_2016-07-06_7.l	P0	UNK-0001	0.000	0	0	0.000
160706_Barbara_H_Teo_2016-07-06_8.l	P68	UNK-0002	0.000	0	0	0.000
160706_Barbara_H_Teo_2016-07-06_9.l	C0	UNK-0003	39.087	19891	423	0.013
160706_Barbara_H_Teo_2016-07-06_10	C68	UNK-0004	0.000	0	0	0.000
Average			37.655	3225247	59028	2.142
%RSD			1.873	93.920	92.480	93.920
Maximum			39.087	7635394	137200	5.070
Minimum			37.272	19891	423	0.013
Standard Deviation			0.705	3029143	54589	2.012

ID#12 Compound Name: Furfural

Title	Sample Name	Sample ID	Ret. Time	Area	Height	Conc.
160706_Barbara_H_Teo_2016-07-06_2.l	Standard Sampl	STD-0001	56.297	7707809	92199	5.292
160706_Barbara_H_Teo_2016-07-06_3.l	Standard Sampl	STD-0002	56.394	5867615	70690	4.029
160706_Barbara_H_Teo_2016-07-06_4.l	Standard Sampl	STD-0003	56.509	3863999	48265	2.653
160706_Barbara_H_Teo_2016-07-06_5.l	Standard Sampl	STD-0004	56.646	1941713	24749	1.333
160706_Barbara_H_Teo_2016-07-06_6.l	Standard Sampl	STD-0005	56.789	381479	5027	0.262
160706_Barbara_H_Teo_2016-07-06_7.l	P0	UNK-0001	0.000	0	0	0.000
160706_Barbara_H_Teo_2016-07-06_8.l	P68	UNK-0002	0.000	0	0	0.000
160706_Barbara_H_Teo_2016-07-06_9.l	C0	UNK-0003	0.000	0	0	0.000
160706_Barbara_H_Teo_2016-07-06_10	C68	UNK-0004	0.000	0	0	0.000
Average			56.527	3952523	48186	2.714
%RSD			0.347	74.382	72.305	74.382
Maximum			56.789	7707809	92199	5.292
Minimum			56.297	381479	5027	0.262
Standard Deviation			0.196	2939953	34841	2.019

Figure 41 - HPLC summarized tables 3

Annex C – SEC diagrams of fractionated streams

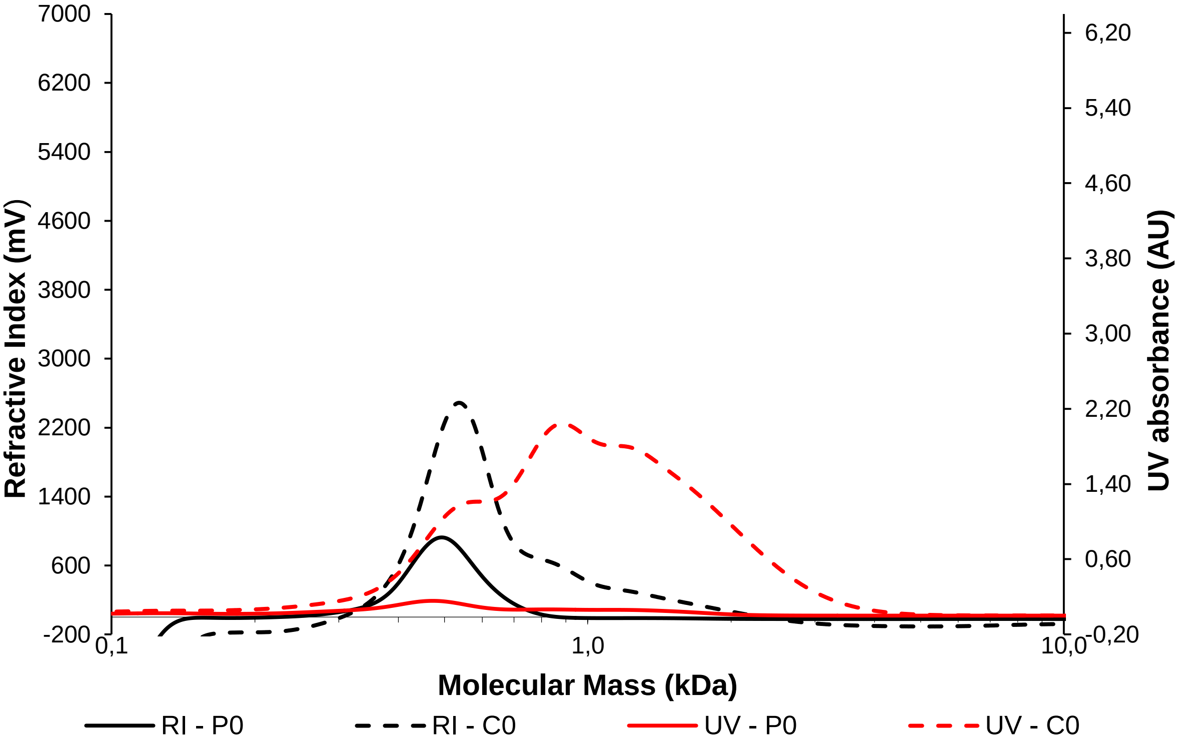

Figure 42 - SEC diagram for retentate and permeate streams at VR=0%

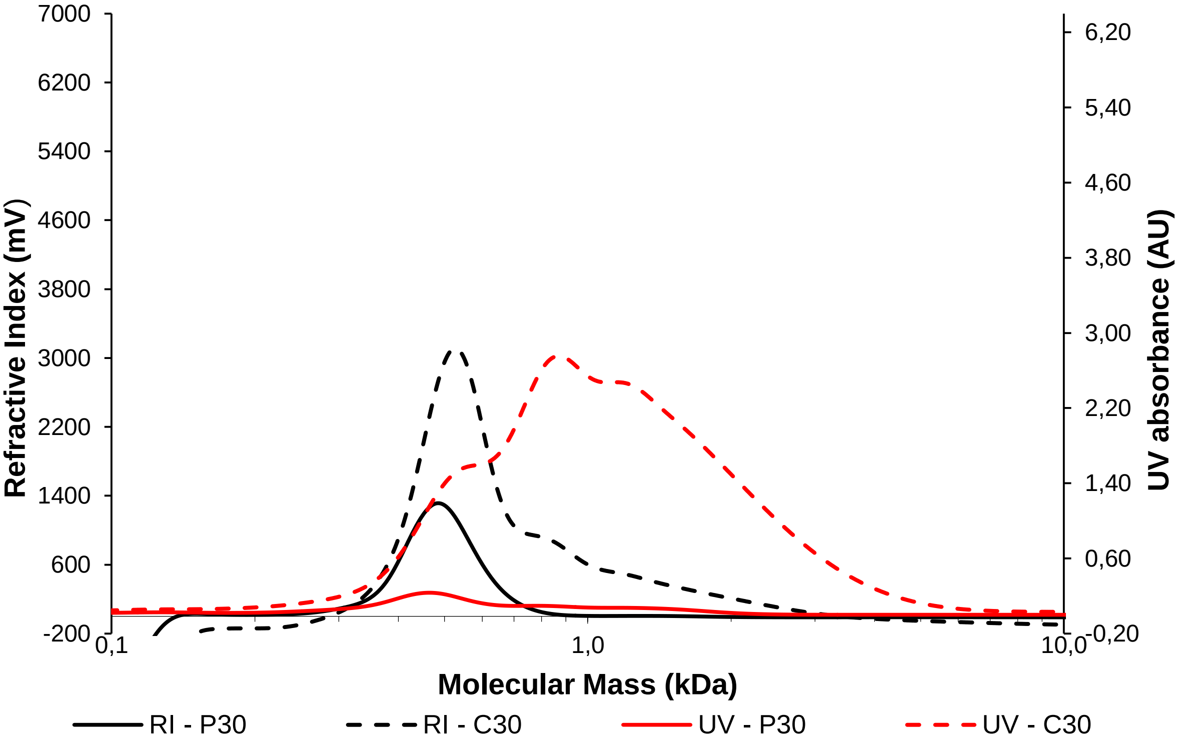

Figure 43 - SEC diagram for retentate and permeate streams at VR=30%

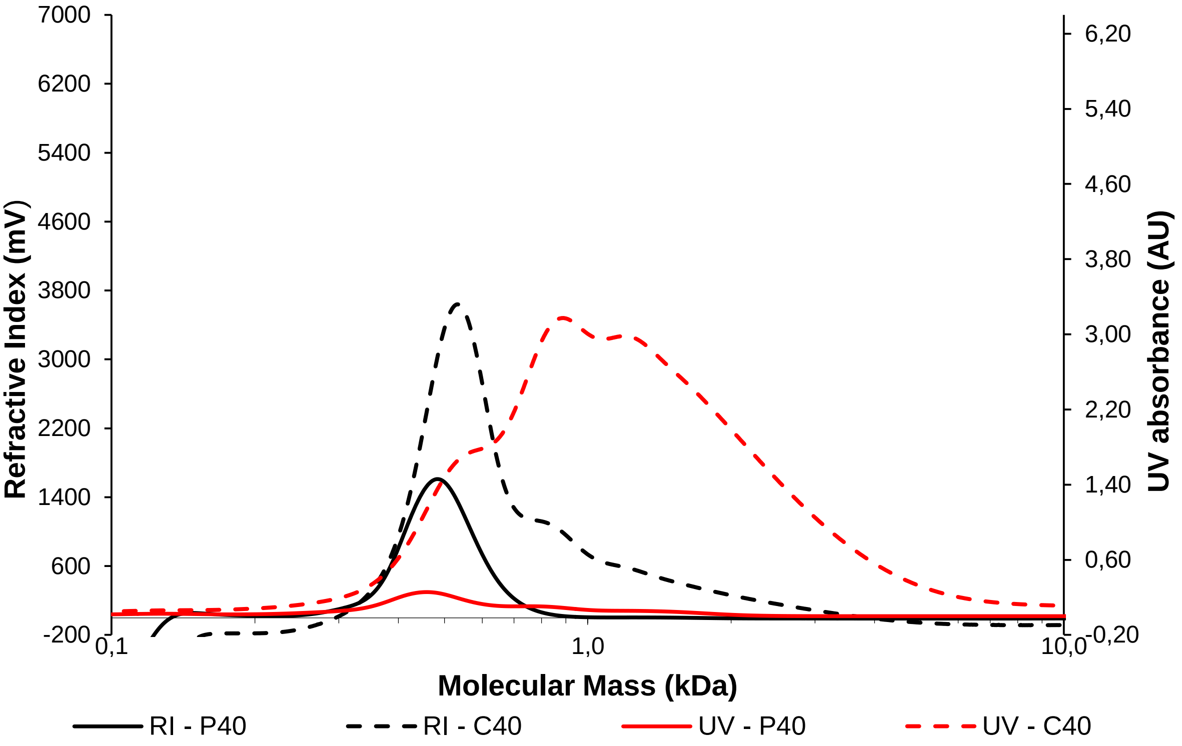

Figure 44 - SEC diagram for retentate and permeate streams at VR=40%

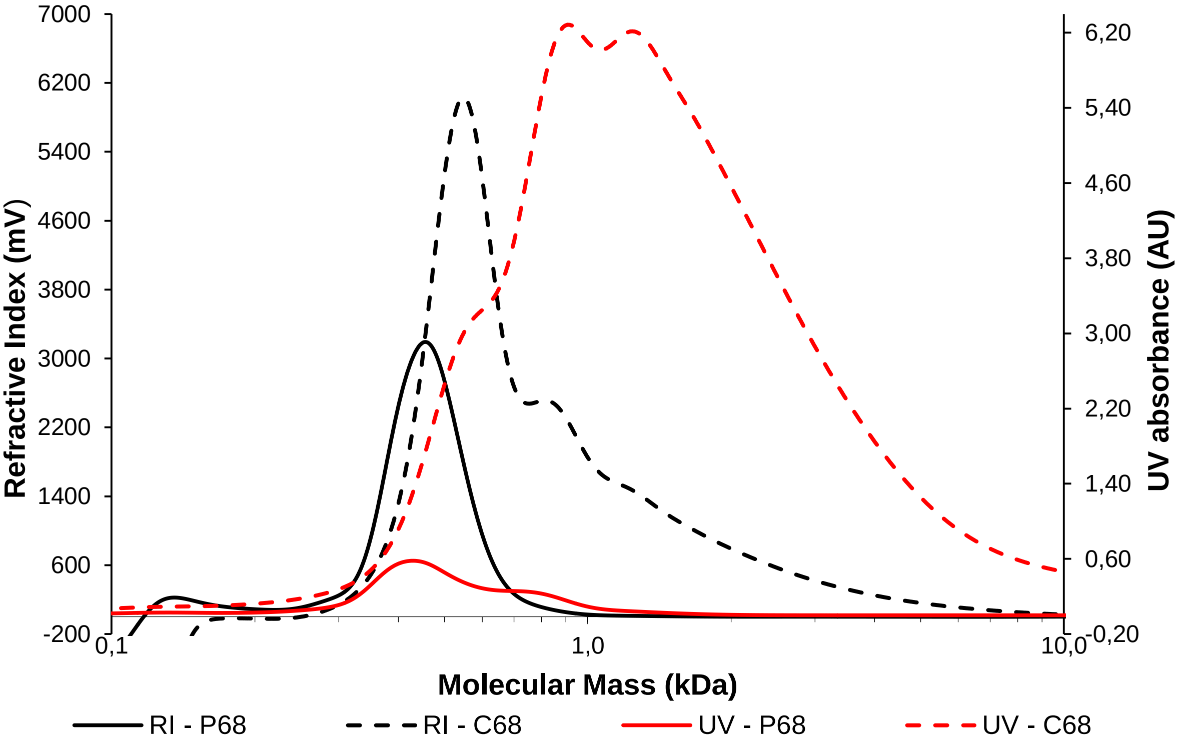

Figure 45 - SEC diagram for retentate and permeate streams at VR=68%